Johann V. Pototschnig, BSc

Theoretical Investigation of the Interaction between Chromium and Helium

Master Thesis

For obtaining the academic degree
Diplom-Ingenieur

Master Programme of
Technical Physics

Graz University of Technology

Supervisor:
Univ.-Prof. Mag. Dr.rer.nat. Wolfgang E. Ernst
Co-Supervisor:
DDr. DI Andreas W. Hauser
Institute of Experimental Physics

Graz, October 2012

Deutsche Fassung:
Beschluss der Curricula-Kommission für Bachelor-, Master- und Diplomstudien vom 10.11.2008
Genehmigung des Senates am 1.12.2008

EIDESSTATTLICHE ERKLÄRUNG

Ich erkläre an Eides statt, dass ich die vorliegende Arbeit selbstständig verfasst, andere als die angegebenen Quellen/Hilfsmittel nicht benutzt, und die den benutzten Quellen wörtlich und inhaltlich entnommene Stellen als solche kenntlich gemacht habe.

Graz, am ……. ……..
(Unterschrift)

Englische Fassung:

STATUTORY DECLARATION

I declare that I have authored this thesis independently, that I have not used other than the declared sources / resources, and that I have explicitly marked all material which has been quoted either literally or by content from the used sources.

……. ……..
date (signature)

Acknowledgments

Right here I want to take some time to thank all the people who supported me and made this thesis possible.

First, I am very grateful to my supervisor Univ.-Prof. Mag. Dr.rer.nat. Wolfgang E. Ernst for the opportunity to do this work. He supported and encouraged me throughout the work and inspired interesting discussions.

The help of the co-supervisor DDr. DI Andreas W. Hauser was very valuable. Without his immense knowledge of quantum chemistry and its applicability to superfluid helium nanodroplets this work would not have been possible.

I especially want to thank Dipl.-Ing. Martin Ratschek who continuously supported me and corrected this thesis. The setting up of the server for the quantum chemical calculations would have been very difficult without him. His understanding of the server-software simplified my work a lot. He had a lot of ideas which he passed on to me in our many discussions.

Additionally I am thankful to Dipl.-Ing. BSc Patrick Kraus who supported me in the preparation of our trip to Moscow for the summer school "Computer Simulations of Advanced Materials".

I also want to give my thanks to Dipl.-Ing. BSc Andreas Kautsch and Dipl.-Ing. BSc Matthias Hasewend who did the experimental investigation of the CrHe-system and gave me a lot of insight.

Ass.Prof. Dipl.-Ing. Dr.techn. Markus Koch also helped a lot and raised many interesting questions.

I want to thank all the people working at the Institute of Experimental Physics for their support.

Additionally I am grateful for all the teachers and professors who motivated and inspired me.

I also want to thank my family, especially my parents Johann and Waltraud Pototschnig. They supported me throughout my education and made this work possible.

This research was supported by the Austrian Science Fund (FWF).

Abstract

Currently chromium (Cr) doped superfluid helium nanodroplets (He_N) are investigated experimentally at the Institute of Experimental Physics at the Graz University of Technology. These Cr doped He-clusters are ionized by optical excitations (photoionization) and the remaining charged complexes are analysed by a quadrupole mass spectrometer. A theoretical description of the CrHe system will be helpful for understanding this process.

The theoretical investigation of the CrHe system was the topic of this thesis. The main focus was the study of the CrHe diatomic molecule and its excited states. To obtain a meaningful description of the CrHe system the Cr atom and the CrHe cation were used as known references. The study of all three systems covers several quantum chemical methods, like the Hartree-Fock method (HF/SCF), the multiconfigurational self-consistent field method (MCSCF), the configuration interaction method (CI), the many body perturbation theory (MBPT), and the coupled cluster method (CC). This thesis is focused on describing two properties. First, the interaction of the Cr atom or ion with He. This interaction will determine the behaviour on He_N. Second, the optical properties of CrHe in the septet-multiplicity were investigated. These properties determine the behaviour of the Cr-He_N during photoionization.

With the results from these calculations predictions for the doped He_N were made. These predictions were based on the so called Ancilotto-parameter. The experimental assumption, Cr sits inside the He_N, but leaves the droplet on excitation, is strongly supported.

Kurzfassung

Zurzeit werden superflüssige Helium Nanotröpfchen (He_N) dotiert mit Chrom (Cr) am Institut für Experimentalphysik an der Technischen Universität Graz untersucht. Diese Cr dotierten Nanotröpfchen werden mit optischen Mehrfachanregungen ionisiert (Photoionisation) und die entstehenden Komplexe mit einem Quadrupol Massenspektrometer untersucht. Für ein Verständnis dieses Experiments ist eine theoretische Beschreibung des CrHe Systems hilfreich.

Diese theoretische Beschreibung des CrHe Systems wird in dieser Arbeit verfolgt. Hauptsächlich wurde der zweiatomige Komplex CrHe und seine angeregten Zustände untersucht. Um den zweiatomige Komplex CrHe möglichst gut beschreiben zu können, wurden auch 2 bekannte Referenzsysteme untersucht, das Cr Atom und das CrHe Kation. Dabei wurden die folgenden quantenchemischen Methoden verwendet: die Hartree-Fock Methode (HF/SCF), die multiconfigurational self-consistent field Methode (MCSCF), die Konfigurations - Wechselwirkungs Methode (CI), die Viel-Körper Störungstheorie (MBPT) und die coupled cluster Methode (CC). Mit dieser Arbeit sollten hauptsächlich zwei Eigenschaften beschrieben werden. Zuerst die Wechselwirkung des Cr Atoms oder Ions mit He. Diese Wechselwirkung bestimmt das Verhalten auf dem He_N. Zweitens wurden die optischen Eigenschaften des CrHe Systems in der Septett - Multiplizität untersucht. Diese Eigenschaften bestimmen das Verhalten von Cr-He_N während der Photoionisation.

Mit den Resultaten dieser Berechnungen wurden Vorhersagen für das Verhalten des dotierten Atoms auf He_N gemacht. Diese Vorhersagen wurden unter Zuhilfenahme des Ancilotto-Parameters gemacht. Das experimentell vermutete Verhalten, dass Cr in He_N sitzt und bei einer Anregung He_N verlässt, konnte damit bestätigt werden.

Contents

List of Figures

For Ångström the abbreviation A is used in the figures. The figures in this thesis have been generated with the programs MATLAB, Microsoft Excel and Avogadro.

List of Tables

Abbreviations, Elements

Cr	chromium
He	helium
He_N	helium-cluster consisting of N atoms
ESR	electron spin resonance
EPR	electron paramagnetic resonance
NIST	National Institute of Standards and Technology [1]
HF/SCF	Hartree Fock / self-consistent field calculation
RHF	restricted Hartree Fock calculation
UHF	unrestricted Hartree Fock calculation
ROHF	restricted open shell Hartree Fock calculation
MCSCF	multiconfigurational self-consistent field calculation
CASSCF	complete active space self-consistent field calculation
CI	configuration interaction calculation
MRCI	multireference configuration interaction calculation
CC	coupled cluster calculation
MRCC	multireference coupled cluster calculation
EOM-CC	equation of motion coupled cluster
(MRCI/CC)S	method with determinants produced by single excitations
(MRCI/CC)SD	method with determinants produced by single and double excitations
CCSD(T)	CC calculation with determinants produced by single and double excitations, most significant triple excitations added perturbatively
MBPT	many body perturbation theory
RS	Rayleigh - Schrödinger perturbation theory
DFT	density functional theory
LDA	local density approximation
LSDA	local spin density approximation
GGA	generalized gradient approximation
STO	slater type orbitals
GTO	gauss type orbitals
ANO	atomic natural orbitals
CSFs	configuration state functions
EMSL database	Environmental Molecular Science Laboratory database [3, 4]
cc	correlation consistent
aug	augmented
BSSE	basis set superposition error
CP	counterpoise correction
MD	molecular dynamics
PES	potential energy surface
PEC	potential energy curve
ZPE	zero point energy
Nr.	number
A	Ångström

Part I

Foundations

Chapter 1

Description of the Problem

At the Institute of Experimental Physics at Graz University of Technology the technique of producing and doping superfluid helium nano droplets (He_N) has been used for several years. Up to now alkali and alkaline-earth atoms, dimers and trimers were investigated [5, 6, 7, 8, 9, 10, 11]. In current experiments at the institute chromium (Cr) is investigated on or inside He_N [12, 13, 14].

Cr was selected due to its outstanding magnetic properties. The solid itself as well as large clusters of Cr atoms are antiferromagnetic. Small chromium clusters, like nanoparticles, on the other hand show superparamagnetism [15].

Chromium as a single atom has a septet ground state with a huge magnetic moment of 6 Bohr magneton (6 unpaired electrons). This large magnetic moment makes it interesting for electron spin resonance (ESR)/ electron paramagnetic resonance (EPR) spectroscopy. Chromium has already been investigated with ESR, but mainly compounds containing Cr [16, 17, 18, 19, 20, 21, 22, 23].

In ESR spectroscopic analyses transitions between magnetically split sub states are induced by microwaves. Since Cr has a septet ground state it has many sub states with a large energy difference due to its large magnetic moment. For the detection of transitions lasers might be used, in order to address a certain spin state as it is shown for alkali metals in [8]. ESR investigations as well as the production of high spin clusters are long term goals.

Cr clusters of different sizes can be produced and investigated by He_N [12]. The He_N environment alters the spectroscopic properties as well as the behaviour of chromium. It is necessary to understand the excitations of chromium and how the He environment influences these excitations in order to be able to understand and design experiments.

Currently this is done experimentally at the Institute of Experimental Physics. Cr is ionized by optical excitations and the ions and complexes of ions are analysed by a quadrupole mass spectrometer (QMS).

This can also be investigated theoretically as it was done within this thesis. Cr and He or Cr and He_N interact through their electron shells. This is a quantum-mechanical many body problem which can be described by quantum mechanics.

A good introduction into quantum mechanics and molecular as well atomic physics are given by Hertel and Schulz [24, 25] and Haken and Wolf [26, 27]. These books were used for writing the first part of this thesis.

1.1 Quantum Mechanics

1.1.1 Schrödinger equation

The main equation of nonrelativistic quantum mechanics is the Schrödinger equation (1.1).

$$\hat{H}\psi\left(\mathbf{r}_i, \mathbf{R}_j, t\right) = i\hbar\frac{\partial}{\partial t}\psi\left(\mathbf{r}_i, \mathbf{R}_j, t\right) \tag{1.1}$$

i is the imaginary unit and $\hbar = \frac{h}{2\pi}$ the reduced Planck constant. $\frac{\partial}{\partial t}$ is the partial derivation with respect to time. The system can be described by ψ, the wave function. In this case it depends on the coordinates of the atomic nuclei $\mathbf{R}_j$ (used for $\mathbf{R}_1, \ldots, \mathbf{R}_{N_n}$), the coordinates of the electrons $\mathbf{r}_i$ (used for $\mathbf{r}_1, \ldots, \mathbf{r}_{N_{el}}$) and the time t (N_n is the number of nuclei in the system, N_{el} the number of electrons). The system is defined by $\hat{H}$, the Hamilton operator, the Hamiltonian. The Hamilton operator can be derived from classical mechanics with the correspondence principle.

One obtains the Hamilton operator (1.2), if the energy of a system (one particle) is given by kinetic and potential energy.

$$E = \frac{1}{2m}\mathbf{p}^2 + V\left(\mathbf{r}\right) \quad \Rightarrow \quad \hat{H} = -\frac{\hbar^2}{2m}\Delta + V\left(\hat{\mathbf{r}}\right) \tag{1.2}$$

m is the mass of the particle, p the momentum of the particle, V the function describing the potential energy which in this case only depends on the position of the particle and $\Delta = \frac{\partial^2}{\partial x^2} + \frac{\partial^2}{\partial y^2} + \frac{\partial^2}{\partial z^2}$ is the Laplace operator.

For a time independent potential the Schrödinger equation can be simplyfied further. The time dependency can be extracted by a time factor $e^{-\frac{iEt}{\hbar}}$. This gives the time-independent Schrödinger equation (1.3) with the energy eigenvalue E.

$$\hat{H}\Psi\left(\mathbf{r}_i, \mathbf{R}_j\right) = E\Psi\left(\mathbf{r}_i, \mathbf{R}_j\right) \tag{1.3}$$

The equation can be simplified further by the Born - Oppenheimer approximation, but this simplification is an approximation which can lead to wrong results. The main idea behind the Born - Oppenheimer approximation is the separation of the electronic and the nuclear system. The ratio of electron mass and proton mass is $m_e : m_P = 1 : 1836$. If a proton and an electron have the same kinetic energy the electrons move about 42 times faster than the protons. If the cores consist of more particles the difference increases. The error introduced by this approximation therefore will be smaller than $1/1836 \approx 5 \times 10^{-4}$.

The method of separation of variables is applied to obtain the Born - Oppenheimer approximation. It is assumed that the wave function of the complete system can be written as a product of a nuclear wave function Φ and an electronic wave function ψ (1.4).

$$\Psi\left(\mathbf{r}_i, \mathbf{R}_j\right) = \Phi\left(\mathbf{R}_j\right)\psi\left(\mathbf{r}_i\right) \tag{1.4}$$

This approach the leads to a separation of the Schrödinger equation into two equations, one for the electrons and one for the cores. In the electronic Schrödinger equation (1.5) the coordinates of the nuclei appear as parameters.

$$\hat{H}_{el}\left(\mathbf{R}_j\right)\psi\left(\mathbf{r}_i\right) = E_{el}\left(\mathbf{R}_j\right)\psi\left(\mathbf{r}_i\right) \tag{1.5}$$

The electronic problem needs to be solved for different configurations of the cores with corresponding Hamiltonians to obtain the energy eigenvalues dependent on the nuclear coordinates $E_{el}(\mathbf{R}_j)$. Different eigenvalues belong to different electronic states. These energy eigenvalues $E_{el}(\mathbf{R}_j)$ define the potential energy surface (PES) or in the case of a dimer the potential energy curve for the nuclear Schrödinger equation (1.6).

$$\hat{H}_{nu}\Phi(\mathbf{R}_j) = E_{nu}\Phi(\mathbf{R}_j) \quad \text{with } \hat{H}_{nu} = E_{kinetic} + E_{el}(\mathbf{R}_j) \tag{1.6}$$

If you solve this equation you can obtain rotational and vibrational states of the system. Sometimes the nuclear problem is solved classically, for example by using the PES in Molecular Dynamics (MD).

1.1.2 Calculating Observables

After determining the wave function of a system observables can be calculated. These observables coincide with properties of the system that may be measured. The expectation value of an observable $\hat{O}$ can be calculated as shown in equation (1.7).

$$\langle O \rangle = \int\int \Psi^*(\mathbf{r}_i, \mathbf{R}_j)\ \hat{O}\ \Psi(\mathbf{r}_i, \mathbf{R}_j)\, d\mathbf{r}_i d\mathbf{R}_j \tag{1.7}$$

Observables can for example be a position operator or a momentum operator. If you want to determine the electron density you would calculate it with the position operators for all electrons (1.8).

$$\langle \rho_{el}(\mathbf{x}) \rangle = \int\int \Psi^*(\mathbf{r}_i, \mathbf{R}_j)\ \sum_i \delta(\mathbf{x} - \hat{\mathbf{r}}_i)\ \Psi(\mathbf{r}_i, \mathbf{R}_j)\, d\mathbf{r}_i d\mathbf{R}_j \tag{1.8}$$

1.1.3 Good Quantum Numbers

The commutator ($[\ldots,\ldots]$) of two operators $(\hat{A}, \hat{B})$ is an important quantity in quantum mechanics (1.9).

$$\left[\hat{A}, \hat{B}\right] = \hat{A}\hat{B} - \hat{B}\hat{A} \tag{1.9}$$

The same set of eigenfunctions can be used if two operators commute ($\left[\hat{A}, \hat{B}\right] = 0$). The system is then in an eigenstate of both operators which means both operators can be measured exactly. On the other hand if the commutator is non-zero it is impossible to measure the observables of both operators exactly. This can be used to calculate the famous Heisenberg uncertainty principle.

An eigenvalue is called a good quantum number if the eigenvalue and eigenstate of an operator remains unchanged over time. A necessary and sufficient condition is that the operator $\hat{O}$ commutes with the Hamiltonian of the system under consideration (1.10).

$$\left[\hat{H}, \hat{O}\right] = 0 \tag{1.10}$$

As the eigenvalues are fixed over time they can be used to identify the states. Examples are angular momentum quantum numbers, spin quantum numbers and others. Good quantum numbers are system dependent and therefore good quantum numbers for an atom may not be good quantum numbers for a molecule.

1.2 Hamilton Operator of the Cr - He System

The wave function describing the Cr - He system can be determined by solving the Schrödinger equation of the system. Therefore we require the Hamiltonian of the system (1.11).

$$\begin{aligned}\hat{H} = &\underbrace{-\frac{\hbar^2}{2m_{Cr}}\Delta_{Cr} - \frac{\hbar^2}{2m_{He}}\Delta_{He}}_{a} + \underbrace{\frac{48\ e^2}{4\pi\epsilon_0}\frac{1}{|\mathbf{R}_{Cr} - \mathbf{R}_{He}|}}_{b} \\ &+ \sum_{i=1}^{26}\Bigg[\underbrace{-\frac{\hbar^2}{2m_e}\Delta_i}_{c} - \underbrace{\frac{2\ e^2}{4\pi\epsilon_0}\frac{1}{|\mathbf{r}_i - \mathbf{R}_{He}|}}_{d} \\ &\underbrace{- \frac{24\ e^2}{4\pi\epsilon_0}\frac{1}{|\mathbf{r}_i - \mathbf{R}_{CR}|}}_{e} + \underbrace{\frac{1}{2}\sum_{j=1, i\neq j}^{26}\frac{e^2}{4\pi\epsilon_0}\frac{1}{|\mathbf{r}_i - \mathbf{r}_j|}}_{f}\Bigg]\end{aligned} \tag{1.11}$$

The first two terms (a) in equation (1.11) are the kinetic energies of the nuclei of the Cr and the He. Next is the term (b) for the electrostatic Coulomb potential of the two cores, with a charge of $48 \cdot e^2$. The sum over the 26 electrons (2 from He, 24 from Cr) follows (terms c-f). The first term (c) in the sum is the kinetic energy of the electrons. Then we have the Coulomb interaction between the cores of He and Cr with the electrons (term d-e). The last term (f) is the so called electron - electron interaction, the Coulomb interaction among the electrons themselves.

A sum over the He atoms is added for a generalization to a system with He_N. The Hamiltonian for a system consisting out of one Cr atom and N He atoms is shown in equation (1.12).

$$\begin{aligned}\hat{H} = &-\frac{\hbar^2}{2m_{Cr}}\Delta_{Cr} + \sum_{I=1}^{N}\left[-\frac{\hbar^2}{2m_I}\Delta_I + \frac{48\ e^2}{4\pi\epsilon_0}\frac{1}{|\mathbf{R}_I - \mathbf{R}_{Cr}|}\right] \\ &+ \sum_{i=1}^{24+2\cdot N}\left[-\frac{\hbar^2}{2m_e}\Delta_i - \frac{24\ e^2}{4\pi\epsilon_0}\frac{1}{|\mathbf{r}_i - \mathbf{R}_{CR}|}\right] \\ &+ \frac{1}{2}\sum_{J=1, I=1, J\neq I}^{N}\frac{4\ e^2}{4\pi\epsilon_0}\frac{1}{|\mathbf{R}_J - \mathbf{R}_I|} + \frac{1}{2}\sum_{i=1, j=1, i\neq j}^{24+2\cdot N}\frac{e^2}{4\pi\epsilon_0}\frac{1}{|\mathbf{r}_i - \mathbf{r}_j|} \\ &- \sum_{i=1}^{24+2\cdot N}\sum_{I=1}^{N}\frac{2\ e^2}{4\pi\epsilon_0}\frac{1}{|\mathbf{r}_i - \mathbf{R}_I|}\end{aligned} \tag{1.12}$$

Chapter 2

Theoretical Background

The solution of quantum-mechanical many body problems is the main concern of quantum chemistry. Several software packages exist, which aim at solving such problems. One of these software packages is MOLPRO [28], which was used for the calculations within this thesis. MOLPRO and most other software packages offer a solution of quantum-mechanical many body problems by applying ab-initio or semi-empirical methods. Some basic principles and especially their methods are described in the sections 2.2, 2.3, 2.4 and 2.4. These methods determine the coefficients of a basis set of functions. Basis sets and basis functions will be described in section 2.1. The classification and identification of states and wave functions is described in the sections 2.8 and 2.9. In the sections 2.7 and 2.10 the main concern will be to find solution for the nuclear Schrödinger equation and describe the behaviour of systems of many particles (He_N).

A deeper insight in the mentioned methods and basis sets can be gained by reading the book of Jensen [29].

2.1 Basis Set

The goal in quantum-mechanical problems is to describe the wave function, as accurate as possible. A perfect description would require an infinite basis set, which is computationally not feasible. Basis sets and basis functions with a form close to real orbitals are used in order to keep the computational effort as small as possible but still obtain meaningful results.

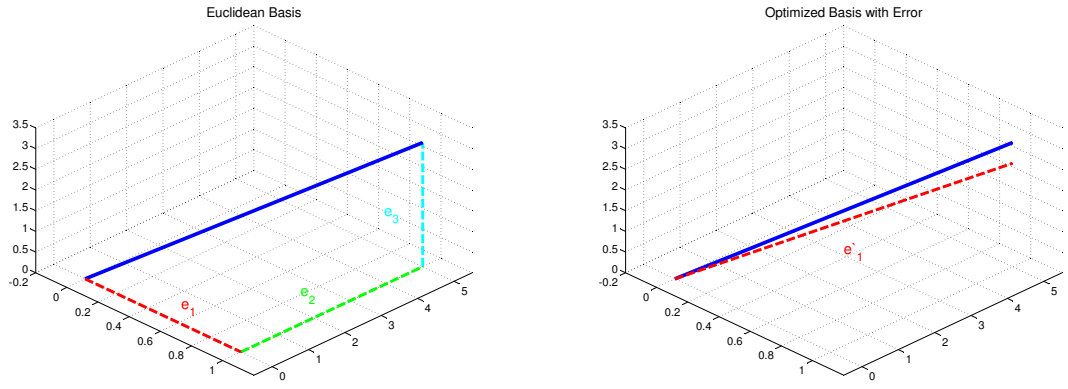

Figure 2.1: Here you see an analogy in three dimensional real space for the infinite function space. The exact description of an arbitrary vector (blue line) requires at least three independent vectors (left side). An approximate description is given by a single vector that has at least approximately the same properties as the one to describe (right side).

For a better understanding a description of an analogy in 3d real space follows, see figure 2.1. The exact solution of the Schrödinger equation, the real wave function corresponds in this analogy to a vector in an arbitrary direction. An exact description of the wave function would require an infinite number of basis functions, as you require three independent coordinates in the three dimensional space (left side of figure 2.1) for an exact description. Now you want to reduce the number of functions (in the analogy: vectors or dimensions) to decrease the computational effort. In the three dimensional space this can be done by a single vector which has at least approximately the same direction as the exact solution (right side of figure

2.1). In the function space this is done by using a finite number of functions which approximate the orbitals as accurately as practicable. This might introduce an error as the right side of figure 2.1 demonstrates, but the calculation remains possible. By using these approximate basis sets meaningful results can be obtained, even if they can not be completely accurate. As will be shown later different properties are described best by different basis sets.

There are three main types of functions which have been established to describe wave functions. The Slater type orbitals (STO) will be described in section 2.1.1. Section 2.1.2 will deal with Gauss type orbitals and section 2.1.3 will refer to plane waves.

2.1.1 Slater Type Orbitals (STO)

The exact solutions of the Schrödinger equation can only be determined for the hydrogen atom. The wave function consists of a product of three functions. The product of two of these functions contains all the angular dependence. These two functions together are the so called spherical harmonics $Y_{lm}(\theta, \varphi)$. The radial function is a product of a finite power series and a negative exponential. The long range behaviour of the solution is dominated by an exponential decay (behaviour: $e^{-a \cdot r}$). The resulting wave function can be used as a basis for more complex systems. Since it is already a solution it is physically meaningful. It should have the right behaviour at small and large distances. This type of basis functions is called Slater type orbitals (STO).

The downside of STOs is the lack of analytic integrals. The integrals can only be evaluated numerically which can take up a lot of computational power. Nevertheless they are still used for certain problems.

2.1.2 Gauss Type Orbitals (GTO)

The wave function can also be described by a set of Gauss functions which are called Gauss type orbitals (GTO). GTOs are very useful for representing real wave functions. They are also localised and have decaying long range behaviour, which means that they can be normalised. They are great for computation because they are easy to evaluate. For the integral of Gauss functions there exist analytical solutions (like (2.1), (2.2)), even for the product of two Gauss functions. (These equations can be found in many collections of equations.)

$$\int_{-\infty}^{\infty} x^{2k} e^{-ax^2} dx = \frac{1 \cdot 3 \cdot \ldots \cdot (2k-1)\sqrt{\pi}}{2^k a^{k+\frac{1}{2}}} \quad \text{for} \quad a > 0 \text{ and } k = 1, 2, \ldots \tag{2.1}$$

$$\int_{-\infty}^{\infty} x^{2k+1} e^{-ax^2} dx = 0 \quad \text{for} \quad a > 0 \text{ and } k = 0, 1, 2, \ldots \tag{2.2}$$

A problem is the difference in short and long range behaviour with respect to the more physical STO because GTO have a quadratic exponential behaviour: $e^{-a \cdot r^2}$. This difference is displayed in figure 2.2.

Another advantage is that the Gauss functions allow for a separation of coordinates (2.3) which simplifies the calculation. The spherical harmonics can be represented with this set of functions.

$$x^n y^m z^l e^{-a \cdot r^2} = x^n y^m z^l e^{-a \cdot \left(x^2+y^2+z^2\right)} = \underbrace{x^n e^{-a \cdot x^2}}_{f(x)} \underbrace{y^m e^{-a \cdot y^2}}_{f(y)} \underbrace{z^l e^{-a \cdot z^2}}_{f(z)} \tag{2.3}$$

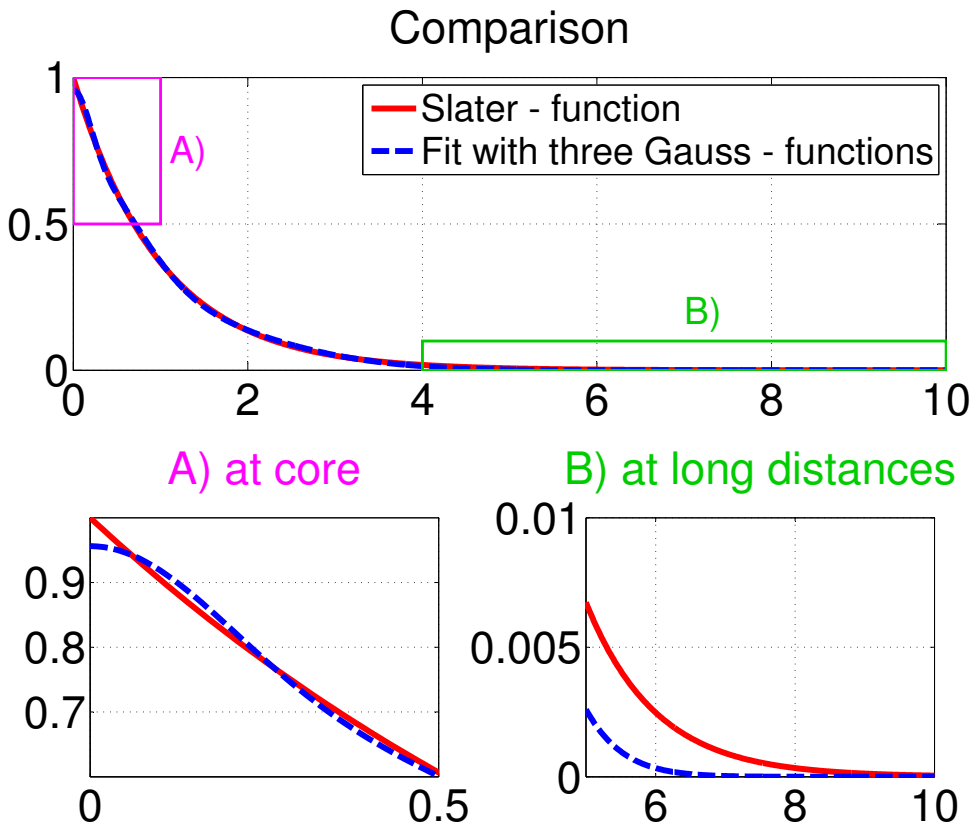

Figure 2.2: comparing a STO with a fit of three GTOs

Most of the programs for calculating molecules use these GTOs. There even is a database where the orbital parameters can be downloaded for different elements and computer programs ([4], https://bse.pnl.gov/bse/portal).

2.1.3 Plane Waves

Plane waves are useful for a different set of problems. They are non-decaying and therefore are for an infinite description. They are also periodic so the result in a certain region describes the result everywhere. These properties make a treatment of localised molecules difficult but help a lot if you want to describe a crystalline structure. Since the interest of this thesis is the description of non-periodic systems this approach is not useful.

2.1.4 Problem dependent Basis Sets

GTO have been developed in order to describe certain properties of an atom or molecule or to simplify the calculation.

A simple GTO is not sufficient to describe an orbital properly. Therefore several GTOs are used. The number of functions can often be deduced from the name of the basis set. So S, D, T, Q, 5, 6 are used to point out that these basis sets have an increasing number of

functions. In each step additional functions are added to describe a orbital and orbitals with increasing angular momentum appear.

Polarized basis sets (marked with p/*) include functions with higher angular momentum in order to describe asymmetric orbitals like polarized atoms.

Since GTOs decay much faster than STOs the correct description of the wave function in large distances is doubtful. This is especially important in weak interactions as van der Waals interactions. This problem can be addressed by diffuse or augmented (marked with aug/+) basis sets which include very weak decaying functions.

All basis sets need to be finite which limits their accuracy. Correlation-consistent (marked with cc) basis sets have been developed to overcome this limitation. They are constructed in a manner that they converge monotonically to the complete basis set limit and give meaningful results in an extrapolation.

There are also basis sets especially developed for relativistic treatment, for example with the Douglas - Kroll formalism (marked with DK). Another efficient way to include relativistic behaviour is the application of effective core potentials (ECPs) which contain relativistic contributions.

Effective core potentials (ECPs) can be used to reduce the computational effort. These potentials describe the core and several inner electrons by an effective potential. So the number of electrons to be treated in the calculation can be reduced. The opposite are all electron basis sets which include all electrons in the calculation.

There are also contracted basis sets. In these basis sets several wave functions are combined and forced to have the same exponential. By this the accuracy gets reduced, but also the computational effort.

2.1.5 MO LCAO

The basis of atomic orbitals (AOs) can now be used to describe the atom under certain conditions. For example an atom can be excited, be in an electric or magnetic field or most importantly form bonds with other atoms, molecules.

A linear combination of atomic orbitals (LCAO, (2.4)) can now be used to describe the wave function of an atom under these conditions.

$$\phi\left(\mathbf{r}_j\right) = \sum_i c_i \psi_i\left(\mathbf{r}_j\right) \tag{2.4}$$

The Pauli principle allows at most two electrons to occupy a single orbital. A system containing n_e electrons requires at least $\frac{n_e}{2}$ orbitals to describe the system accordingly. The Pauli principle can also be accounted for by adding two spin orbitals for every spatial orbital.

A simple linear combination is insufficient to describe antisymmetry required by the Pauli principle. But if the total wave function is described by a Slater determinant (2.5) antisymmetry is guaranteed.

$$\phi\left(\mathbf{r}_j\right) = \begin{vmatrix} \psi_1\left(\mathbf{r}_1\right) & \psi_2\left(\mathbf{r}_1\right) & \dots & \psi_n\left(\mathbf{r}_1\right) \\ \psi_1\left(\mathbf{r}_2\right) & \psi_2\left(\mathbf{r}_2\right) & \dots & \psi_n\left(\mathbf{r}_2\right) \\ \dots & \dots & \dots & \dots \\ \psi_1\left(\mathbf{r}_{n_e}\right) & \psi_2\left(\mathbf{r}_{n_e}\right) & \dots & \psi_n\left(\mathbf{r}_{n_e}\right) \end{vmatrix} \tag{2.5}$$

Also molecular orbitals can be described by a linear combination of atomic orbitals (MO LCAO). The coefficients of the linear combination (c_i in equation (2.4)) are determined by

the methods used by quantum chemical programs. The quantum chemical methods will be discussed in the sections 2.3 and 2.4.

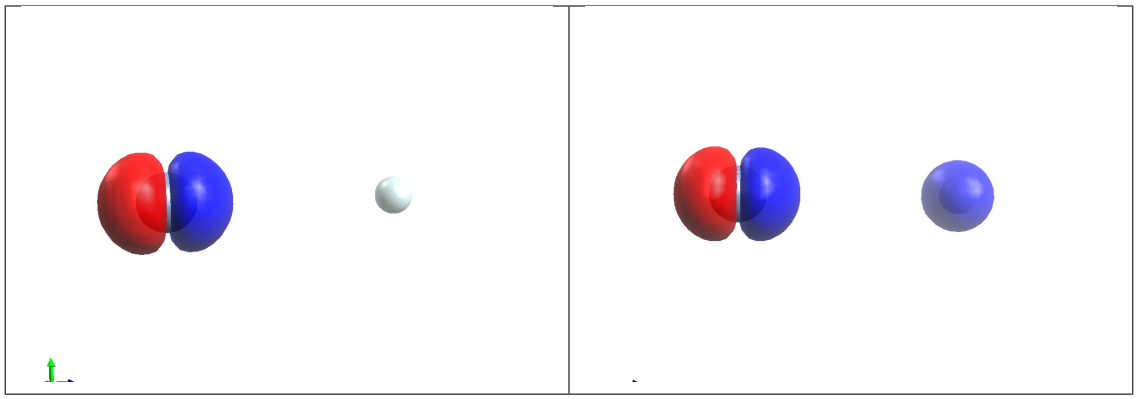

Figure 2.3: The 5^{th} MO of CrHe calculated with the Hartree Fock method (HF, left) and the multiconfigurational self-consistent field method (MCSCF, right). This is a calculation of the CrHe system at 5 $\mathring{A}$.

In figure 2.3 the MO orbitals for CrHe can be seen calculated with two different methods at a distance of 5$\mathring{A}$ between the Cr and He. The white spheres are added to illustrate the position of the Cr (left) and the He nuclei (right). The orbitals are displayed in red and blue. Whether it is blue or red depends on the sign of the wave function. The wave functions are continuous and the red and blue surfaces display the iso-probability surface of the electron probability density.

2.1.6 Towards an Infinite Basis Set

As previously explained the solutions obtained with a finite basis set are inaccurate. Therefore it is desirable to estimate the change with an increasing number of functions. The goal is to obtain a reliable extrapolation for an infinite basis set. There are two approaches that will be presented here.

In order to perform an extrapolation, basis sets are required that converge systematically which is true for correlation-consistent basis sets (marked with cc). Also polarisation consistent or atomic natural orbitals (ANO) basis sets may be used for extrapolation.

Extrapolation Formula

Equation (2.6) is the formula for extrapolating to the basis set limit [29, 30, 31].

$$\Delta E_{corr,\infty} = \frac{N^3 \Delta E_{corr,N} - M^3 \Delta E_{corr,M}}{N^3 - M^3} \tag{2.6}$$

M and N denote the largest angular momentum quantum numbers of the two basis sets used for the extrapolation. $E_{corr,N}$ is the correlation energy calculated with the basis set with N as the largest angular momentum quantum number. An exact definition of the correlation energy will be given in section 2.4. Note that this formula gives an estimation for the correlation energy itself, which has to be added to the Hartree-Fock result to obtain the estimated total energy.

Fitting Function

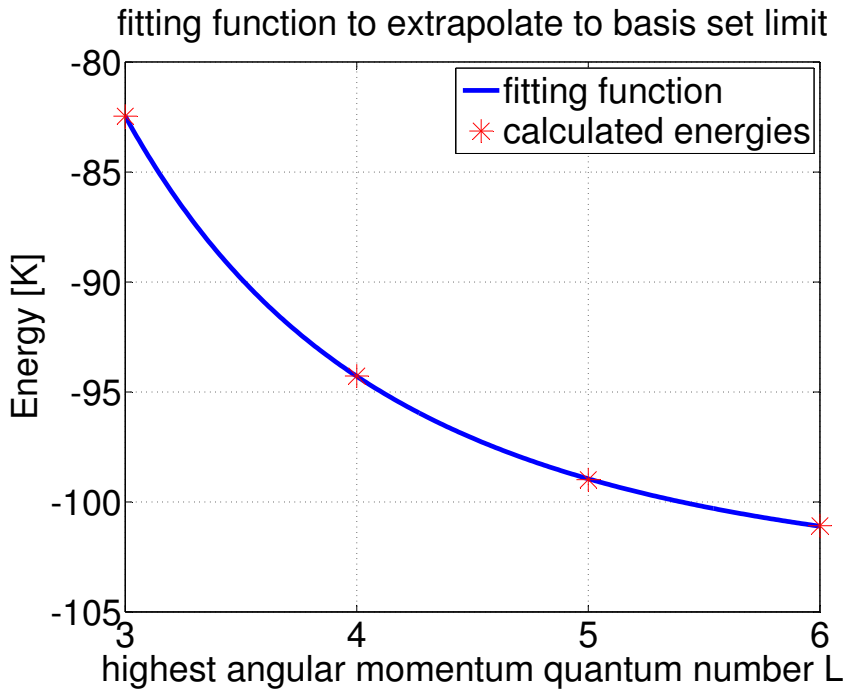

Figure 2.4: several calculated points and a function fitted to these points.

Extrapolation by fitting a function to the data is not easy because at most 6 points have been calculated and the functions have between 2 and 4 parameters that should be determined. Even if the extrapolation gives meaningful results the accuracy is not very high. Figure 2.4 shows the results for a single point of the CrHe potential.

There are several suggestion how to go about the fitting and which function to use [32, 33, 34, 35, 31, 36, 37, 38, 39, 29]. Some suggest only using the correlation energy others use the total energy.

2.1.7 Basis Set Superposition Error (BSSE)

The basis set superposition error occurs in calculations with more than one atom and if the interatomic distances change. Within the MO LCAO approach the AOs are centered around the nuclei. If the nuclei change their distances to each other the AOs do the same and they might start overlapping. If this happens the wave function of one nucleus gains additional basis functions and so its description becomes more accurate. So the accuracy changes in the same calculation due to change in the interatomic distances. This gives rise to a systematic error, the basis set superposition error.

Counterpoise Correction (CP) after Boys und Bernardi [40]

For molecules of several atoms the counterpoise correction needs several calculations and optimizations. For the diatomic molecule, which was the main concern here, the correction is much simpler. The correction for a diatomic molecule consisting of atom A and atom B is

given in equation (2.7). The subscripts give the basis which is used, in this case it is always the same, including all AOs of both atoms. The brackets contain the system for which the energy is calculated. $E^{CP}(AB)$ is the diatomic potential which should approach zero as the distance between the atoms increases.

$$E^{CP}(AB) = E_{AB}(AB) - E_{AB}(A) - E_{AB}(B) \tag{2.7}$$

The counterpoise correction has been proven to improve the results, especially for simple complexes and van der Waals interaction [41]. The best manner to apply it to molecules with strong interactions and its usefulness in these calculations is still disputed. The application to excited states is also not defined.

2.1.8 Ghost Atoms and Bond Functions

Ghost atoms or dummy atoms are atoms with no charge and without electrons. They are simply used to add additional basis functions with a centre different from the existing nuclei.

There are two main applications of ghost atoms. First they can be used for CP calculations, where you add the basis functions but neglect the rest, see equation (2.7).

Another application are the so called bond functions. In order to describe the interaction of atoms better you add additional functions centered between the existing atoms. With this basis the description of interaction should improve. However it is not completely clear how to perform the CP correction including bond functions, especially if more then 2 atoms are involved. Nevertheless this method has been successfully used for diatomic molecules [42, 43, 44, 45].

2.2 Solving the Schrödinger Equation approximately

The Schrödinger equation cannot be solved exactly for many body problems with more than two distinct bodies. Therefore methods have been developed to determine approximate solutions. Two different methods have been applied within this thesis, the variational principle and the perturbation theory. Both methods will be introduced in this section.

2.2.1 Variational Principle

$$E\left(\psi\left(\mathbf{r}_i\right)\right) = \frac{\langle\psi\left(\mathbf{r}_i\right)|\,\hat{H}\,|\psi\left(\mathbf{r}_i\right)\rangle}{\langle\psi\left(\mathbf{r}_i\right)|\,\psi\left(\mathbf{r}_i\right)\rangle} \geq E_0 \tag{2.8}$$

The variational principle (2.8) states:

- Any arbitrary function $\psi\left(\mathbf{r}_i\right)$ used to evaluate the Hamiltonian gives an energy equal or greater than the exact ground state energy E_0.
- If you obtain E_0 then the used function is exactly the wave function for the ground state.

In this manner you can determine the best description for the ground state. If you evaluate the Hamiltonian for different functions, the function which gives the lowest energy describes the ground state the best.

2.2.2 Perturbation Theory

For applying the perturbation theory an unperturbed system (2.9) is necessary of which the exact solution is known.

$$\hat{H}_0\psi_i = \epsilon_i\psi_i \tag{2.9}$$

Then a sufficiently small perturbation of the system is considered ($\lambda\ \hat{H}_1$) with λ being a small parameter.

$$\hat{H} = \hat{H}_0 + \lambda\ \hat{H}_1 \tag{2.10}$$

The solutions of the system are expanded in this small parameter and put into the exact equation(2.13).

$$E = E_0 + \lambda\ E_1 + \lambda^2\ E_2 + \lambda^3\ E_3 + \ldots \tag{2.11}$$

$$\varphi = \varphi_0 + \lambda\ \varphi_1 + \lambda^2\ \varphi_2 + \lambda^3\ \varphi_3 + \ldots \tag{2.12}$$

$$\hat{H}\varphi = E\varphi \tag{2.13}$$

By identifying terms of the same order of λ and demanding that the wave function is normalised the correction terms $(E_1, \varphi_1, E_2, \varphi_2, \ldots)$ can be determined (2.14). $\varphi_{1,j}$ is the first correction for the wave function belonging to the eigenvalue ϵ_j of the unperturbed system. E_1 is the first correction for the ground state energy. In the equations only the solution for non-degenerate states are displayed. In the case of degeneracies you would treat the degenerate state in a subspace and find exact solutions for this subspace.

$$
\begin{aligned}
E_1 &= \int \psi_0^* \hat{H}_1 \psi_0 d\mathbf{r} \\
\varphi_{1,j} &= \sum_{i,i\neq j} \psi_i \frac{\int \psi_i^* \left(\mathbf{r}\right) \hat{H}_1 \psi_j \left(\mathbf{r}\right) d\mathbf{r}}{\epsilon_j - \epsilon_i} \\
E_2 &= \sum_{i,i\neq 0} \frac{\int\int \psi_i^* \left(\mathbf{r}\right) \hat{H}_1 \psi_0 \left(\mathbf{r}\right) \psi_0^* \left(\mathbf{r'}\right) \hat{H}_1 \psi_i \left(\mathbf{r'}\right) d\mathbf{r} d\mathbf{r'}}{\epsilon_0 - \epsilon_i}
\end{aligned}
\tag{2.14}
$$

If the perturbation λ is sufficiently small, the expansion in λ can be truncated. Evaluating only a finite number of correction terms limits the accuracy, but for a small λ it might be sufficient for the desired accuracy.

Due to the expansion in a power series the results show oscillating convergence, contrary to the results obtained by the variational principle which converge monotonically.

2.3 Hartree - Fock (HF), Self-Consistent Field (SCF)

This and the next section will describe the methods used for solving the electronic Schrödinger equation (1.5). First the electronic Hamiltonian of a general system (2.15) will be discussed. Then the Hartree-Fock method will be described in detail. Since the Hartree-Fock method has its limitations it is necessary to extend the considerations to Post Hartree-Fock methods (section 2.4) for an accurate description.

2.3.1 Electronic Hamiltonian of a General System

$$\begin{aligned}
\hat{H}_{el}\left(\mathbf{R}_1,\ldots,\mathbf{R}_{N_n}\right) &= T_{el} + V_{el,n}\left(\mathbf{R}_1,\ldots,\mathbf{R}_{N_n}\right) + V_{el,el} + V_{n,n}\left(\mathbf{R}_1,\ldots,\mathbf{R}_{N_n}\right) \\
T_{el} &= -\sum_{i}^{N_{el}} \frac{\hbar^2}{2m_e}\Delta_i \\
V_{el,n}\left(\mathbf{R}_1,\ldots,\mathbf{R}_{N_n}\right) &= -\sum_{i}^{N_{el}}\sum_{I=1}^{N_n} \frac{Z_I\ e^2}{4\pi\epsilon_0}\frac{1}{|\mathbf{r}_i-\mathbf{R}_I|} \\
V_{el,el} &= \sum_{i,j,i<j}^{N_{el}} \frac{e^2}{4\pi\epsilon_0}\frac{1}{|\mathbf{r}_i-\mathbf{r}_j|} \\
V_{n,n}\left(\mathbf{R}_1,\ldots,\mathbf{R}_{N_n}\right) &= \sum_{I,J,I<J}^{N_n} \frac{Z_I Z_J\ e^2}{4\pi\epsilon_0}\frac{1}{|\mathbf{R}_I-\mathbf{R}_J|}
\end{aligned} \tag{2.15}$$

$\hat{H}_{el}$ is the Hamiltonian of the electronic part of the system. This Hamiltonian appears after applying the Born-Oppenheimer approximation, compare with the equations (1.6) and (1.5). T_{el} is the term for the kinetic energy of the electrons, where N_{el} is the total number of electrons. $V_{el,n}$ is the interaction potential between electrons and nuclei, where N_n is the total number of nuclei. Since the coordinates of the nuclei are fixed this term defines a potential in which the electrons move. The most challenging term is $V_{el,el}$, the electron-electron interaction. Approximations and approaches to determine this term will follow. The last term is $V_{n,n}$, the interaction of nuclei among themselves. For fixed coordinates of the cores this term becomes a constant which can be added to the solution of the electronic Schrödinger equation.

Without the term $V_{el,el}$ there would be no operator connecting two different electrons, the problem would be separable. The solution of the electronic problem would simply be a product of one electron functions that satisfy a single particle Schrödinger equation with the Hamiltonian $\hat{h}_i$ (2.16).

$$\hat{h}_i = -\frac{\hbar^2}{2m_e}\Delta_i - \sum_{I=1}^{N_n}\frac{Z_I\ e^2}{4\pi\epsilon_0}\frac{1}{|\mathbf{r}_i-\mathbf{R}_I|} \tag{2.16}$$

2.3.2 Self Consistent Calculation

The self-consistent calculation makes use of the variational principle (section 2.2.1) and the LCAO ansatz (section 2.1.5). The LCAO wave function is used to evaluate the Hamiltonian (2.17).

$$E = \frac{\sum_i \sum_j c_i^* c_j H_{ij}}{\sum_i \sum_j c_i^* c_j S_{ij}} \tag{2.17}$$

$$\text{with } H_{ij} = \int \psi_i^* \hat{H} \psi_j d\mathbf{r} \tag{2.18}$$

$$S_{ij} = \int \psi_i^* \psi_j d\mathbf{r} \tag{2.19}$$

This solution can be differentiated with respect to the coefficients of the LCAO ansatz (c_i, equation (2.4)) in order to determine the best possible wave function for the ground state. This gives a system of linear equations (2.20).

$$\sum_j \left(H_{ij} - E \cdot S_{ij}\right) c_j = 0 \tag{2.20}$$

Solving this system of linear equations gives the coefficients of the LCAO ansatz (c_i). So far the calculation has a unique solution and solving it self-consistently would not be necessary. But evaluating (2.18) requires already knowledge about the solution of the system. Therefore a self-consistent approach is necessary. Some arbitrary coefficients are chosen, the Hamiltonian is evaluated and new coefficients are determined. This is repeated until the coefficients do not change any more.

2.3.3 Compute the Hamiltonian

With the single particle Hamiltonian the general Hamiltonian can be rewritten (2.21).

$$\hat{H}_{el} = \sum_i^{N_{el}} \hat{h}_i + \sum_{i,j,i<j}^{N_{el}} \frac{e^2}{4\pi\epsilon_0} \frac{1}{|\mathbf{r}_i - \mathbf{r}_j|} + V_{n,n} \tag{2.21}$$

This Hamiltonian needs to be computed for the SCF-calculation (2.18). This is done with a Slater determinant (2.5). By using the orthonormality of the orbitals the different terms can be simplified. $V_{n,n}$ is a constant which is left unaltered. The single electron Hamiltonian is evaluated with a single orbital from the Slater determinant (2.22).

$$\epsilon_i = \int \psi_i^* (\mathbf{r}_i) \;\; \hat{h}_i \;\; \psi_i (\mathbf{r}_i) \;\; d\mathbf{r}_i \tag{2.22}$$

The electron-electron potential needs two orbitals for evaluation (2.23),(2.24).

$$CO_{i,j} = \int\int \psi_i^* (\mathbf{r}_i) \, \psi_j^* (\mathbf{r}_j) \, \frac{e^2}{4\pi\epsilon_0} \frac{1}{|\mathbf{r}_i - \mathbf{r}_j|} \psi_i (\mathbf{r}_i) \, \psi_j (\mathbf{r}_j) \, d\mathbf{r}_i d\mathbf{r}_j \tag{2.23}$$

$$EX_{i,j} = \int\int \psi_i^* (\mathbf{r}_i) \, \psi_j^* (\mathbf{r}_j) \, \frac{e^2}{4\pi\epsilon_0} \frac{1}{|\mathbf{r}_i - \mathbf{r}_j|} \psi_j (\mathbf{r}_i) \, \psi_i (\mathbf{r}_j) \, d\mathbf{r}_i d\mathbf{r}_j \tag{2.24}$$

The first expression (2.23) is called Coulomb operator and accounts for the Coulomb repulsion between two electrons. The second expression (2.24) is a quantum mechanical contribution, the exchange operator.

2.3.4 Mean Field - Approximation

This approach is a mean field calculation. One electron is considered in the field of the other electrons.

$$V_{el,el} = \sum_{i,j,i<j}^{N_{el}} \frac{e^2}{4\pi\epsilon_0} \frac{1}{|\mathbf{r}_i - \mathbf{r}_j|} \Longrightarrow \langle V_{el,el} \rangle = \sum_{j}^{N_{el}} (CO_{i,j} + EX_{i,j}) \tag{2.25}$$

The interaction between two electrons is only considered by the mean field. In order to overcome this deficiency Post - Hartree Fock methods (section: 2.4) were developed which also include electron correlation.

2.3.5 Open / Closed Shell Systems

Closed shell systems are only containing doubly occupied orbitals and they always have a singlet multiplicity. These systems are treated more easily with the so called restricted Hartree-Fock calculations (RHF).

For open shell system, like Cr with a septet multiplicity, two methods can be chosen. In unrestricted Hartree-Fock calculations (UHF) every spin orbital is treated separately. On the other hand in restricted open shell Hartree-Fock calculations (ROHF) the doubly occupied orbitals are treated by RHF and the rest by UHF. For the calculations in this thesis the ROHF proved to be more successful than UHF calculations.

The HF calculations were performed in MOLPRO with programs developed by Polly and Werner [46].

2.4 Post - Hartree Fock Methods

The motivation for developing these methods was that the electron-electron interaction is insufficiently described by the HF calculations. It is lacking the electron correlation. The correlation energy is exactly defined in equation (2.26).

$$\mathrm{E_{corr}} = \mathrm{E_{exact,\ nonrelativstic}} - \mathrm{E_{HF,\ complete\ basis\ set}} \tag{2.26}$$

The HF method made use of a single slater determinant. If you want to describe electron correlation this is no longer sufficient. A description with more slater determinants is required (2.27).

$$\psi(\mathbf{r}_i) = a_0\phi_{HF} + \underbrace{\sum_i a_i\phi_i}_{S} + \underbrace{\sum_{i,j} a_{i,j}\phi_{i,j}}_{D} + \ldots \tag{2.27}$$

Methods applying this approach are either called multiconfigurational (optimizing several states) or multireference (using several states as reference). Another advantage of this approach is that excited states can also be calculated.

Since an infinite number of slater determinants cannot be computed some determinants are selected. They are generated by putting one or more electrons from one orbital with low energy in an orbital with higher energy (a previously empty orbital, so called virtual orbital). Different numbers of electrons are used for this excitations and this is indicated within the abbreviation of the method. Common approaches use following excitations:

singles (S) only one electron is in a virtual orbital

doubles (D) two electrons change orbitals

triples (T) three electrons change orbitals

The Slater determinants are also called configuration state functions (CSFs) and as their number increases the accuracy increases too. So if the CSFs of a calculation are similar the results should be similar, too.

In this context the expression active space is often used. This is the space of functions which is used in a certain calculation. The active space is often given by the number of orbitals and the number of electrons which are used to generate the function space. The function space is generated by putting the electrons in the orbitals in all possible combinations as far as they are allowed because the Pauli principle still has to be fulfilled. Sometimes all possible states are generated and this is called a complete active space (CAS). For restricted active space (RAS) additional conditions need to be fulfilled.

2.4.1 Multiconfigurational SCF (MCSCF)

The multiconfigurational SCF (MCSCF) is also based on the variational principle and can be seen as a HF calculation for multiple states. Multiple states are calculated and each state has its own energy. So the question arises which energy should be minimized to obtain the best possible set of wave functions. Since the orbitals need to be orthonormalized, the determinants influence each other. In general a state average is used. The energy average of several states is minimized, sometimes a weighted average is used. This method optimizes the coefficients c_i of equation (2.4) and the coefficients $a_0, a_i, ...$ of equation (2.27).

The complete active space SCF (CASSCF) is a special case of the MCSCF. This calculation uses all possible CSFs with a predefined number of orbitals and electrons.

The opposite is a restricted active space SCF (RASSCF) in which there are additional restrictions to decrease the number of CSFs.

In a MCSCF calculation the determinants are still optimized and the energies are also improved. The succeeding methods (MRCI, CC, RS) leave the orbitals unchanged, but calculate improved energies and other improved observables.

The MCSCF programs of MOLPRO were developed by Werner, Knowles and Meyer [47, 48, 49].

2.4.2 Multireference Configuration Interaction (MRCI)

The foundation for this method is equation (2.27). The ground state and the excited states which need to be calculated are expressed as series of determinants. The determinants are kept fixed contrary to the SCF methods (HF, MCSCF) but the coefficients of the determinants are optimized.

Again the variation principle (section 2.2.1) is used and the energy of the system is minimized under the constraint that the wave function is normalized. This leads to a system of linear equations which can be solved (2.28).

$$(\underline{\mathbf{H}} - \mathbf{E}\underline{\mathbf{I}}) \cdot \mathbf{a} = 0 \tag{2.28}$$

$\mathbf{a}$ are the coefficients of the series. The eigenvalues $\mathbf{E}$ are multiplied with the identity matrix $\underline{\mathbf{I}}$. The matrix $\underline{\mathbf{H}}$ is generated by evaluating the Hamiltonian for the combination

of different determinants. For the states described by the different series energies and other observables can be calculated.

The statements so far also hold for simple CI. The difference between CI and MRCI is the starting wave function. In CI a wave function of a single determinant HF - calculation is used. In MRCI you start from multiconfigurational wave functions which most of the time have been generated by MCSCF. Then excitations between these states are considered.

Full CI/ truncated CI

In full configuration interaction (CI) all possible excitations are considered for a certain space (like CASSCF). This is only feasible for small systems with a small set of basis functions. Most of the time truncated CI is used. For example only single and doubly excited determinates are considered (CISD) in the calculation. A deficiency of the truncated method is that the system is no longer size consistent.

Size consistency means that if you calculate one molecule and a system of N non-interacting molecules you obtain N times the value for the single system. Size inconsistency is not physical and may alter the results.

There are approximate corrections of this missing size consistency, for example the Davidson correction[50]. The MRCI was used as implemented in MOLPRO by Werner and Knowles [51, 52, 53].

2.4.3 Coupled Cluster (CC)

The coupled cluster method uses also an expansion like CI but the coupled cluster method is size consistent. The cluster operator (2.29) can be used to write the coupled cluster wave function (2.32) which is generated by the cluster operator acting on the Hartree-Fock wave function. The single excitations are generated by the operator in equation (2.30). The expression t_i^a is a coefficient which gives the strength of contribution of ϕ_i^a. The function ϕ_i^a is the Hartree-Fock wave function with the electron that previously was in orbital i and now is in orbital a. The first sum in (2.30) is over the occupied orbitals, the second over the virtual orbitals. The operator (2.31) generates in a similar way functions where two electrons have changed their orbital. This can be continued to an operator where all electrons change their orbital. The operator (2.29) can be called an excitation operator because it generates excited states.

$$\mathbf{T} = \mathbf{T}_1 + \mathbf{T}_2 + \mathbf{T}_3 + \ldots + \mathbf{T}_N \tag{2.29}$$

$$\mathbf{T}_1\ \phi_0 = \sum_{i}^{occ} \sum_{a}^{vir} t_i^a \phi_i^a \tag{2.30}$$

$$\mathbf{T}_2\ \phi_0 = \sum_{i,j,i<j}^{occ} \sum_{a,b,a<b}^{vir} t_{ij}^{ab} \phi_{ij}^{ab} \tag{2.31}$$

$$\ldots$$

$$\psi_{CC} = e^{\mathbf{T}} \phi_0 \tag{2.32}$$

exponential sorted by order:

$$e^{\mathbf{T}} = \mathbf{1} + \mathbf{T}_1 + \left(\mathbf{T}_2 + \frac{1}{2}\mathbf{T}_1^2\right) + \ldots \tag{2.33}$$

This method uses a single reference wave function. The wave function is then modified by the cluster operator. This cluster operator (2.33) has the great advantage to give size consistent results contrary to truncated CI calculations. If such an approach, that only uses a single determinant, gives meaningful results needs to be evaluated. Especially in cases where some states have similar energy it will not work. For the evaluation of this approach the so called T_1-diagnostics can be used[54]. It is calculated with $|\mathbf{t}_1|$, the norm of the singles amplitudes. A value larger than 0.02 indicates that single-reference methods are inadequate to describe the problem.

Equation of Motion Coupled Cluster (EOM-CC), Multireference Coupled Cluster (MRCC)

Since coupled cluster uses a single reference function the calculation of excited states is not possible. Therefore EOM-CC has been developed which is related to linear response CC. For further details see [55]. EOM-CC was not successfully applied in order to calculate excited state of the diatomic molecule CrHe. Multireference coupled cluster uses several reference states and is currently being developed [56]. It is compatible with MOLPRO and might be applied.

The coupled cluster algorithm implemented in MOLPRO by Knowles, Werner and Hampel [57, 58] was used.

2.4.4 Many Body Perturbation Theory (MBPT), Rayleigh - Schrödinger Perturbation Theory (RS)

The many body perturbation theory or Rayleigh - Schrödinger perturbation theory is based on the perturbation theory (section 2.2.2). The unperturbed system is given by the HF or MCSCF system with a mean field approach (2.34). The difference between the mean field and the potential of the correlated electrons is the perturbation.

$$\begin{aligned} \hat{H}_0 &= \sum_i^{N_{el}} \hat{h}_i + \langle V_{el,el} \rangle \\ \hat{H}_1 &= V_{el,el} - \langle V_{el,el} \rangle \end{aligned} \tag{2.34}$$

The zeroth order gives the HF or MCSCF energies and wave functions. The first order correction for the energy is zero. In first order the operator $\hat{H}_1$, the perturbation, is zero, because you still only evaluate functions where a single electron is excited. So the first correction appears in the second order. The application to a quantum mechanical many body problem is often called Møller - Plesset perturbation theory.

In use are many body perturbation corrections of $2^{nd}, 3^{rd}$ and 4^{th} order. Since they are based on perturbation theory, they have oscillating convergence.

The Rayleigh - Schrödinger perturbation theory was implemented in MOLPRO by Werner and Celani [59, 60].

2.5 Density Functional Theory (DFT)

Density functional theory determines the density and not the wave function of the ground state. This simplifies the calculation enormously since the density is a function in the three spatial coordinates, while the wave functions has 3 N (N is the number of particles) coordinates, see equation (2.35). This reduces the complexity of the problem greatly and so it can be expected that the density alone cannot describe all phenomena accurately. By a so called hybrid functional the complexity is increased and the description is improved (section 2.5.1).

$$\psi\left(\mathbf{r}_1, \mathbf{r}_2, \ldots, \mathbf{r}_N\right) \Longrightarrow \rho\left(\mathbf{r}\right) \tag{2.35}$$

The foundations of the density functional theory (DFT) are the theorems of Hohenberg and Kohn [61] which have been generalized later.

The first theorem states that there is a unique function $\rho_0\left(\mathbf{r}\right)$ describing a system (theorem I).

The second theorem was proved by applying the variational principle (section 2.2.1). It states that if you know the functional describing the total energy of the system $F\left[\rho\left(\mathbf{r}\right)\right]$, the density minimizing this functional is the ground state density $\rho_0\left(\mathbf{r}\right)$ (theorem II).

The difficulty now is to find an accurate functional describing the energy of the system.

2.5.1 Functionals

Many functionals have been developed. They are always for a certain problem or system. For example different functionals are used for bosonic and fermionic systems. Functionals are either derived from theory without involving results (ab initio) or adjusted to reproduce the results of experiments (semi empirical).

Kohn and Sham found a functional and formulated the so called Kohn - Sham equations [62], (2.36) which form the foundation of many modern DFT-approaches. They treated the electronic Schrödinger equation as follows (2.36):

$$\begin{aligned}
F\left[\rho\left(\mathbf{r}\right)\right] &= V_n\left[\rho\left(\mathbf{r}\right)\right] + V_{el}\left[\rho\left(\mathbf{r}\right)\right] + T\left[\rho\left(\mathbf{r}\right)\right] + E_{xc}\left[\rho\left(\mathbf{r}\right)\right] \\
V_n\left[\rho\left(\mathbf{r}\right)\right] &= \int v\left(\mathbf{r}\right)\rho\left(\mathbf{r}\right)d\mathbf{r} \\
V_{el}\left[\rho\left(\mathbf{r}\right)\right] &= \frac{1}{2}\int\int \frac{\rho\left(\mathbf{r}\right)\rho\left(\mathbf{r'}\right)}{\left|\mathbf{r}-\mathbf{r'}\right|} d\mathbf{r}d\mathbf{r'} \\
T\left[\rho\left(\mathbf{r}\right)\right] &= \sum_i^{N_{el}} \int \psi_i^*\left(\mathbf{r}\right)\left(-\frac{1}{2}\nabla^2\right)\psi_i\left(\mathbf{r}\right)d\mathbf{r} \text{ mit } \rho\left(\mathbf{r}\right) = \sum_i^{N_{el}}\left|\psi_i\left(\mathbf{r}\right)\right|^2
\end{aligned} \tag{2.36}$$

V_n is the potential energy of the electron density in the external potential ($v\left(\mathbf{r}\right)$ in equation (2.36)) which is given by the positively charged cores. T is the kinetic energy of the electrons. V_{el} is the energy due to the Coulomb interaction of the electron with themselves. E_{xc} is the exchange energy which is the most demanding term since it is non-local. There are three main approaches for approximating this energy: the local density approximation (LDA),the generalized gradient approximation (GGA) , hybrid methods. They will be explained in the following text.

Local Density Approximation (LDA)

The exchange energy is derived by assuming a local uniform density. If there are open shells and the spins do not compensate each other, the LDA approach is extended to the local spin density approximation (LSDA).

Generalized Gradient Approximation (GGA)

GGA extends LDA by including also the gradient of the density in the calculation of the exchange energy.

Hybrid Methods

So called hybrid functionals can also be used. These functionals use pseudo wave functions to calculate the exchange energy on a Hartree-Fock level (compare equation (2.24)). The rest is still calculated with the density. This approach has been developed to capture more details in DFT.

2.5.2 Calculations

The DFT calculations are again self-consistent calculations. The density of the electrons is calculated. This density generates a new potential for the calculation which leads to a different density. This is repeated until the density changes no more.

DFT is less demanding than HF or the previously mentioned post - Hartree - Fock methods. Therefore DFT can be used to calculate much larger systems.

2.6 Relativistic Approach

So far the quantum-mechanical problem has only been treated in a non-relativistic way and for light atoms this is sufficiently accurate. But the Cr atom shows already weak influences of relativism (see part II), especially if one is interested in weak Van der Waals interaction. Furthermore spin-orbit coupling for excited states can not be neglected.

2.6.1 Scalar-relativistic Corrections

The scalar-relativistic corrections were considered by the Douglas-Kroll-Hess Hamiltonian as implemented by Reiher and Wolf in MOLPRO [63, 64, 65]. This correction is applied in the HF calculations by modifying the Fock matrix with a correction term.

This correction is obtained by a Douglas Kroll Transformation of the Dirac Hamiltonian (2.37). Equation (2.37) has been taken from [64].

$$H_D = c\ \boldsymbol{\alpha} \bullet \mathbf{p} + (\beta - 1)mc^2 + V = \begin{pmatrix} V & c\ \boldsymbol{\sigma} \bullet \mathbf{p} \\ c\ \boldsymbol{\sigma} \bullet \mathbf{p} & V - 2mc^2 \end{pmatrix} \tag{2.37}$$

V is the potential, m the mass and $\mathbf{p}$ the momentum. $\boldsymbol{\sigma}$ is a vector of the Pauli matrices which allows a compact notation.

The Dirac Hamiltonian is a 4×4 matrix with four wave functions as solutions. Two have positive (matter), the other two (antimatter) negative energy eigenvalues. The other difference between the wave functions is a property which can be associated with the spin of the particle.

This 4 dimensional term is mapped with the Douglas - Kroll transformation on to a one dimensional correction term which is added on the Hartree - Fock level. The correction term would be added to the expression in equation (2.18).

2.6.2 Breit-Pauli Operator

The spin that appears in the Dirac equation is associated with a magnetic moment which has a direction. The angular momentum of the orbitals also is connected with a directed magnetic moment. These magnetic moments couple which is called spin - orbit coupling. This is also a relativistic effect, but not a scalar one.

This effect plays an important role in the calculation of excited states (see part II) and can be considered by the Breit - Pauli Hamiltonian (2.38). Equation (2.38) has been taken from [66].

$$\hat{H}_{SO} = \frac{e^2\hbar}{2m^2c^2} \sum_i \sum_K \frac{Z_K \mathbf{r}_{iK} \times \hat{\mathbf{p}}(i)}{r_{iK}^3} \cdot \hat{\mathbf{s}}(i) - \frac{e^2\hbar}{2m^2c^2} \sum_{i,j,i\neq j} \frac{\mathbf{r}_{ij} \times \hat{\mathbf{p}}(i)}{r_{ij}^3} \left[\hat{\mathbf{s}}(i) + 2\hat{\mathbf{s}}(j)\right] \tag{2.38}$$

This operator calculates the interaction between the angular momentum of a particle ($\mathbf{r}_{ij} \times \hat{\mathbf{p}}(j)$) and the spin ($\hat{s}_\alpha(i)$). It considers interactions between the spin of a particle and its angular momentum as well as the angular moment of other electrons. Z_K is the charge of the nuclei K. $\mathbf{r}_{iK}$ is the distance between a nuclei and the electron and $\mathbf{r}_{ij}$ is an electron - electron distance.

The Breit - Pauli Hamiltonian has been used as implemented in MOLPRO by Berning and Schweizer [67].

2.7 The Nuclear Schrödinger Equation

After obtaining the solution for the electronic Schrödinger equation the nuclear problem can be treated. The potential energy surface (PES, $E_{el}(\mathbf{R}_j)$, section 1.1.1) for the ground state and maybe for excited states will be used in the nuclear Schrödinger equation ((1.6), (2.39)).

$$\left[-\sum_{I=1}^{N_n}\frac{\hbar^2}{2m_I}\Delta_I + V_n\right]\Phi(\mathbf{R}_1,\ldots,\mathbf{R}_{N_n}) = E_{\nu,J}\Phi(\mathbf{R}_1,\ldots,\mathbf{R}_{N_n})$$
$$\text{with}\quad V_n = E_{el}(\mathbf{R}_1,\ldots,\mathbf{R}_{N_n}) \tag{2.39}$$

The first expression in the square brackets in (2.39) is the kinetic energy of the atomic cores. The second expression is the potential of the cores which contains the electronic contributions as well as the core-core interaction. The energy eigenvalues of this equation have three quantum numbers, the electronic state, the vibrational state (ν) and the rotational state (J). N_n is the number of nuclei (atoms).

Most of the calculations within this thesis are concerned with describing a diatomic molecule. If there are only two atoms the PES becomes a potential energy curve (PEC) that only depends on the distance between the atoms.

2.7.1 Potentials

In order to describe the PES or the PEC many analytical formulas have been applied, as well as interpolation and extrapolation. With these potentials the nuclear Schrödinger equation can be solved. This description is necessary because solving the electronic problem is costly and can only be done for a limited number of core positions. In order to find solutions for the nuclear problem on the other side many points are needed. So these formulas generate the missing information.

Since the main interest is in diatomic molecules only potentials for this case will be introduced.

The Lennard-Jones (m,n) Potential

The Lennard-Jones potential consists of two terms in different powers of the internuclear distance ((2.40), [68]). The small power (n) represents the attractive force at intermediate distances. The greater power (m) represents the strong repulsion at small distances. D_e gives the depth of the potential and r_{min} the distance at which the minimum of the potential appears. The most common is the (12,6) Lennard-Jones potential (n=6, m=12).

$$V_n(R) = D_e\left[\left(\frac{n}{m-n}\right)\left(\frac{r_{min}}{R}\right)^m - \left(\frac{m}{m-n}\right)\left(\frac{r_{min}}{R}\right)^n\right] \tag{2.40}$$

In figure 2.5 the Lennard-Jones and the Morse potential for the same D_e and r_{min} are compared.

The Morse Potential

The Morse potential was developed by Philip M. Morse [69]. In this case the potential is described by an exponential. Similar parameters as in the Lennard-Jones potential are used, but also an exponential factor of a.

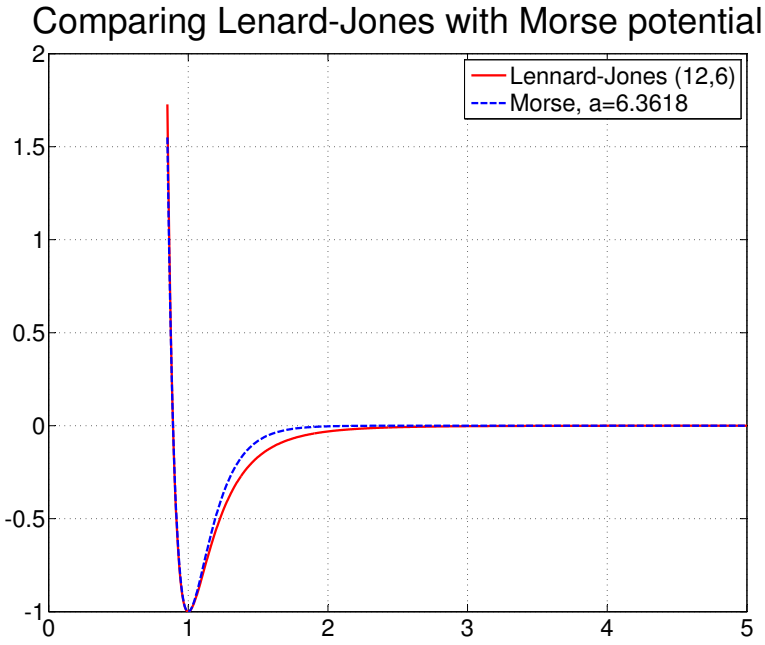

Figure 2.5: The Lennard-Jones and the Morse potential for a D_e of 1 unit and r_{min} of 1 unit.

$$V_n(R) = D_e \left[1 - e^{a\cdot(R-r_{min})}\right]^2 \tag{2.41}$$

There is an analytical formula for the vibrational levels of the Morse potential (2.42).

$$E_\nu = \omega_0 \left(\nu + \frac{1}{2}\right) - \omega_0 x_e \left(\nu + \frac{1}{2}\right)^2 + D_e \quad \text{mit} \quad \nu = 0, 1, \ldots, \max \tag{2.42}$$

$$\omega_0 = 2\pi a \sqrt{\frac{2D_e}{\mu}} \tag{2.43}$$

$$x_e = \frac{\omega_0}{4D_e} \tag{2.44}$$

$$\mu = \frac{m_1 m_2}{m_1 + m_2} \quad \text{reduced mass of a dimer} \tag{2.45}$$

m_1 and m_2 are the masses of the nuclei forming the diatomic molecule. They are used to calculate the reduced mass μ with (2.45). D_e, a, and r_{min} are the parameters of the potential which are used to evaluate equation (2.43). After calculating the parameter x_e with equation (2.44) the vibrational levels E_ν can be determined (2.42).

2.7.2 LEVEL-program

The LEVEL-program of Robert J. Le Roy [70] solves a quasi or effective one dimensional Schrödinger equation (2.46) numerically. This may be used to determine the vibrational and rotational levels of a diatomic molecule. For a diatomic molecule equation (2.39) can be reduced to equation (2.46).

$$\left[-\frac{\hbar^2}{2\mu}\frac{d^2}{dR^2} + V_J(R)\right]\Phi_{\nu,J}(R) = E_{\nu,J}\Phi_{\nu,J}(R) \tag{2.46}$$

The potential $V_J(R)$ depends on the rotational quantum number J because every rotational state has a different centrifugal force. Every vibrational state has a different average internuclear distance between the atoms. This changes the moment of inertia and by that the rotational states. This means that the rotational and vibrational states influence each other and cannot be treated separately.

In the LEVEL-program the potential is split up in a rotation independent part $V(R)$, caused by the electronic interaction and a centrifugal potential (2.47). Ω is the projection of the electronic angular momentum on the internuclear axis. In the program the charge modified reduced mass is used (2.48) with the total charge Q.

$$V_J(R) = V(R) + \frac{\hbar^2\left[J(J+1) - \Omega^2\right]}{2\mu R^2} \tag{2.47}$$

$$\mu = \frac{m_1 m_2}{m_1 + m_2 + m_e \cdot Q} \tag{2.48}$$

Numerov Algorithm/ Shooting Method

The shooting method can be used to solve a boundary value problem of an ordinary differential equation. Such a differential equation is for example the Schrödinger equation in one dimension (2.46). The boundary conditions of the Schrödinger equation are that the wave functions go to zero as infinity is approached. In the case of the radial Schrödinger equation one boundary is altered. The wave function needs to be zero at zero distance. The program itself has two parameters (R_{min}, R_{max}) which define the points where the wave function needs to be zero. These two points should be set to classically forbidden regions.

The differential equation is now solved by treating the problem as an initial value problem, one point is selected and the calculation starts there. The wave function for a certain energy eigenvalue is altered according to the given differential equation until the second point is reached. If the wave function has the demanded value at this point a solution has been found, otherwise the process is repeated with different values for the energy.

In this manner several states can be determined.

2.8 Symmetry

Symmetries are often used for describing molecules as well as solids. They can simplify the calculation and general rules can be deduced from general symmetry considerations.

There are 32 crystallographic point groups in three dimensions. Every point group has a number of symmetry operations under which the elements of this point group remain unchanged. In this thesis the Schönflies notation will be used to address the point groups.

In order to use and understand point groups character tables and product tables can be used (tables 2.1, 2.2). These tables can be found in various books and other resources (for example [25]). A heteronuclear diatomic molecule (different atoms) has the same symmetries as the point group $C_{\infty v}$ a homonuclear dimer belongs to the point group $D_{\infty h}$. Since these point groups are not implemented in MOLPRO and most quantum chemical software, instead, the point groups C_{2v} and D_{2h} will be used.

2.8.1 Character Table

Most of the times the point group C_{2v} will be used. So the properties of point groups will be discussed with this example. A character table is helpful in understanding a point group (table 2.1).

	E	$C_2(z)$	$\sigma_v(xz)$	$\sigma_v(yz)$	linear, rotations	quadratic
A_1	1	1	1	1	z	x^2, y^2, z^2
A_2	1	1	-1	-1	R_z	xy
B_1	1	-1	1	-1	x, R_y	xz
B_2	1	-1	-1	1	y, R_x	yz

Table 2.1: character table for C_{2v}

The headers of the first four columns contain the symmetry operations possible in this point group. The number of possible symmetry operations depends on the point group. C_1, the point group with the lowest symmetry, contains only one symmetry operation, the identity (doing nothing) E. D_{2h} on the other hand has 8 symmetry operations. There are the identity, rotations, inversion and reflections.

Rotations are defined by two details. The axis of the rotation is given in the brackets while the index gives the number of similar rotations to return exactly to the start configuration (rotation by 360°). An example is the rotation around the z-axis with 180° which is labelled as $C_2(z)$.

The reflections are also a group of symmetry operations. They are defined by a plane through the origin, for example xz means that the mirror plane is spanned by the x- and the z-axis. It is labelled by $\sigma(xz)$. As can be determined from table 2.1 C_{2v} has one rotational symmetry and two mirror planes.

Another symmetry operation is the inversion, a reflection in the origin with the label i.

The column "linear, rotations" can be used to determine to which irreducible representation certain axes and rotations belong to. As the p-orbitals in xyz-representation can be assigned to axes this gives also the irreducible representation of the p-orbitals. The p_x-orbital for example would belong to the irreducible group B_1 in C_{2v}.

The column "quadratic" can be used in a similar way to determine the irreducible representations of the d-orbitals. The orbitals belonging to x^2, y^2 and z^2 are linearly dependent and form only two independent orbitals.

2.8.2 Product Table

Irreducible representations are representations for a group of objects. It is called irreducible if it only contains the least necessary information. Other representations are called reducible. If you determine the irreducible representation of an object, for example a wave function or an orbital, you know its behaviour under the symmetry operations.

An example for the C_{2v} point group would be a p_x-orbital. It belongs to the irreducible representation B_1. That means the identity operation and the reflection on the xz-plane leave the orbital unchanged, while the sign changes during a rotation around the z-axis and a reflection about the yz-plane.

The behaviour of the product of two objects can be determined by a product table (table 2.2). The p_x-orbital belongs to B_1 the p_y-orbital belongs to B_2. Their product $p_x \cdot p_y$ belongs to A_2.

	A_1	A_2	B_1	B_2
A_1	A_1	A_2	B_1	B_2
A_2	A_2	A_1	B_2	B_1
B_1	B_1	B_2	A_1	A_2
B_2	B_2	B_1	A_2	A_1

Table 2.2: product table for C_{2v}

Symmetry can be helpful to reduce computational effort and allows to establish general rules (section 2.9.5).

These point groups are sufficient to describe molecules and localised objects. If you want to describe large objects, like solids, with a periodic unit the point groups are no longer sufficient. Then the 230 space groups can describe the possible symmetries.

2.9 Electronic States of Linear Molecules

This section will mainly serve to discuss the identification of electronic states of a linear molecule and transitions between these states. Sections 2.9.1 to 2.9.4 give an insight into electronic states of atoms and linear molecules. A good description of the electronic states of linear molecules as well as non-linear molecules and their relation to point groups can be found in the review of Sponer and Teller [71]. There are general rules for the transition between electronic states, so called selection rules. These rules define exactly which transitions are allowed and which are not. A more general approach is calculating the transition moments between the states which will be described in the sections 2.9.5, 2.9.6 and 2.9.7.

2.9.1 Single Electron States of Atoms

In section 1.1.3, it was already explained that eigenvalues of certain operators can be used to identify or classify states. The condition for the operators is that they commute with the Hamiltonian. If they commute their eigenvalues are so called good quantum numbers.

The state of a single electron bound to an atom can be identified by the principle quantum number n, the orbital angular momentum quantum number l, the magnetic quantum number m_l, and the spin quantum number m_s. The quantum numbers n and l are also used to address orbitals and their occupation in a multi electron atom. The term designation for a single electron can be seen in (2.50). In this case N would give the occupation of the orbital.

$$n\, l^N \tag{2.49}$$

The quantum number l is often labelled with lower case letters instead of ascending numbers, see table 2.3.

l	0	1	2	3	4	...
	s	p	d	f	g	... (alphabetically)

Table 2.3: lower case letters for the orbital angular momentum quantum number l

An example would be $1s^2 2p^1$. This means that the s orbital of the first shell is occupied by two electrons and the p orbital of the second shell is occupied by one electron. The complete expression for chromium in the ground state would be $1s^2 2s^2 2p^6 3s^2 3p^6 4s^1 3d^5$ (or: $[Ar]\, 4s^1 3d^5$) and for helium $1s^2$. These expressions are called the electronic configuration of an atom.

2.9.2 Multi Electron States of Atoms

A multi electron state of an atom is characterized by different quantum numbers. It depends on the coupling of the angular momentum and spins of the electrons which quantum numbers can be used. There are the LS-coupling and the jj-coupling. For the LS-coupling (Russel-Saunders coupling) the total orbital angular momentum L and the total spin S are good quantum numbers. These quantum numbers are determined by coupling the electrons in open shells, because in closed shells the angular moments of all electrons compensate each other. This type of coupling applies to light atoms. Heavy atoms show jj-coupling. In the case of jj-coupling the angular orbital momentum and the spin of each electron couple individually to an angular momentum j. L and S or the j's couple afterwards to the total angular momentum J.

The term designation in the LS-coupling is given by (2.50).

$$^{2S+1}L_J \tag{2.50}$$

For the total orbital angular momentum upper case letters are used (table 2.4).

L	0	1	2	3	4	...
	S	P	D	F	G	... (alphabetically)

Table 2.4: upper case letters for the total orbital angular momentum quantum number L

$2S + 1$ is the so called multiplicity of the state, see table 2.5. The multiplicity gives the number of degenerate states for this quantum number.

S	multiplicity	expression
0	1	singlet
$\frac{1}{2}$	2	doublet
1	3	triplet
$\frac{3}{2}$	4	quartet
2	5	quintet
$\frac{5}{2}$	6	sextet
3	7	septet
...	...	...

Table 2.5: total spin quantum number S, multiplicity and expression for the multiplicity

J represents the total angular momentum.

Preceding the LS-term, lower case letters may be used for counting the different states of one atom with the same quantum numbers. The even states are counted in alphabetical order starting with a, the odd states are counted in a reversed alphabetical order starting with z. Sometimes odd states are additionally marked.

The ground state of the chromium atom is addressed with $a\ ^7S_3$ and the expression for the helium atom is $^1S_0$.

2.9.3 Single Electron States of Linear Molecules

So far we always had a spherically symmetric potential (a single atom). Molecules consist of at least two atoms. Therefore spherical symmetry is destroyed and the orbital angular momentum quantum number is no longer a good quantum number. Linear molecules (as for example diatomic molecules) have cylindrical symmetry. The orbital angular momentum is no conserved quantity, but its projection on the symmetry-axis. For a diatomic molecule this would be the axis connecting the nuclei. The quantum number λ of the projected orbital angular momentum is labelled by lower case Greek letters, see table 2.6.

λ	0	1	2	3	...
	σ	π	δ	ϕ	...

Table 2.6: lower case Greek letters for the projected orbital angular momentum quantum number λ

The spin of the electron remains to be a good quantum number. The wave function can additionally be assigned to even or odd symmetry, if the molecule has a centre of inversion (as for example a homonuclear dimer). An even wave function is labelled with g (gerade) and an odd wave function is labelled with u (ungerade). Another differentiation is possible due to their contributions to bonding. A non-bonding orbital is marked with a star ($*$).

A single electron orbital of a linear molecule is labelled by (2.51). In front of the term a number might be used to count the orbitals with the same λ, starting with one for the energetically lowest orbital.

$$\text{numbering } \lambda_{(g/u)}^{(\ /*)} \tag{2.51}$$

These terms can be used to give the electronic configuration in a similar way as for an atom (section: 2.9.1).

For CrHe the expected electronic configuration would be
$(1\sigma)^2\,(2\sigma)^2\,(3\sigma)^2\,(1\pi)^4\,(4\sigma)^2\,(5\sigma)^2\,(2\pi)^4\,(6\sigma)^2\,(7\sigma)^1\,(8\sigma)^1\,(3\pi)^2\,(1\delta)^2$.

2.9.4 Multi Electron States of Linear Molecules

It is necessary to consider the coupling of the electrons if the molecule contains more than one electron. The spins of the electrons couple as explained in section 2.9.2 to a total spin of the molecule Σ which is labelled by multiplicity again. The projected orbital angular momentums can be added up to the total projected orbital angular moments Λ. Greek letters are used for different states, see table 2.7.

Λ	0	1	2	3	...
	Σ	Π	Δ	Φ	...

Table 2.7: upper case Greek letters for the total projected orbital angular momentum quantum number Λ

For molecules with a centre of inversion the state can again be identified as even or odd (g, u). Another classification is used for multi electron states of linear molecules. The behaviour during a reflection with respect to a plane orthogonal to the symmetry axis is indicated by a sign, either '-', if the sign changes during the reflection, or '+', if it stays the same.

The coupling becomes quite complicated, because the angular momentum of the molecules has to be included. The coupling can happen in different orders which are described by the Hund's coupling cases. Sometimes the total angular momentum of the electrons Ω is used. It can be determined by coupling Σ and Λ.

The term designation for multi electron states of linear molecules is given by (2.52).

$$^{2\Sigma+1}\Lambda_{(\Omega)}^{(+/-)} \tag{2.52}$$

The groundstate of CrHe can be addressed as $^7\Sigma_3^+$. Sometimes the states are additionally labelled to be able to refer to them. The ground state gets an upper case X. The rest of the states are labelled with upper case letters in alphabetical order starting with A for the lowest energy.

2.9.5 Transition Moments

A measurable quantity of spectroscopic lines are their absolute or relative intensities. The intensity is closely related to the transition moment. The transition moment is an observable and can be calculated as shown in section 1.1.2.

Different transitions are possible with decreasing probability: an electric dipole transition (2.53), a magnetic dipole transition (2.54), an electric quadrupole transition (2.55)), and transitions of higher order.

A detailed discussion of such transitions can be found on the pages 127 - 189 in [24].

$$\hat{\mathbf{d}} = -e\hat{\mathbf{r}} \quad \ldots \quad \text{electric dipole transition} \tag{2.53}$$

$$\hat{\boldsymbol{\mu}}_M = \frac{e}{2m_e} \cdot \left(\hat{\mathbf{l}} + 2\hat{\mathbf{s}}\right) \quad \ldots \quad \text{magnetic dipole transition} \tag{2.54}$$

$$\hat{Q}_{i,j} \propto \left(3\hat{r}_i\hat{r}_j - \delta_{ij}\hat{\mathbf{r}}^2\right) \quad \ldots \quad \text{electric quadrupole transition} \tag{2.55}$$

$\hat{r}$ is the position operator, $\hat{l}$ the angular momentum operator and $\hat{s}$ the spin operator. The indices i, j of the quadrupole transition tensor $\hat{Q}_{i,j}$ can take the values of the three spatial coordinates (x, y, z). The magnetic transition dipole moment can be different depending on the spin-orbit coupling.

For a transition these operators are evaluated between an initial state a and a final state b.

$$\left\langle a \left| \hat{O} \right| b \right\rangle = \int\int \Psi_a^* \left(\mathbf{r}_i, \mathbf{R}_j\right) \; \hat{O} \; \Psi_b \left(\mathbf{r}_i, \mathbf{R}_j\right) d\mathbf{r}_i d\mathbf{R}_j \tag{2.56}$$

The Born-Oppenheimer approximation can be applied again. The transition probability will then be determined by two quantities: the Franck-Condon integral and the transition moment. The Franck-Condon integral is independent from the transition operator $\hat{O}$. Since the transition operators only apply to the electronic wave functions the wave function for the nuclei can be evaluated independently. The important quantity is the overlap of the nuclear wave functions, the Franck-Condon integral (2.57). This value gives the probability for the same nuclear configuration in the initial and final state.

$$I_{FC} = \int \Phi_a^* \left(\mathbf{R}_j\right) \Phi_b \left(\mathbf{R}_j\right) d\mathbf{R}_j \tag{2.57}$$

The second quantity is the evaluation of the transition operator $\hat{O}$ for two electronic states (2.58).

$$\left\langle a \left| \hat{O} \right| b \right\rangle_{el} = \int \psi_a^* \left(\mathbf{r}_i\right) \; \hat{O} \; \psi_b \left(\mathbf{r}_i\right) d\mathbf{r}_i \tag{2.58}$$

Allowed transitions are indicated by non-vanishing values of the integral (2.58). If the function $\psi_a^* \; \hat{O} \; \psi_b$ is antisymmetric the integral becomes zero and there is no probability for this transition. General symmetry considerations sometimes are sufficient to determine if the function is antisymmetric or not. So called selection rules are determined in this manner.

Point groups are another way to judge the symmetry of $\psi_a^* \; \hat{O} \; \psi_b$. A wave function of a molecule with a certain point group can be assigned to a certain irreducible representation. The position operator as well as the angular momentum operator can also be associated with a certain irreducible representation. The symmetry of the function $\psi_a^* \; \hat{O} \; \psi_b$ can be determined quite simply by using product tables (for example table 2.2), if you have determined the irreducible representations of the operators and wave functions. The total product needs to be the completely symmetric representation (for example A_1 for C_{2v}), otherwise the integral becomes zero. The completely symmetric representation is the irreduzible representation which remains the same for all symmetry operations in the character table (section 2.8.1). This is a way to reduce the computational effort and formulate general rules.

2.9.6 Electric Dipole Transition

The most intense transition is the electric dipole transition. The intensity of different electric dipole transitions can be compared by their transition dipole moment (2.59).

$$\mathbf{DM}_{a\to b} = -e \int \psi_a^* (\mathbf{r}_i) \;\; \hat{\mathbf{r}} \;\; \psi_b (\mathbf{r}_i) \, d\mathbf{r}_i \tag{2.59}$$

2.9.7 Measurable Quantities

In experiments the Einstein coefficient A_{ab}, the oscillator strength f_{ab} or the line strength S_{ab} are determined. These quantities are proportional and can therefore be converted to each other. The line strength can be calculated with the transition dipole moment (2.60).

$$S_{ab} = S_{ba} = \sum_{i,j} \left| \mathbf{DM}_{a_i \to b_j} \right|^2 \tag{2.60}$$

The summation in (2.60) adds the contribution of degenerate states if the states a or b consist of several states with the same energy.

The oscillator strength for a single initial state a is given by equation (2.61) where $\omega_{ab} = \frac{E_{ab}}{\hbar}$ is the angular frequency given by the energy difference of the states. m_e is the mass of an electron and e is the elementary charge. g_a is a factor compensating the degeneracy of the state a. It can be calculated with $g_a = \sum_i (2J_i + 1)$

$$f_{ab} = \frac{4\pi m_e \omega_{ab}}{3h} \sum_j \left| \mathbf{DM}_{a\to b_j} \right|^2 = \frac{4\pi m_e \omega_{ab}}{3e^2 h} \frac{1}{g_a} S_{ab} \tag{2.61}$$

The Einstein coefficient for a transition from a to b is calculated as shown in (2.62).

$$A_{ab} = \frac{2e^2 \omega_{ab}^3}{3\epsilon_0 h c^3} \sum_j \left| \mathbf{DM}_{a\to b_j} \right|^2 = \frac{2\omega_{ab}^3}{3\epsilon_0 h c^3} \frac{1}{g_a} S_{ab} \tag{2.62}$$

Instead of ω_{ab} the wavelength of the transition λ_{ab} can be used.

$$f_{ab} = \frac{8\pi^2 m_e c}{3h\lambda_{ab}} \sum_j \left| \mathbf{DM}_{a\to b_j} \right|^2 = \frac{8\pi^2 m_e c}{3e^2 h \lambda_{ab}} \frac{1}{g_a} S_{ab} \tag{2.63}$$

$$A_{ab} = \frac{16\pi^3 e^2}{3\epsilon_0 h \lambda_{ab}^3} \sum_j \left| \mathbf{DM}_{a\to b_j} \right|^2 = \frac{16\pi^3}{3\epsilon_0 h \lambda_{ab}^3} \frac{1}{g_a} S_{ab} \tag{2.64}$$

These equations have been taken from [72, 1].

2.10 Ancilotto-Parameter

The Ancilotto-parameter was introduced by Francesco Ancilotto [73] to describe the behaviour of dopants interacting with superfluid He_N.

The Ancilotto-parameter λ_A is determined by the changes of the He_N introduced by the dopant. There are two changes. First, the dopant displaces the He atoms. An additional surface is generated which costs the energy σR^2. σ is the surface tension of superfluid He with a value of $\sigma = 0.179\ cm^{-1}\mathring{A}^2$ [74]. Second, the dopant pulls He atoms towards itself if there is a potential with a minimum ϵ_d. The gain in interaction energy can be estimated by $\epsilon_d \rho_{He} R^3$. ρ_{He} is the He-density of the unperturbed droplet. The value of $\rho_{He} = 0.022\ \frac{atoms}{\mathring{A}^3}$ has been taken from [75, 76]. These values are for a cluster of ^{4}He. The ratio of these contributions is the Ancilotto-parameter λ_A (2.65).

$$\lambda_A = \frac{\rho_{He} \epsilon_d r_{min}}{\sigma 2^{1/6}} \tag{2.65}$$

It is a dimensionless parameter with a threshold value. If λ_A is below the threshold (< 1.9) a location on the surface of the He_N is likely. A value above the threshold indicates (> 1.9) a position inside the He_N.

However, quantum mechanical influences like the zero point energy (ZPE) have to be considered, too. The de Boer quantum parameter λ_{Boer} gives an estimation of the quantum mechanical influences.

For its calculation the mass of the dopant m_d, the potential depth of the diatomic potential ϵ_d and the position r_{min} of the minimum of the diatomic potential are required (2.66).

$$\lambda_{Boer} = \frac{h^2}{m_d \epsilon_d r_{min}^2} \tag{2.66}$$

If the de Boer quantum parameter is significantly large (> 0.1) the quantum effects influence the position and a location on the surface may be stabilised.

The Ancilotto-parameter and the de Boer quantum parameter for different systems can be seen in section 6.1.

Part II

Results

Chapter 3

The CrHe - Cation

3.1 Introduction

In order to obtain a first impression of the difficulties and challenges which may arise in describing the CrHe - system, the ionized system was studied first. The CrHe-cation was already investigated experimentally [77] and theoretically [78, 79]. Calculations of the cation can be expected to be less sensitive to different basis sets and computational methods than the neutral CrHe diatomic molecule. Since one of the partners needs to be ionized, a much stronger interaction is to be expected, compared to the neutral system, where we have only a weak van der Waal interaction. The interaction in the ionized system can more or less be described as an interaction between ionized chromium and a neutral helium. This statement can be justified if one compares the ionization energies of chromium and helium. Cr has an ionization energy of 54 575.6 cm^{-1}, which is small compared to the ionization energy of He of 198 310.7 cm^{-1}. Both values have been obtained from the National Institute of Standards and Technology (NIST) - Database [1].

The experimental results for the CrHe - Cation of [77] give a potential depth of $0.98 \pm 0.1 \left[\frac{kcal}{mol}\right] \approx 4.1 \pm 0.4 \left[\frac{kJ}{mol}\right]$ and a bond length of 2.25 $\mathring{A}$.

Due to the large values the results are displayed in $\left[\frac{kJ}{mol}\right]$ which converts to Kelvin with $1 \left[\frac{kJ}{mol}\right] = 120\ K$

3.2 Basis Sets

Choosing a suitable basis set is essential to describe the CrHe-cation sufficiently accurate. Appropriate basis sets for the ionized system are described in the papers of Wilson [78, 79].

For the single ionized CrHe - Cation a potential depth of 5.7 $\left[\frac{kJ}{mol}\right]$ and a bond length of 2.36 $\mathring{A}$ can be found in [78].

Some attempts were made to reproduce the described basis sets and of course the results.

As a starting point Wilson used the Wachters+f [80, 81] basis set, as was done here. The d-functions were afterwards replaced with the functions of Rappe [82]. Afterwards these basis sets were extended with even tempered wave functions (by two d- and two p - functions). This basis set was used in subsequent calculations and will be addressed as “complete”.

Another approach is to add bond functions as described in the paper by Tong [44] who used the functions of Tao[43].

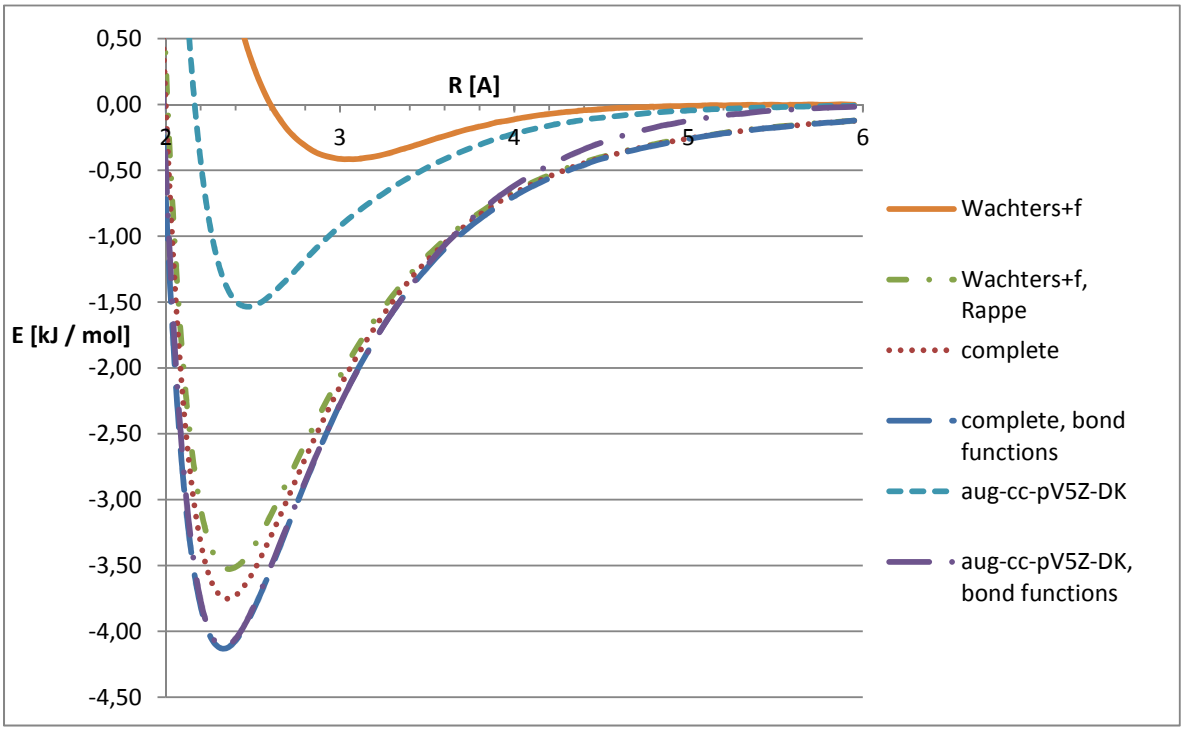

Figure 3.1: The CrHe cation - potential is calculated with CCSD(T) for different basis sets. Bond functions lead to a significant improvement.

Besides the above mentioned approaches figure 3.1 also shows the aug-cc-pV5Z-DK Basis set of Balabanov [83]. Helium was always described by the aug-cc-pV5Z of Woon and Dunning [84].

All calculations were done by the 2006 version of MOLPRO. First a ROHF calculation was performed and afterwards an UCCSD(T) calculation. All potentials are displayed with counterpoise correction (CP).

3.3 Methods

Apart from testing basis sets, different quantum chemical methods were tested on the CrHe cation.

The coupled cluster methods show the best performance for the ground state of the cation as can be seen in figure 3.2. There is a slight difference if triple corrections are included or not (the methods with triple corrections are labelled with a (T)). For this single reference method the Hartree-Fock orbitals seem to be sufficient. A preceding MCSCF calculation does not improve the result considerably. However, the CI method improves significantly when combined with pre-optimized MCSCF determinants. The Rayleigh - Schrödinger many body perturbation method also fails to provide meaningful results, but could probably be improved by adding orbitals to the active space. All calculations were performed with the same basis set, the " complete " basis set with bond functions and the aug-cc-pV5Z basis set for helium.

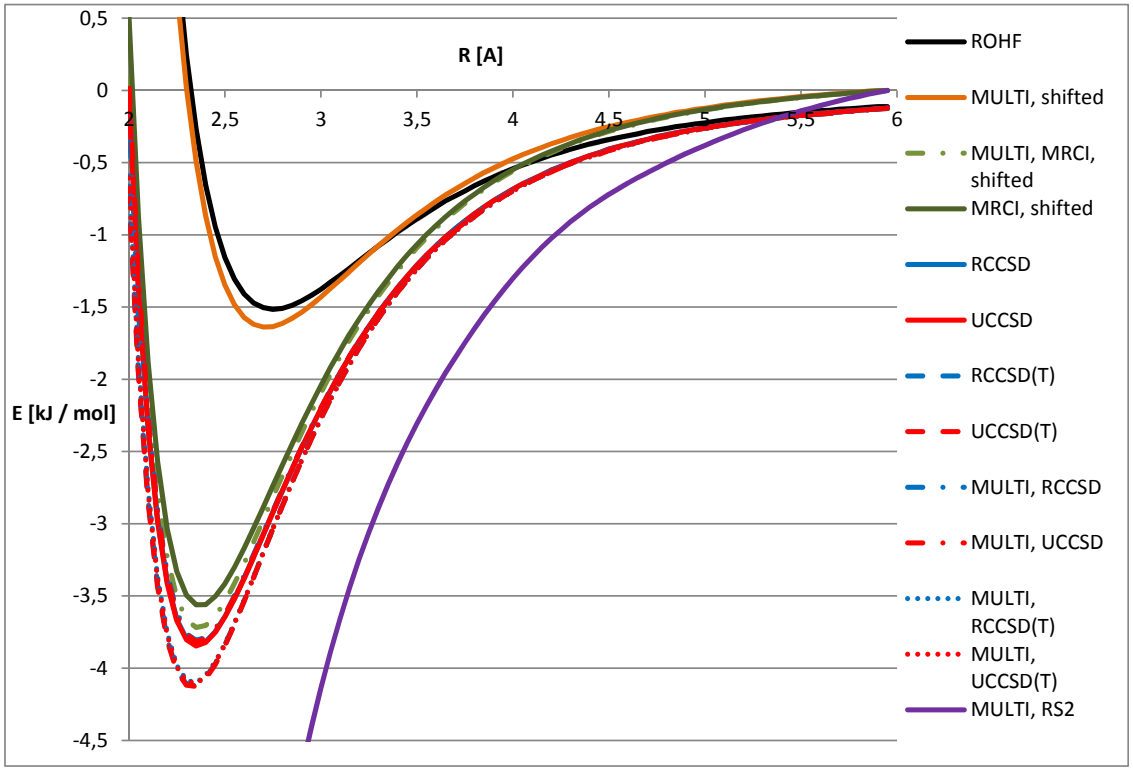

Figure 3.2: In this figure the CrHe cation - potential is calculated with different methods but the same basis set.

A single reference coupled cluster method seems to be the best approach for describing the ground state.

Relativistic corrections are not negligible as shown in figure 3.3. The Douglas-Kroll (DK) correction was used for these calculations.

3.4 Rovibrational Analysis comparing with Wilson

Three approaches were used for the most promising potential curve (complete basis set, RCCSD(T), DK) to determine the rovibronic levels.

First, the vibrational levels were calculated using a MATLAB - program written by Andreas Hauser. This program uses the calculated points and discretises the problem. Then the eigenenergies and eigenfunctions are calculated.

Second, a Morse potential was fitted to the calculated points and the vibrational levels were calculated using the analytical formula, see section 2.7.1. The fitting function gives the parameters in table 3.1.

$D_e[cm^{-1}]$	$r_{min}[A^{circ}]$	a [d.u.]
356.5618	2.3151	1.7860

Table 3.1: Morse parameter for the CrHe cation

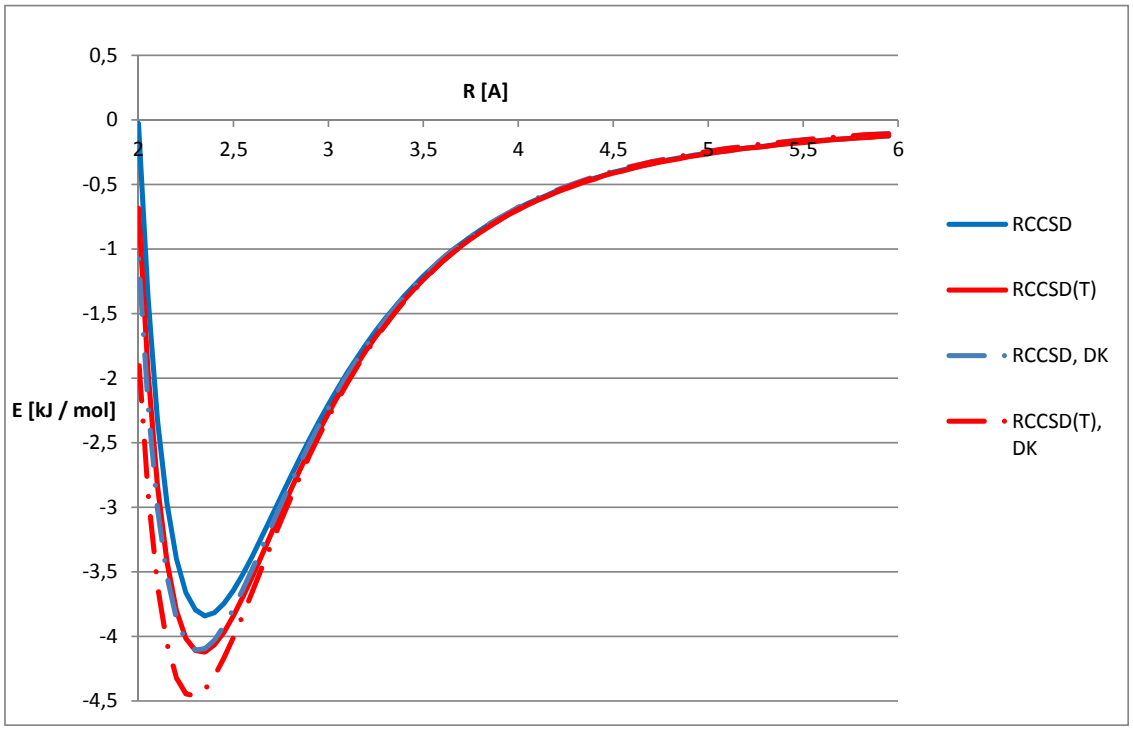

Figure 3.3: In this figure the CrHe cation - potential is calculated by two different methods. The change if you add relativistic corrections is shown (DK).

Third, the LEVEL program of Robert J. Le Roy was applied, see section 2.7.1. In order to obtain reliable results for the rovibronic levels with the LEVEL-program two steps proved to be necessary. First, an analytic potential is fitted to the calculated points of the potential. Second, the parameters of the function are passed on to the LEVEL program. The program uses a Lennard-Jones potential with parameters which can be seen in table 3.2.

m [d. u.]	n [d. u.]	$D_e[cm^{-1}]$	$r_{min}[A^{circ}]$
8	5	381.0908	2.2829

Table 3.2: Lennard-Jones parameter for the CrHe cation

The potential of the CrHe cation shows several vibrational and rotational levels. These levels are displayed in table 3.3 and in table 3.4.

Table 3.3 contains the vibrational levels for all above mentioned approaches. ν is the vibrational quantum number which might take values from 0 to 4. The typical level distances of vibrational states can be observed. A harmonic potential would give equidistant levels, but due to anharmonicity of the potentials the level difference of the vibrational states is reduced with increasing quantum number. (This behaviour is obvious from the formula for the vibrational levels of the Morse-potential, (2.42).)

ν	MATLAB $[cm^{-1}]$	MORSE $[cm^{-1}]$	LEVEL 8 $[cm^{-1}]$
0	-282.25	-299.52	-294.73
1	-162.35	-177.93	-169.67
2	-81.50	-90.25	-87.14
3	-31.70	-36.47	-37.69
4	-3.76	-16.59	-12.12

Table 3.3: This table shows the vibrational levels of the cation determined with different approaches. The rotational quantum number J is zero for all values in this table.

ν	0	1	2	3	4
J					
0	-294.73	-169.67	-87.14	-37.69	-12.12
1	-293.18	-168.40	-86.14	-36.95	-11.63
2	-290.07	-165.86	-84.14	-35.47	-10.66
3	-285.41	-162.07	-81.16	-33.26	-9.23
4	-297.21	-157.02	-77.194	-30.35	-7.37
5	-271.48	-150.73	-72.27	-26.77	-5.12
6	-262.22	-143.22	-66.41	-22.54	-2.58
7	-251.46	-134.50	-59.64	-17.72	
8	-239.20	-124.59	-52.00	-12.37	
9	-225.46	-113.52	-43.52	-6.58	
10	-210.28	-101.32	-34.27	-0.49	
11	-193.66	-88.045	-24.32		
12	-175.66	-73.72	-13.76		
13	-156.29	-58.41	-2.72		
14	-135.61	-42.20			
15	-113.67	-25.17			
16	-90.52	-7.45			
17	-66.24				
18	-40.92				
19	-14.66				

Table 3.4: This table displays the rovibrational levels for the CrHe-cation calculated with the LEVEL-program. J is the rotational, ν the vibrational quantum number.

Table 3.4 contains the rovibronic levels calculated with the LEVEL-program. J is the rotational quantum number. The typical behaviour of rotational levels can be seen in the table, the more or less quadratic behaviour of the levels of rotational states.

Wilson [78] obtained a harmonic vibrational frequency of $\omega_e = 138\ cm^{-1}$. This would coincide in a first approximation with the level difference of the first and second level. With the applied approaches differences of 119.90 cm^{-1}, 121.25 cm^{-1} and 125.06 cm^{-1} were determined. The frequency for the linear contribution in equation (2.42), the harmonic part of the Morse levels, would be $\omega_0 = 155.49\ cm^{-1}$. This is even larger than the value obtained by Wilson.

Chapter 4

The Cr Atom

4.1 Introduction

Chromium (Cr) has interesting magnetic properties. It has a septet ground state and therefore one of the highest magnetic moments of single atoms. If one goes from single Cr atoms to the Cr bulk the magnetic properties depend on size. The bulk as well as particles above a certain size show antiferromagnetic behaviour, while nanoparticles have been shown to have superparamagnetic properties [15]. An investigation of chromium by means of electron spin resonance (ESR) seems quite intriguing because the spin states can be addressed individually in such an investigation. The analysis of magnetic properties of small clusters seems also very interesting.

Currently the optical properties of Cr doped He_N are under investigation by our group. A theoretical description should be helpful in their understanding.

The ground state of chromium has been determined to be a septet state, for example by spectroscopic analysis (NIST, [1]). This is also the result of my calculations (the septet state has the lowest energies and leads to converging results).

Since transitions between different multiplicities are still unlikely, the investigation was mostly focused on the septet multiplicity. While the levels of quintet multiplicity lie in different energy ranges, the levels of triplet multiplicity are in the same range as septet-excitations, as can be seen in table 8.1 in the appendix.

The Cr atom was investigated mainly for two reasons. The first reason was gaining a better insight into the system, its challenges, and the approaches, for example to determine which basis sets give good results. The second reason was to obtain the results of the unperturbed system (The results should be the same as for CrHe at large distances.) which can be compared to experimental results (NIST, [1], table 8.1 in the appendix).

4.2 First Excitation

First the excitation $a\ ^7S \rightarrow z\ ^7P$ was investigated. During this transition one electron changes its orbital from the 4s-orbital to the 4p-orbital. The states have the electronic configurations $[Ar]\,4s^1 3d^5$ for $a\ ^7S$ state, and $[Ar]\,3d^5 4p^1$ for $z\ ^7P$ state (see section 2.9.1).

This transition was investigated using the MRCI - method, see section 2.4.2. The wave function was first calculated using ROHF, then MCSCF was applied for an active space consisting of 10 orbitals filled with 6 electrons. Then the MRCI calculation was performed with the same active space. This gives approximately $15 \cdot 10^3 - 30 \cdot 10^3$ configuration state

functions (CSFs). A more detailed dicussion of the active spaces can be found in section 4.3.1. The complete number of electrons used in the calculations changed because partly effective core potentials (ECP) have been used.

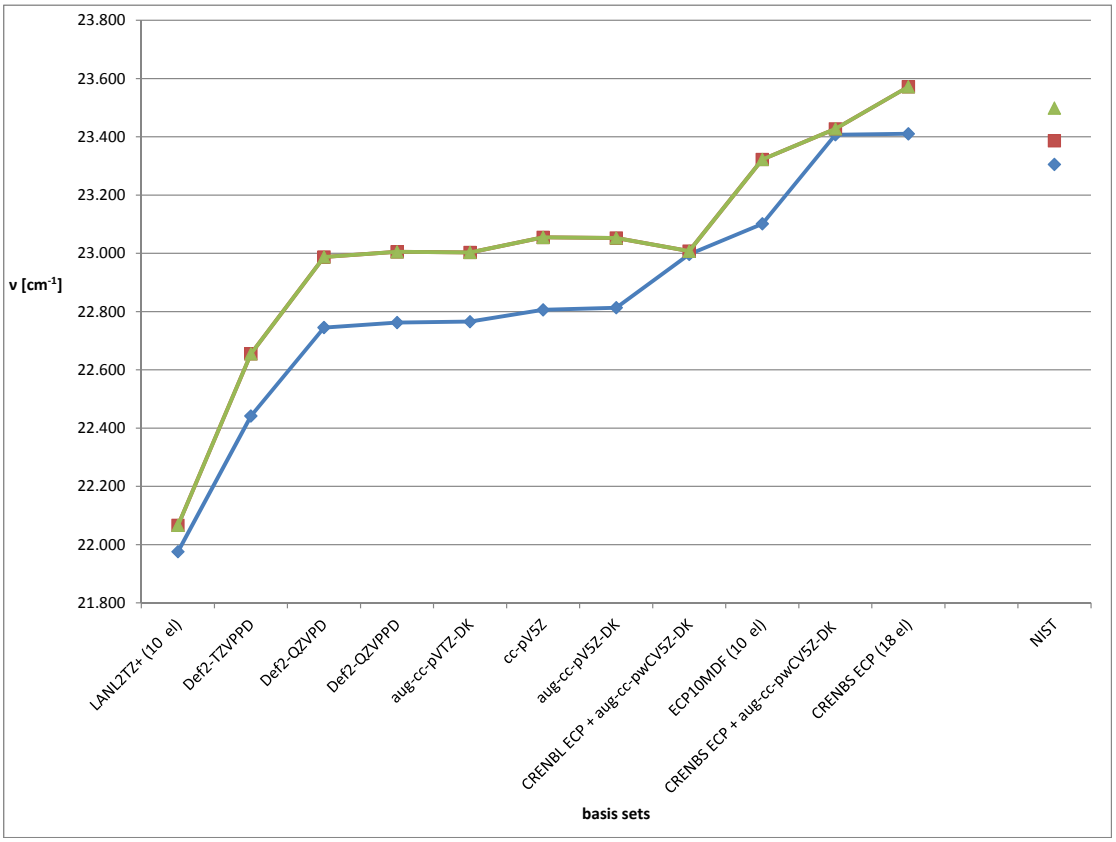

Figure 4.1: The first excitation of chromium $a\ ^7S \rightarrow z\ ^7P$ is displayed. It was calculated with different basis sets. The calculated results are split because of different treatment of the symmetries, while the NIST - values are split due to spin-orbit coupling.

The different basis sets used in figure 4.1 were obtained from the EMSL Basis Set Exchange database [3, 4]. In general increasing the number of functions gives better results (for example a QZ basis set gives a better result than a TZ basis set). ECP prooved to be a successful approach. Three ECP (CRENBL ECP, ECP10MDF, LANL2TZ+), which included 10 electrons in the potential, and one ECP (CRENBS ECP), which included 18 electrons in the potential, were applied. The best result was obtained with the CRENBS ECP and the aug-cc-pwCV5Z-DK basis set. The level splitting in the calculation occurs due to different treatment of different symmetries and should actually be degenerate. The experimental values (NIST) are split because of spin-orbit coupling.

4.3 The Septet-Multiplicity for Excitations in the Experiment

Mainly the excitations $a\ ^7S \rightarrow z\ ^7P$ and $a\ ^7S \rightarrow y\ ^7P$ are currently investigated experimentally by our group. So the main concern was the description of these excitations. To consider all possible septet states in this energy region, mainly two configurations are required for the excited states: The excitation from an s-orbital to a p-orbital into the configuration $[Ar]\,3d^5 4p^1$

($z\ ^7P$) and the excitation from a d-orbital to a p-orbital into the configuration $[Ar]\,4s^1 3d^4 4p^1$ ($y\ ^7P$).

The first configuration only describes the state $z\ ^7P$, whereas the second configuration describes the three states $z\ ^7F$, $z\ ^7D$, $y\ ^7P$ in this multiplicity.

The calculations in MOLPRO were restricted to the point group C_{2v} in order to be able to address and identify orbitals. C_{2v} has four irreducible representations which are A_1, the completely symmetric representation, A_2, B_1, and B_2. In MOLPRO they appear in following order: (A_1 / B_1 / B_2 / A_2), which will be used from now on. The ground state is totally symmetric, belongs to the completely symmetric representation A_1. If you want to calculate all states up to $y\ ^7P$ you need to calculate the following number of states (6/ 5/ 5/ 3), in the respective irreducible representations. This means 6 states are calculated in the A_1 symmetry, 5 in the B_1 and in the B_2 symmetries, and 3 states in the A_2 symmetry.

In this symmetry the s-orbital has the irreducible representation A_1 which is addressed in MOLPRO by (1/ 0/ 0/ 0). The three p-orbitals belong to the irreducible representations A_1, B_1, and B_2, addressed as (1/ 1/ 1/ 0). The five d-orbitals can appear in all irreducible representations (2 / 1 / 1 / 1), as well as the seven f-orbitals (2/ 2/ 2/ 1).

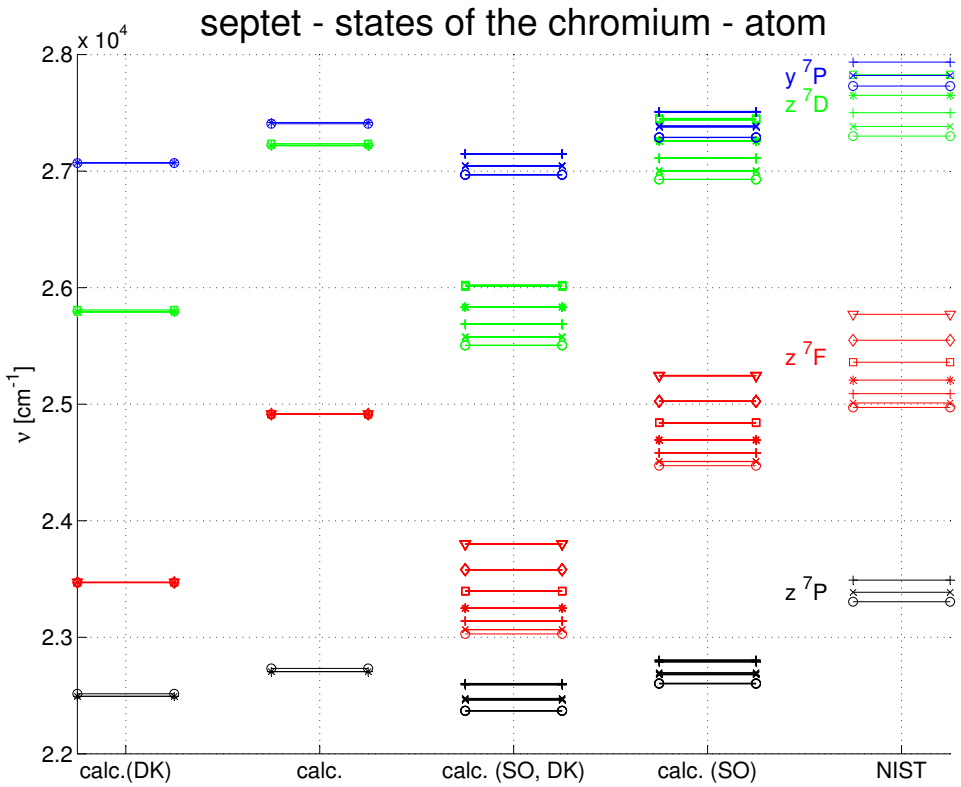

Figure 4.2: Excited states of the chromium atom with different approaches compared to the experimental values (NIST). Calculations were performed either with or without spin-orbit coupling (SO) or Douglas-Kroll correction (DK).

The first step was a Hartree-Fock calculation, to be exact a ROHF calculation. This calculation has been performed with and without scalar relativistic corrections by the Douglas-Kroll formalism at Hartree Fock level. As is shown in figure 4.2 the Douglas-Kroll correction does not improve the result in terms of level difference.

For the successive state averaged CASSCF - calculation it was necessary to define the active space. Nine orbitals were defined as "closed", that means that they are optimized during the calculations but always kept completely filled (2 electrons per orbital). These orbitals consist of 3 s orbitals and $2 \cdot 3$ p orbitals which are defined in MOLPRO in the C_{2v} point group as (5 / 2 / 2 / 0). The other orbitals need to be singly occupied in order to obtain septet multiplicity (six spins aligned). These electrons were freely distributed in $4s$, $3d$ and $4p$. The available orbitals were defined by (4 / 2 / 2 / 1). Therefore the active space of the CASSCF calculation consisted of 6 electrons in 9 orbitals. The results of the MCSCF are not very accurate. The energy differences are far off and not even the order of the states is reproduced for some active spaces.

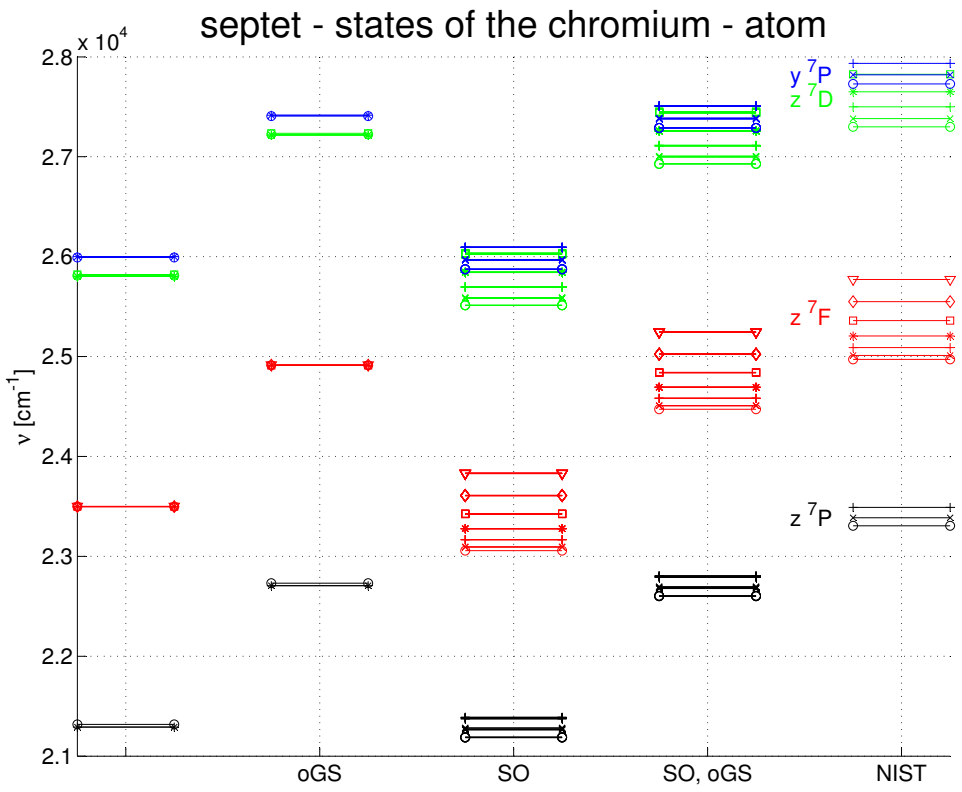

Figure 4.3: Excited states of the chromium atom with different approaches compared to the experimental values (NIST). Calculations were performed either with or without spin-orbit coupling (SO). Additionally the results for a separately optimized ground state were included (oGS) contrary to a state-averaged optimization.

Next the MRCISD - method was applied for each symmetry separately. Additionally the active space was increased. Two sets of d - orbitals were added, as they are significant for

transition metals, and one s - orbital. That gives a total of twenty active orbitals in the irreducible representations (9 / 4 / 4 / 3).

This active space was chosen after a study of several possibilities which can be seen in section 4.3.1.

As scalar relativistic corrections were not very encouraging, another promising approach was used, so called Breit - Pauli operator. The spin - orbit coupling can be described using the so called Breit - Pauli operator, see section 2.6.2. The NIST table (table 8.1) shows level splitting's of about a few hundred wavenumbers, which can be reproduced with this approach. The level splitting of the atomic lines is determined quite accurately by these calculations, see figures 4.2 and 4.3.

In figure 4.2 another correction was applied in order to improve the results. The state-averaged MCSCF calculations lead to a more inaccurate description of the ground state. So the ground state was optimized in an additional calculation that improved the result for the level energies as can be seen in figure 4.3.

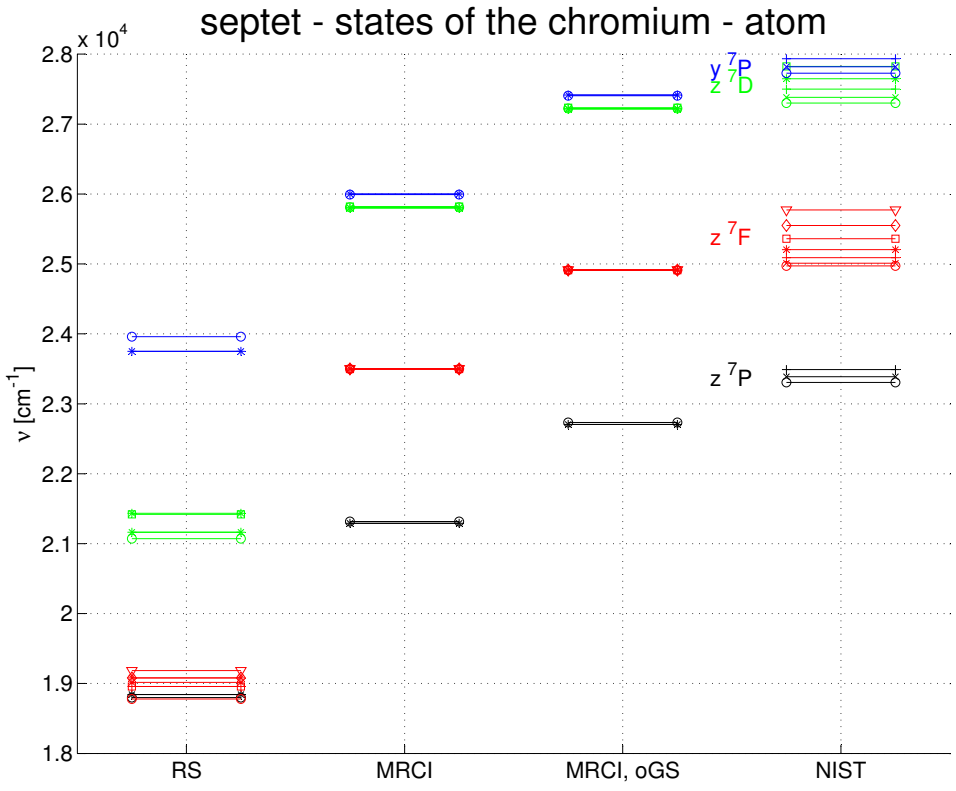

Figure 4.4: The excited states of Cr calculated with a perturbative method (RS) are compared to the MRCI results as well as NIST-values.

Calculating the excited states with Rayleigh-Schrödinger perturbation theory seemed not very promising (figure 4.4).

4.3.1 Study of different Active Spaces

Several possible active spaces were investigated and are compared in figure 4.5 and table 4.1. The definition of the spaces in the table is based on the definition in MOLPRO where you define the total number of orbitals and which of them are closed.

For an active space of (9 / 4 / 4 / 3) and a closed space of (5 / 2 / 2 / 0) the total number of orbitals is (14 / 6 / 6 / 3). The calculations consist of a ROHF calculation, a MCSCF calculation and a MRCI calculation. Neither the Dougals-Kroll correction, nor the Breit-Pauli operator were applied.

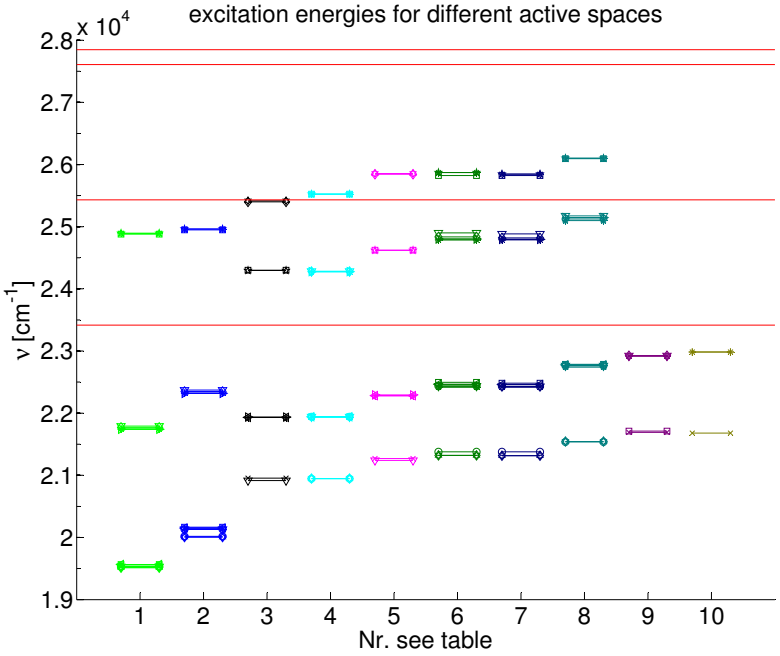

Figure 4.5: Excited states of the chromium atom calculated with different active spaces. For active spaces refer to table 4.1. The NIST-values are shown as thin lines spreading over the complete figure.

If you take a look at the results you see that the results improve in general if you add orbitals to the active space as long as you leave the core unchanged. The first two calculations in figure 4.5 give results which deviate stronger from the NIST-values, although they have a smaller core and by that a very large active space. A smaller core means that orbitals are added to the active space, but more importantly, also electrons. The configuration state functions (CSFs) are the functions used in a MRCI calculation and the number of CSFs also is an estimation of the computational demands of the calculation. The last two columns in table 4.1 show the contracted and uncontracted CSFs. Some methods are able to use the contracted functions, other calculations need uncontracted ones. The difference between the contracted and uncontracted CSFs lies in the treatment of the orbitals. For the contracted orbitals several functions are combined and used as one. In the uncontracted treatment all orbitals are treated independently. If you take a look at table 4.1 you can see that the first two calculations have a lot more CSFs and also need significantly more computational effort

Nr.	MCSCF (core)	MCSCF (total)	MRCI (core)	MRCI (total)	con. CSFs	uncon. CSFs
1	4 / 1 / 1 / 0	9 / 4 / 4 / 1	5 / 2 / 2 / 0	11 / 5 / 5 / 2	16912175	200232763
2	5 / 2 / 2 / 0	9 / 4 / 4 / 1	4 / 1 / 1 / 0	11 / 5 / 5 / 2	16910729	200232763
3	5 / 2 / 2 / 0	11 / 5 / 5 / 1	5 / 2 / 2 / 0	14 / 6 / 6 / 3	1460907	6146320
4	5 / 2 / 2 / 0	9 / 4 / 4 / 1	5 / 2 / 2 / 0	12 / 5 / 5 / 2	654571	1874919
5	5 / 2 / 2 / 0	9 / 4 / 4 / 1	5 / 2 / 2 / 0	14 / 6 / 6 / 3	1334251	6146320
6	5 / 2 / 2 / 0	11 / 5 / 5 / 2	5 / 2 / 2 / 0	11 / 5 / 5 / 2	732508	1395051
7	5 / 2 / 2 / 0	11 / 5 / 5 / 2	5 / 2 / 2 / 0	12 / 6 / 6 / 2	1004810	3167892
8	5 / 2 / 2 / 0	12 / 5 / 5 / 2	5 / 2 / 2 / 0	14 / 6 / 6 / 3	1503167	6153557
9	5 / 2 / 2 / 0	13 / 6 / 6 / 2	5 / 2 / 2 / 0	13 / 6 / 6 / 2	979784	4005752
10	5 / 2 / 2 / 0	15 / 6 / 6 / 3	5 / 2 / 2 / 0	15 / 6 / 6 / 3	1480352	7465644

Table 4.1: The active spaces for the results in figure 4.5 are displayed. The format for the C_{2v} in MOLPRO is used. The core and the total orbitals for the MCSCF and the succeeding MRCI calculation are shown. The last two columns give the number of the contracted and uncontracted CSFs.

but give less meaningful results. By comparing calculation number (Nr.) 3 and Nr. 5 you can see that increasing the active space for the MCSCF calculation does not always improve the result. For the calculations in the previous section the active space Nr. 5 was applied, which gives good results and is not too costly.

Another interesting aspect that can be deduced from figure 4.5 and table 4.1 is that the active space should be selected in a meaningful manner, considering the symmetry of orbitals. The calculation labelled Nr. 3 gives results with strong deviations compared to the calculations Nr. 5, Nr. 6 and Nr. 7. The latter three, however, have a smaller active space and therefore less CSFs. This can be explained by the symmetry of the active space. While Nr 3. uses additional s- and p-orbitals, Nr. 6 and 7 use additional d-orbitals. D-orbitals, however, are especially important for transition metals.

4.4 Dipole Moment and Transition Probability

Since Cr is a light atom LS-coupling dominates and its selection rules need to be fulfilled. The selection rules for LS-coupling prohibit a change of multiplicity, that is a spin flip, in an electric dipole transition. Therefore an investigation of the septet-manifold should be sufficient to describe the transitions starting from the groundstate ($a\ ^7S$).

Additional restrictions can be deduced using the symmetry as described in section 2.9.5. All following considerations are referring to the point group C_{2v}. The total electronic wave functions can be assigned to a certain irreducible representation, the ground state for example is of A_1-symmetry. The transition operator also belongs to an irreducible representation as described in section 2.8.1.

The triple product, ground state times electric dipole moment times excited state, has to belong to the completely symmetric representation A_1 for an allowed transition (section: 2.9.5). This restriction allows to determine the symmetry of an excited state, if the symmetry of the ground state and the transition operator are known.

The ground state can be assigned to the irreducible representation A_1. The $\hat{d}_z$, the part of the dipole moment operator in the z-direction, belongs also to A_1. By applying the product table (section 2.8.2) it can be determined that only excited states with the A_1-symmetry can be reached. The $\hat{d}_x$ operator is associated with the irreducible representation B_1. The according excited states also need to be of the B_1-symmetry to obtain a non-zero transition probability. The operator $\hat{d}_y$ can be represented by the irreducible representation B_2. Its excited states also have the irreducible representation B_2. A state in the symmetry A_2 can not be reached from the ground state with a dipole transition. These rules are observed in the tables 4.2, 4.3, 5.5 and 5.6. The symmetry is addressed as in MOLPRO by numbering (1: A_1, 2: B_1, 3: B_2, 4: A_2).

Table 4.2 contains the transition dipole moments for a MCSCF calculation. The energies and the ordering of the states are not reproduced correctly and so an identification with a certain state is rather difficult.

The first column (sym.) tells the symmetry of the state according to MOLPRO symmetry numbering. The second column (st.) contains a numbering of the states in each symmetry. The direction of the nonzero dipole operator can be found in the third column ($\hat{d}$). The next column (E_1) contains the energy difference to the ground state. The transition dipole moment ($\hat{d}_1$) can be found in the fifth column. It is displayed in the atomic units $a_0 \cdot e$ (Bohr times elementary charge). An empty field in the column for the dipole moments means a negligible transition probability. The sixth column gives the square of the transition dipole moment in the atomic units $a_0^2 \cdot e^2$. These 3 columns are repeated with the results from a second calculation. The calculations are indicated by an index (first and second calculation).

The first calculation was performed using the aug-cc-pwCVTZ-DK basis set and (9 / 4 / 4 / 1) total and (5 / 2 / 2 / 0) closed orbitals in the MCSCF calculation. The MRCI calculation used (11 / 5 / 5 / 1) total and (5 / 2 / 2 / 0) closed orbitals. The second calculation applied the aug-cc-pVTZ-DK basis set. For MCSCF and MRCI the same active space consisting of (11 / 5 / 5 / 2) total and (5 / 2 / 2 / 0) closed orbitals was used.

Table 4.3 contains the transition dipole moment for the excited states of Cr. An association with certain states is possible and was included in the table. Apart from this additional column “terms” it is the same as the previous table.

sym.	st.	$\hat{d}$	E_1 $[cm^{-1}]$	$\hat{d}_1$ $[a.u.]$	$\left\|\hat{d}_1\right\|^2$ $[a.u.]$	E_2 $[cm^{-1}]$	$\hat{d}_2$ $[a.u.]$	$\left\|\hat{d}_2\right\|^2$ $[a.u.]$
2	1	x	5732.67			11623.25	3.49E-02	1.22E-03
2	2	x	5732.67			11720.04	-6.93E-02	4.80E-03
2	3	x	6326.62	-3.26E-01	1.06E-01	12107.34	-1.53E-01	2.33E-02
2	4	x	7983.89			14129.60	-9.13E-02	8.33E-03
2	5	x	19102.53	2.08E+00	4.33E+00	20486.40	2.34E+00	5.46E+00
3	1	y	5732.67			11623.25	3.49E-02	1.22E-03
3	2	y	5732.67			11720.04	6.93E-02	4.80E-03
3	3	y	6326.62	3.26E-01	1.06E-01	12107.34	1.53E-01	2.33E-02
3	4	y	7983.89			14129.60	9.13E-02	8.33E-03
3	5	y	19102.53	2.08E+00	4.33E+00	20486.40	-2.34E+00	5.46E+00
1	2	z	5732.67			11657.51	-3.27E-02	1.07E-03
1	3	z	5732.67			11678.62	2.55E-08	6.49E-16
1	4	z	6326.62	-3.26E-01	1.06E-01	12357.64	1.74E-01	3.01E-02
1	6	z	19102.53	-2.08E+00	4.33E+00	20448.36	-2.26E+00	5.12E+00

Table 4.2: The excited states and transition properties for Cr from a MCSCF calculation are shown. Symmetry (sym.) gives the irreducible representation of the state. The column states (st.) contains a numbering of the states in their respective symmetries. The third column shows the direction of the dipole operator which gives a non-zero contribution to the transition dipole moment. E_1 are the energy differences of the states in the first calculation, E_2 in the second calculation. $\hat{d}_1$ and $\hat{d}_2$ are the dipole moments in atomic units $(a_0 \cdot e)$ for the first and second calculation, respectively. Their squares can also be found in the table in atomic units $(a_0^2 \cdot e^2)$

In the second calculation the 5^{th} state in the first symmetry and the 4^{th} state in the second and third symmetry had the higher dipole moment. These states were shifted to the last position (6^{th} and 5^{th}) because they certainly are the y^7P states.

The dipole moments can now be compared with experimental values from the NIST-database, see table 4.4. The main features are reproduced quite well, although there is a difference in the absolute values. Since only one ground state and one excited state are considered in the MRCI calculation, the degeneracy of the states is neglected. The last two columns in table 4.4 deal with this deficiency. The line strength S is first divided by the degeneracy of the excited state g_k, then by the degeneracy of the ground state g_i. The units of S and $\left|\hat{d}\right|^2$ are the same. After removing the degeneracy their values should be comparable. Quite good agreement can be found if you compare the line strength with one removed degeneracy and the dipole moments. The order of the intensities is clearly reproduced by the calculation, but not the absolute values.

terms	sym.	st.	$\hat{d}$	E_1 $[cm^{-1}]$	$\hat{d}_1$ $[a.u.]$	$\left\|\hat{d}_1\right\|^2$ $[a.u.]$	E_2 $[cm^{-1}]$	$\hat{d}_2$ $[a.u.]$	$\left\|\hat{d}_2\right\|^2$ $[a.u.]$
$z\ ^7P$	1	2	z	21123.51	-1.15E+00	1.32E+00	21448.64	-1.27E+00	1.61E+00
	2	1	x	21112.33	1.15E+00	1.32E+00	21380.18	1.26E+00	1.60E+00
	3	1	y	21112.33	-1.15E+00	1.32E+00	21380.18	-1.26E+00	1.60E+00
$z\ ^7F$	1	3	z	23348.29	-1.29E-05	1.67E-10	24032.15	1.37E-02	1.87E-04
	1	4	z	23349.25	4.45E-03	1.98E-05	24035.08	-6.16E-08	3.79E-15
	2	2	x	23346.68	8.14E-03	6.62E-05	24045.97	2.10E-02	4.43E-04
	2	3	x	23349.77	6.68E-03	4.47E-05	24074.12	-6.05E-03	3.65E-05
	3	2	y	23346.68	8.14E-03	6.62E-05	24045.97	-2.10E-02	4.43E-04
	3	3	y	23349.77	-6.68E-03	4.47E-05	24074.12	6.05E-03	3.65E-05
$z\ ^7D$	1	5	z	25669.00	1.84E-04	3.40E-08	26386.60	-1.69E-06	2.85E-12
	2	4	x	25665.14	1.21E-02	1.47E-04	26404.29	5.66E-01	3.21E-01
	3	4	y	25665.14	-1.21E-02	1.47E-04	26404.29	-5.66E-01	3.21E-01
$y\ ^7P$	1	6	z	25825.92	-1.91E+00	3.66E+00	26301.67	-1.84E+00	3.39E+00
	2	5	x	25828.63	1.92E+00	3.69E+00	26358.21	-1.77E+00	3.13E+00
	3	5	y	25828.63	-1.92E+00	3.69E+00	26358.21	1.77E+00	3.13E+00

Table 4.3: The excited states and transition properties for Cr from a MRCI calculation are displayed. The headings are described in table 4.2. An additional column was added in the front for the term designations.

Terms	λ_{vac} $[nm]$	E_i - E_i $[cm^{-1}]$	g_i - g_k	A_{ki} $[s^{-1}]$	f_{ki}	S $[a.u.]$	$\frac{S}{g_k}$ $[a.u.]$	$\frac{S}{g_i g_k}$ $[a.u.]$
a 7S - z 7P*		0 - 23415.19	7 - 21	3.13E+07	2.57E-01	2.52E+01	1.20E+00	1.71E-01
	425.435	0.00 - 23498.84	7 - 9	3.15E+07	1.10E-01	1.08E+01	1.20E+00	1.71E-01
	427.480	0.00 - 23386.35	7 - 7	3.07E+07	8.42E-02	8.29E+00	1.18E+00	1.69E-01
	428.972	0.00 - 23305.01	7 - 5	3.16E+07	6.23E-02	6.16E+00	1.23E+00	1.76E-01
a 7S - z 7D*								
	361.564	0.00 - 27649.71	7 - 9	5.10E+04	1.30E-04	1.10E-02	1.22E-03	1.75E-04
		0.00 - 27500.37	7 - 7	1.50E+04	3.00E-05	2.50E-03	3.57E-04	5.10E-05
a 7S - y 7P*		0 - 27847.78	7 - 21	1.52E+08	8.81E-01	7.29E+01	3.47E+00	4.96E-01
	357.869	0.00 - 27935.26	7 - 9	1.48E+08	3.66E-01	3.02E+01	3.36E+00	4.79E-01
	359.349	0.00 - 27820.23	7 - 7	1.50E+08	2.91E-01	2.41E+01	3.44E+00	4.92E-01
	360.533	0.00 - 27728.87	7 - 5	1.62E+08	2.26E-01	1.88E+01	3.76E+00	5.37E-01

Table 4.4: The excited states and transition properties for selected states of Cr extracted from NIST - database [1, 2] are shown. The column "Terms" gives the term designation of the involved states. The second column shows the wave length of the transition and the third column the energy levels of the involved states. g_i and g_k are the degeneracies of the involved states. A_{ki} is the Einstein coefficient, f_{ki} is the oscillator strength. The last three columns show the line strength with different degeneracies.

4.5 Conclusion

The Cr atom and its excitation were analysed by the ROHF, MCSCF and the MRCI methods. The RS method was also attempted but yielded less meaningful results than the MRCI method. Several basis sets were compared and the aug-cc-pwCV5Z-DK showed the best reproduction of experimental values. An additional optimization of the ground state improved the results (figure 4.3). The calculation was performed for different active spaces (section 4.3.1). In general the accuracy increased with an increasing active space.

In the last part the results for a dipole transition moment calculation are shown. The y^7P state has the highest transition dipole moment, closely followed by the z^7P state which is also in agreement with experimental findings (NIST, [1]).

Chapter 5

The CrHe Diatomic Molecule

5.1 Ground State

A description of the interaction between chromium and a helium cluster can be deduced from a description of the interaction between the two atoms Cr and He. Therefore the diatomic potential was analysed extensively. In comparison to the ionic system, the interaction between the neutral atoms is extremely weak. For the cation a potential minimum of 538.88 K at 2.27 $\AA$ was obtained, in contrast to the neutral system with a potential minimum of about 7.08 K at about 5.01 $\AA$. This difference in the strength of the interaction can easily be understood. The interaction for the cation is based on the interaction of an ion and a neutral atom, a monopole - induced dipole interaction. The interaction between the neutral atoms is based on two induced dipoles, therefore extremely weak. The weakness of the bond can easily be illustrated. The potential minimum sets an upper limit for the bond breaking at a temperature of 7 K or $-266.15\ ^{\circ}C$.

5.1.1 Basis Sets

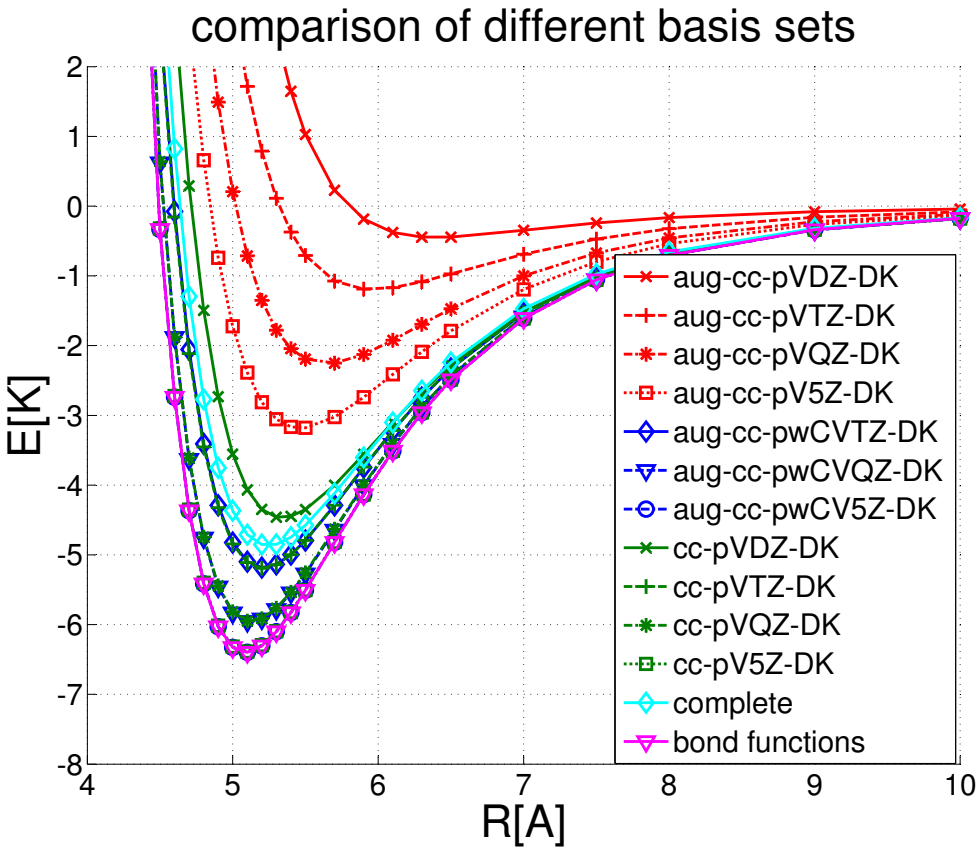

Figure 5.1: The CrHe potential is displayed for three different basis set families. The curves were determined with a ROHF calculation and a CCSD(T) calculation.

Since the interaction between chromium and helium is weak, basis sets that describe the atoms very well should work well in this case, too. So for chromium the aug-cc-pwCVNZ-DK (N= T, Q, 5)[83] was selected and for helium the aug-cc-pVNZ-DK (N= T, Q, 5)[84]. In

figure 5.1 the curves for different basis sets are shown. It can be seen that an augmented basis set is essential. Augmented basis sets contain slowly decaying functions and therefore are able to describe long range interaction, as for example weak van der Waals interactions. The figure also contains the results for the basis sets that gave the best results for the CrHe - cation (complete). This basis set is not as good as the augmented basis sets (TZ - 5Z) in describing the interaction. If you add bond functions to the aug-cc-pwCV5Z-DK basis set the results remain more or less the same (bond functions).

5.1.2 Methods

Many methods were applied to calculate the interaction between chromium and helium. Even density functional theory (DFT) was attempted but the results were unsatisfactory, so this approach was not pursued.

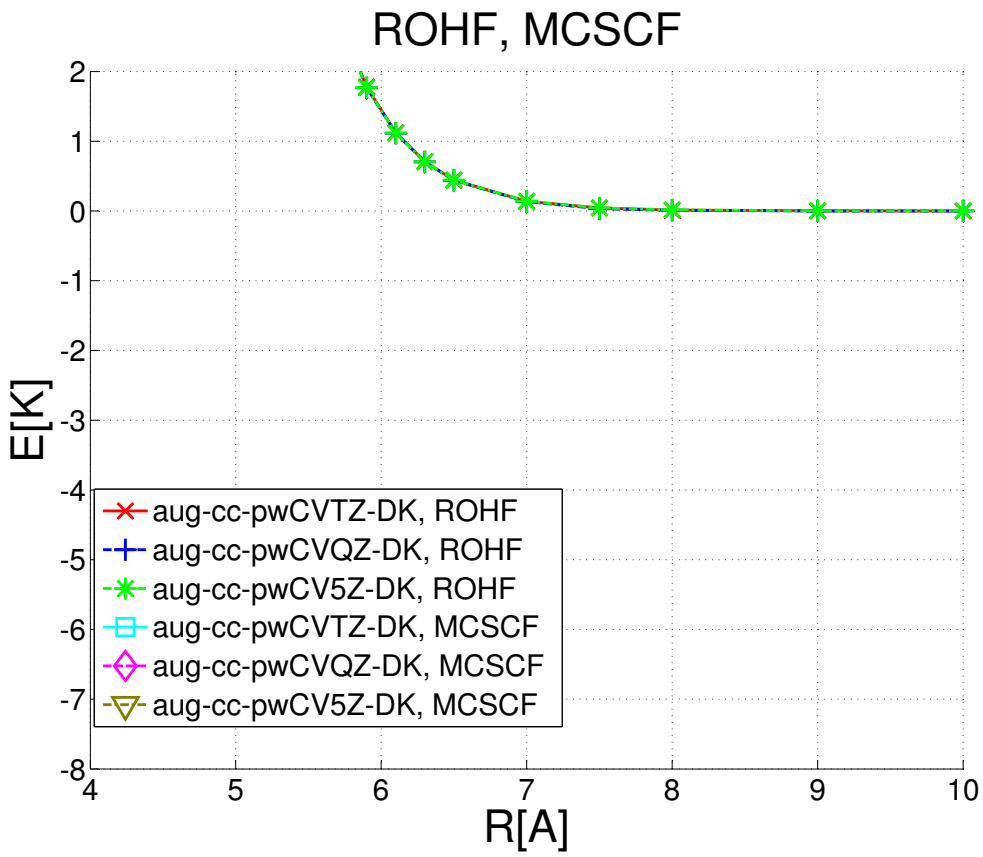

Figure 5.2: The CrHe potential is displayed for three different basis set families. The calculations were performed on the Hartree-Fock level, therefore no electron correlation is considered and no bonding is obtained. All potential curves lie on top of each other.

The Cr-He diatomic molecule has a septet - multiplicity in the ground state, like the atom. Therefore open shell methods and calculations are required. For a first calculation, always a Hartree Fock calculation is applied. Since it is an open shell system either unrestricted Hartree Fock calculations (UHF) or restricted open shell Hartree Fock calculations (ROHF) can be applied. UHF showed less meaningful results and convergence problems. Therefore

ROHF was the method of choice. The weak van der Waals interaction of the CrHe diatomic molecule is based on electron correlation. Since electron correlation is not included on the Hartree-Fock level, no bonding is indicated by ROHF calculations (figure 5.2).

A reasonable potential curve requires a sufficient spatial resolution. Therefore numerous single point calculations are necessary to capture the features of a potential curve. To keep the overall computational effort reasonable, the accuracy of single point calculations is reduced. So the active space of the CASSCF calculation was restricted to (4 / 1 / 1 / 1) in C_{2v}-symmetry, seven orbitals with six electrons. The results of this calculation, the orbitals, were used in following calculations see figures 5.4 and 5.5. The potential curves obtained by this calculation are shown in figure 5.2.

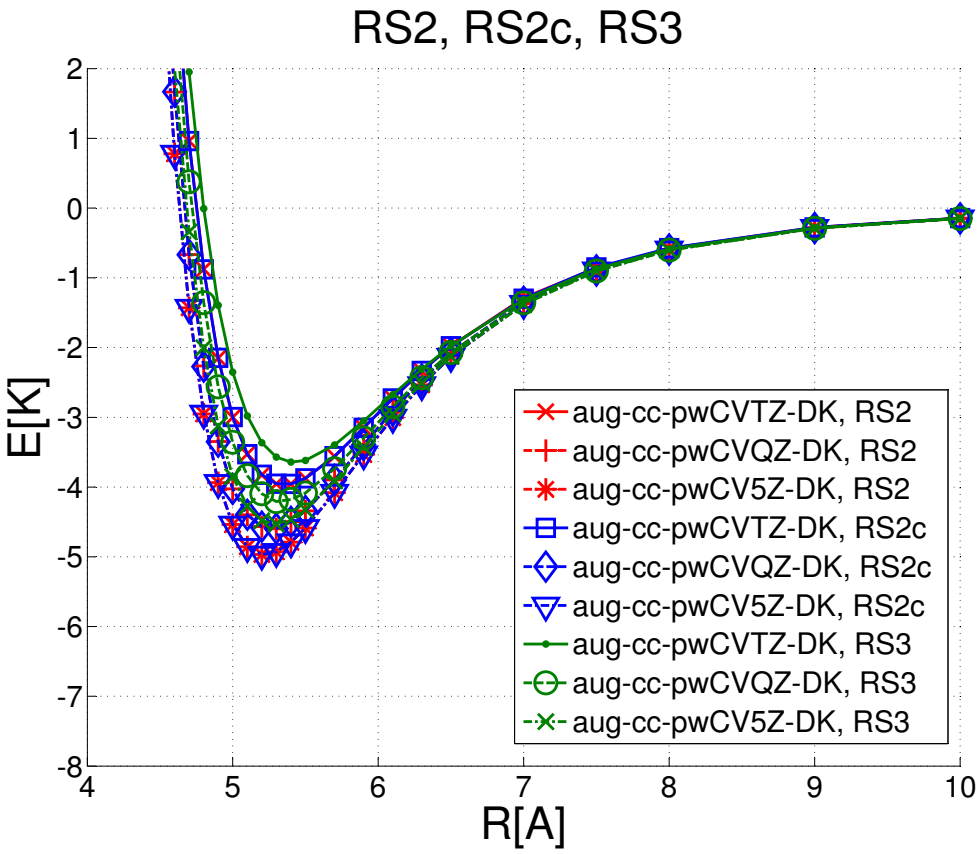

Figure 5.3: The CrHe potential curve for the Rayleigh Schrödinger perturbative approach of different order. An oscillating convergence is indicated.

The Rayleigh Schrödinger perturbation theory gives the results in figures 5.3 and 5.4. For these calculations the active space remained the same as for the CASSCF calculations. In the beginning the calculations did not converge because of the intruder state problem. The intruder state problem appears if the different states get energetically close to each other and states of different spaces start interacting. There are several methods to resolve this problem. Either a modified Fock - operator [85] can be used or level shifts [86]. Here a level shift of 0.6 was applied as implemented in MOLPRO by Roos and Andersson [86]. An optimization of the wave function with CASSCF showed no significant improvement of the result (figure 5.4).

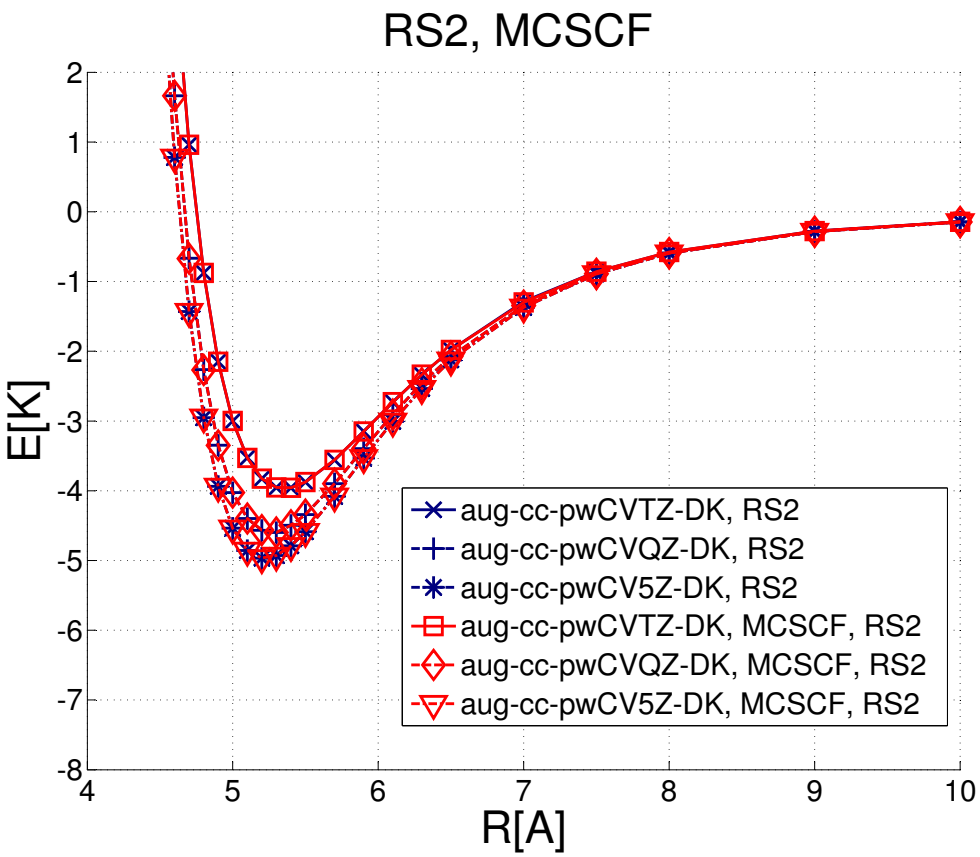

Figure 5.4: The CrHe potential curves are shown with or without a MCSCF calculation before the Rayleigh Schrödinger perturbative approach. No improvement is achieved with MCSCF.

Different orders of Rayleigh - Schrödinger Perturbation Theory (RS) have been applied and their results are displayed in figure 5.3. The second order methods (RS2, RS2c) show about the same results, which is to be expected. These methods only differ in their computational effort due to different treatment of contracted wave functions. The third order calculation (RS3) shows shallower potential curves which indicate oscillating convergence. The Rayleigh - Schrödinger Perturbation Theory is based on perturbation theory which also shows such a convergence. An extrapolation to infinite order is not possible because there are not sufficient orders.

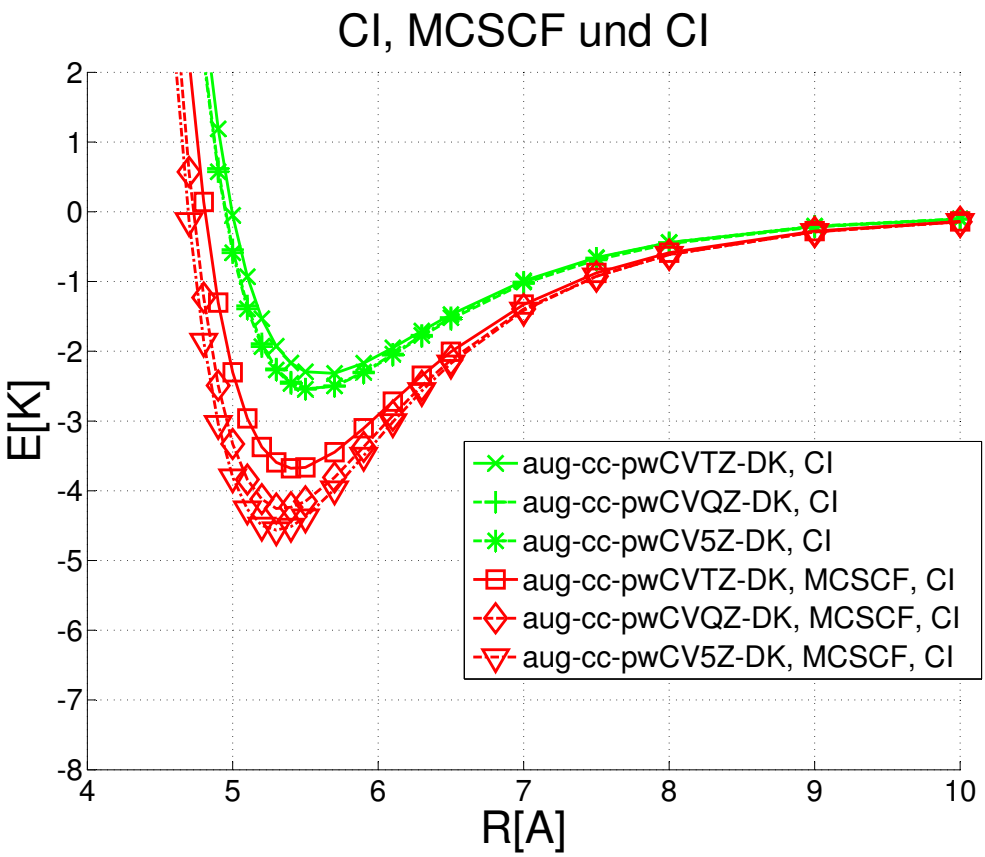

Figure 5.5: The CrHe potential curve has been calculated with CI. The additional optimization with MCSCF improves the result significantly.

A Full - CI calculation should give the best results. Contrary to expectation CI - calculations are not very accurate (figure 5.5). The CI - calculations need a large active space as well as sufficient virtual excitations to create the required configurations to become accurate. The CI implemented in MOLPRO is truncated and only uses single and double excitations (CISD). The potential is even shallower than RS2 results, but the convergence is monotonically which makes the results more predictable.

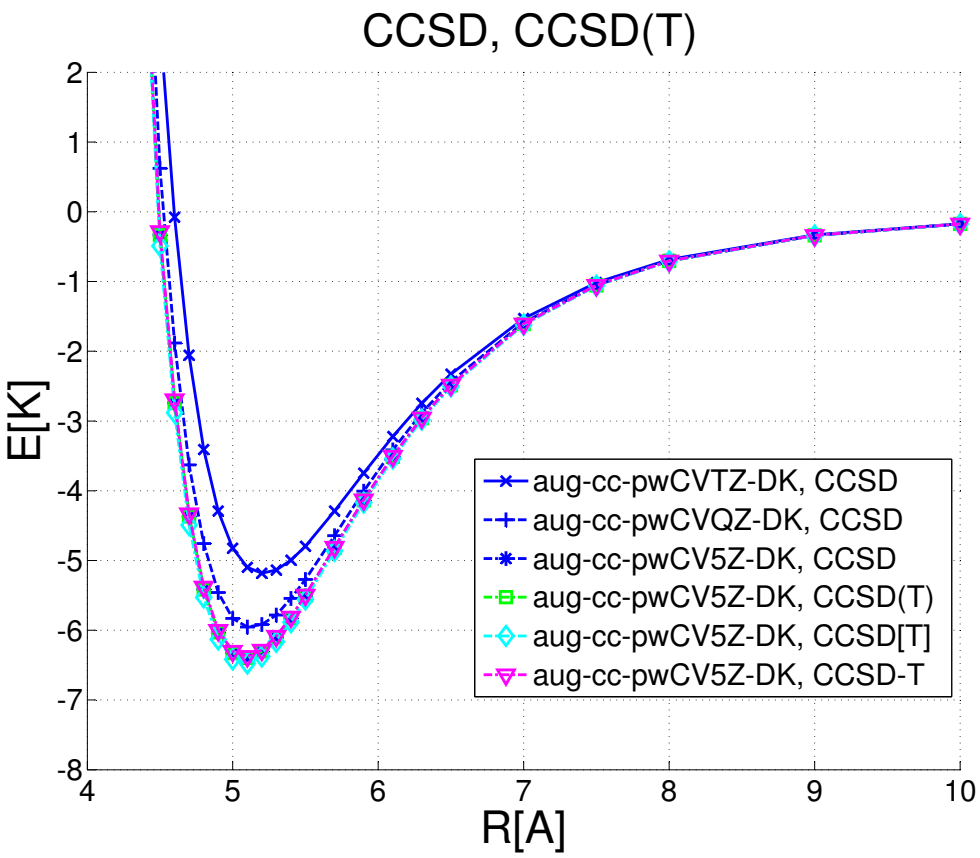

Figure 5.6: The CrHe potential curve calculated with CC methods. Different approaches to include the triples are shown. These results are used later on to extrapolate to the basis set limit.

The coupled cluster approach showed the most promising results as already mentioned. The coupled cluster method was applied as it is implemented in MOLPRO for open shell systems. The results were significantly improved by correlating all electrons, this means also including the core electrons. An additional feature of MOLPRO is that the coupled cluster program offers different inclusion of triple excitations. The single excitations and the double excitations are completely taken into account, but only the most significant contributions of the triple excitations are added perturbatively. There are different methods for selecting and evaluating these contributions. Figure 5.6 contains the CCSD results and the different methods for adding the triples ((T), [T], -T). These calculations were performed using a single reference coupled cluster method. So the question arises if the ground state can be described sufficiently with a single determinant. The validity of this approach can be judged by the so called T1-diagnostics [54]. In the calculations the value of T1 reaches at most 0.012 which indicates that the ground state is reasonably well described by the approach (compare with section 2.4.3). These results are used for the extrapolation to the basis set limit.

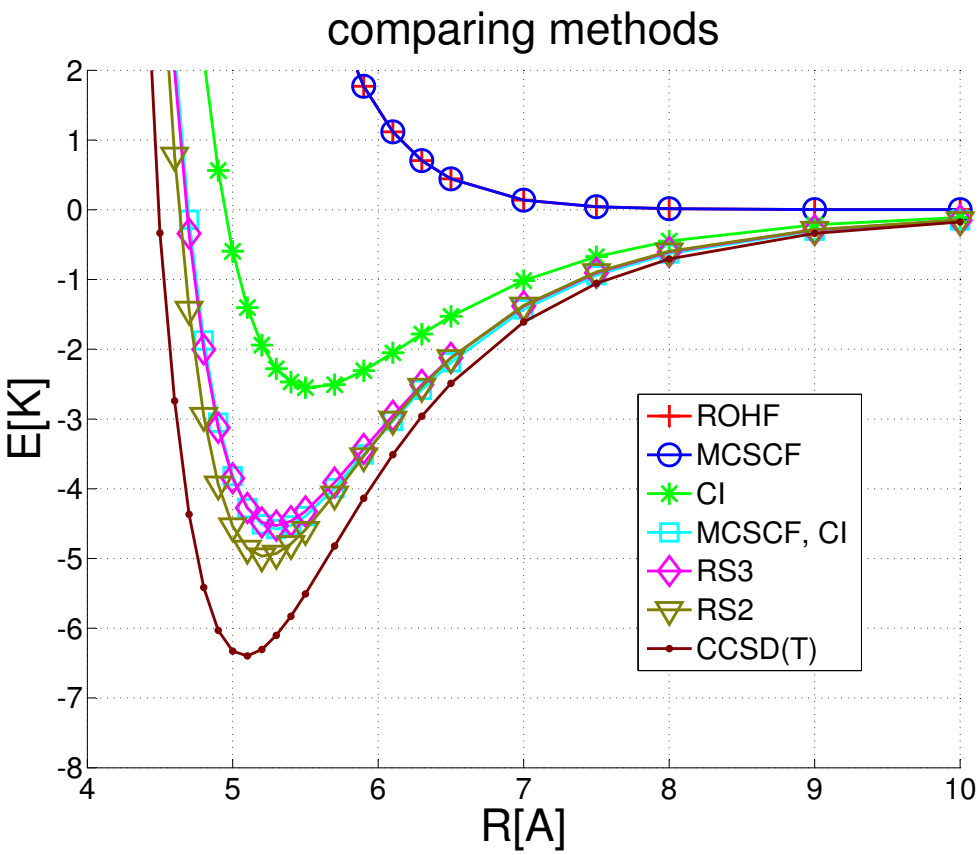

Figure 5.7: The CrHe potential curve calculated with different methods. The CC method gives the most promising potential curve and also the deepest one.

The results obtained by different methods are compared in figure 5.7. CC and CI methods both are based on the variational principle and they show a monotonic convergence towards deeper potential wells. Therefore the deepest potential should be the most realistic one. In contrast, RS calculations are based on the perturbation theory and have therefore mostly oscillating convergence. Nevertheless all methods show convergence towards deeper potential wells if the number of basis functions is increased. In comparing the RS method of second order and CI with CASSCF calculations, the RS calculations give slightly deeper potential wells, if they all use a similar active space.

5.1.3 Relativistic Approach

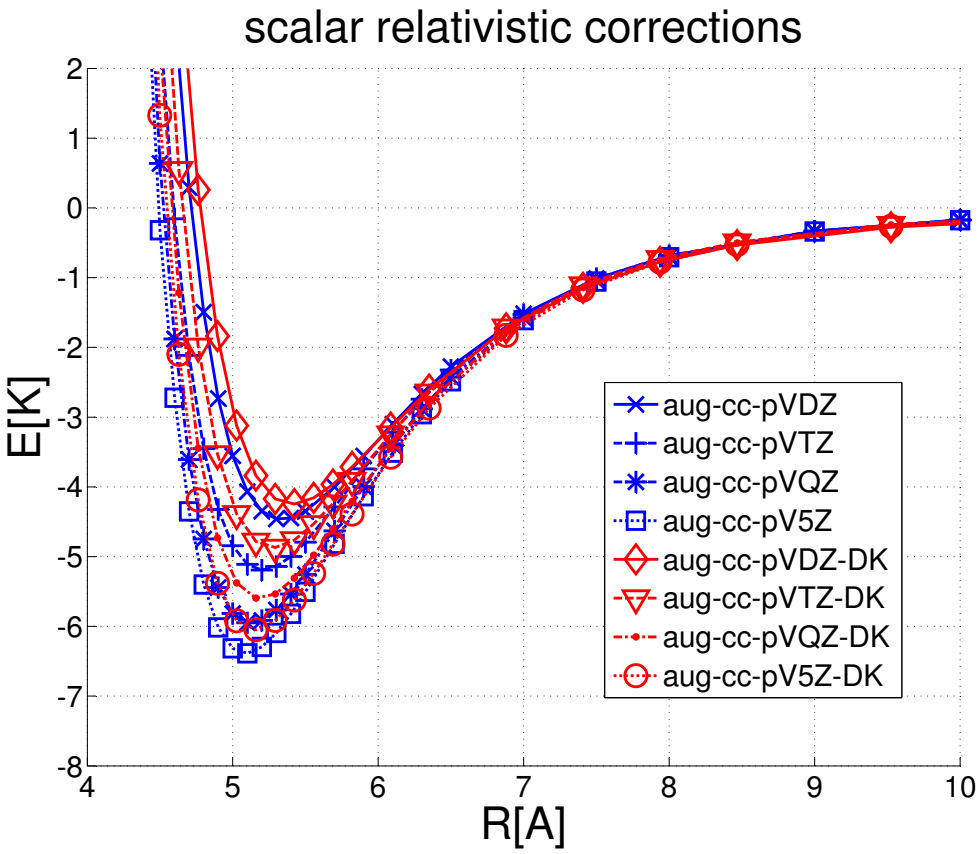

Figure 5.8: This figure shows the significance of including the scalar relativistic Douglas-Kroll correction in calculating the potential for CrHe. The relativistic curves are shifted slightly and show deeper potential wells.

Although Cr is a light atom, the relativistic contributions are significant for the neutral system. Cr and He are bound by a weak van der Waals interaction. Therefore even small relativistic contributions need to be considered (figure 5.8). Additionally the contributions seem to be independent of the basis set. The relativistic effects were considered here by the Douglas-Kroll correction on the Hartree-Fock level. In this approach the expression in equation (2.18) contains additional terms to account for relativistic effects. This results in a change of the form of the orbitals. One relativistic effect is the change of mass with velocity which results in a higher probability density near the nucleus. Different orders of the Douglas Kroll correction can be applied (figure 5.9). As can be observed it is essential to include the Douglas Kroll correction but the order is more or less insignificant. It has an oscillating convergence but in this case it is already mostly converged for the second order. In most calculations the Douglas-Kroll correction of 8^{th} order was applied. The inclusion of the Douglas-Kroll correction does not require a lot of computational effort. The calculations take only slightly longer.

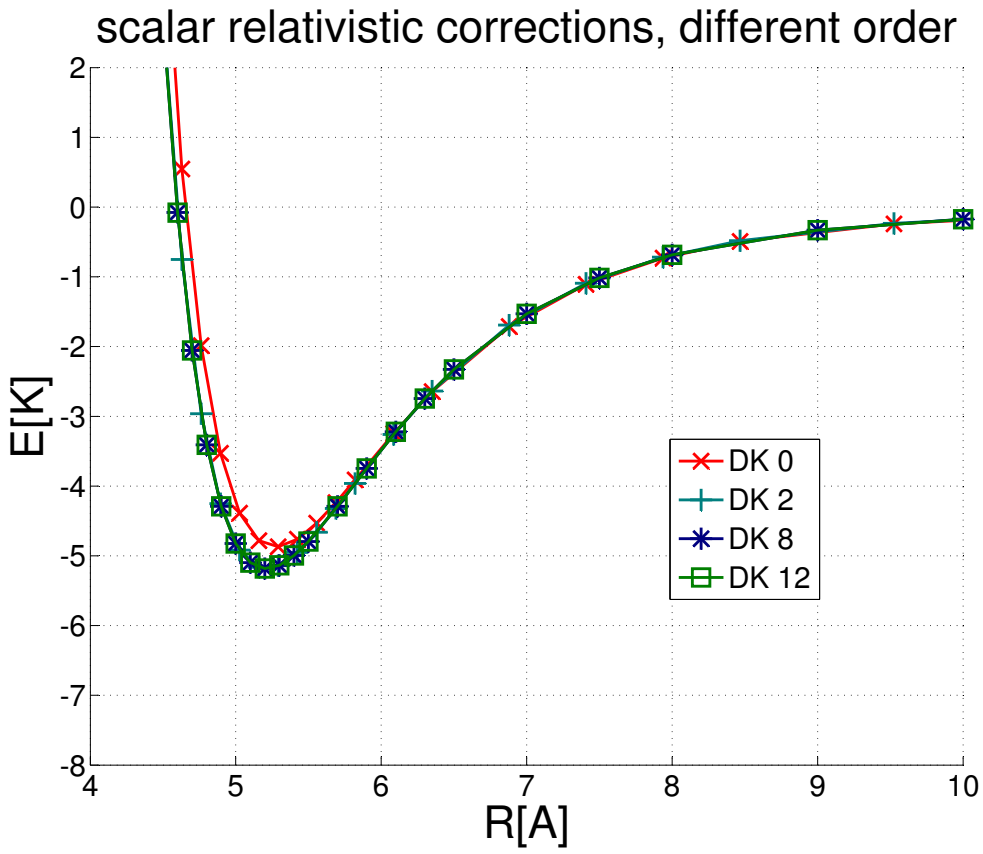

Figure 5.9: This figure shows the Douglas-Kroll correction of different order for the CrHe system. There is a clear difference if the correction is included or not, but the order of the correction influences the result barely.

5.1.4 Extrapolation

A finite basis set is insufficient to describe the problem exactly. Therefore basis sets especially adjusted to this problem are used, as already explained. Correlation consistent basis sets are applied in order to estimate the solution for an infinite basis set or to approximate it. These basis sets allow for an extrapolation to the basis set limit. Two different basis set families were used and both show similar behaviour if they are extrapolated to the basis set limit.

For He the aug-cc-pVNZ (N=D,T,Q,5) family of Woon and Dunning [84] was applied in all calculations. Cr was either described by the aug-cc-pVNZ-DK (N=D,T,Q,5) basis set family of Balabanov [83] or the aug-cc-pwCVNZ-DK (N=T,Q,5) basis set family of Balabanov [83]. The second basis set family is recommended for calculations correlating all electrons.

Functions

There are many functions for the extrapolation to the basis set limit. Sometimes it is proposed to extrapolate the total energy (E), sometimes formulas suggest using the Hartree-Fock energy (E_{HF}) or the correlation energy ($E_{corr} = E - E_{HF}$). The extrapolation formulas either use the highest angular quantum number of all functions in the basis set (l_{max}) or some cardinal number (n, for example $D \rightarrow 2, T \rightarrow 3, \ldots$). Some authors also differ between different Post-Hartree Fock methods. Sometimes the formulas also refer to a certain basis set family.

Halkier took a closer look at the convergence of first and second row atoms with the correlation consistent basis sets of Dunning (cc-pVNZ, [87]). In the papers he proposed a splitting into Hartree-Fock energy and correlation energy [32, 33]. For the Hartree-Fock energy he used functions of exponential form or power form as in (5.1).

$$\begin{aligned} E_{HF}(n) &= E_{HF}(\infty) + Ae^{-\alpha n} \\ E_{HF}(n) &= E_{HF}(\infty) + An^{-\alpha} \end{aligned} \tag{5.1}$$

These functions were not applied here because the change in the Hartree-Fock energy for the CrHe - ground state is negligible. A constant was used to approximate the Hartree-Fock energy, if the energy was split into the Hartree-Fock energy and the correlation energy. The functions describing the correlation energy are mostly motivated theoretically by some expansion of the wave function and use fixed powers, like in equation (5.2). For the correlation energy Halkier used CCSD(T) and MP2 calculations.

$$E_{corr}(n) = E_{corr}(\infty) + A(n)^{-3} \quad \text{(Halkier 1)} \tag{5.2}$$

Another function for the correlation energy was mentioned by Feller ((5.3), [39]). The value of γ depends on the level of theory and the used basis sets. In the figures 5.10 and 5.11 γ was used as an additional parameter which needed to be optimized.

$$E_{corr}(n) = E_{corr}(\infty) + A(n+\gamma)^{-3} \quad \text{(Feller 1)} \tag{5.3}$$

For the behaviour of the total energy in a CCSD(T) calculation Martin suggested different power series ([34], (5.4)).

$$
\begin{aligned}
E\left(l_{max}\right) &= E\left(\infty\right) + \frac{A}{\left(l_{max}+\frac{1}{2}\right)^{\alpha}} \quad \text{(Martin 1)} \\
E\left(l_{max}\right) &= E\left(\infty\right) + \frac{A}{\left(l_{max}+\frac{1}{2}\right)^{4}} \quad \text{(Martin 2)} \\
E\left(l_{max}\right) &= E\left(\infty\right) + \frac{A}{\left(l_{max}+\frac{1}{2}\right)^{4}} + \frac{B}{\left(l_{max}+\frac{1}{2}\right)^{6}} \quad \text{(Martin 3)}
\end{aligned} \tag{5.4}
$$

Feller proposed an exponential form or an mixed exponential and Gaussian function for extrapolating to the basis set limit ([35], (5.5)) for the total energy in a CCSD(T) calculation.

$$
\begin{aligned}
E\left(n\right) &= E\left(\infty\right) + Ae^{-B\cdot n} \quad \text{(Feller 2)} \\
E\left(n\right) &= E\left(\infty\right) + Ae^{-(n-1)} + Be^{-(n-1)^2} \quad \text{(Feller 3)}
\end{aligned} \tag{5.5}
$$

Lara-Castells used the cardinal number instead of l_{max} ([36], (5.6)) for a power series.

$$
\begin{aligned}
E\left(n\right) &= E\left(\infty\right) + \frac{A}{\left(n+\frac{1}{2}\right)^{\alpha}} \quad \text{(Lara-Castells 1)} \\
E\left(n\right) &= E\left(\infty\right) + \frac{A}{\left(n+\frac{1}{2}\right)^{4}} + \frac{B}{\left(n+\frac{1}{2}\right)^{6}} \quad \text{(Lara-Castells 2)}
\end{aligned} \tag{5.6}
$$

Feller also mentions single inverse power functions ([39], (5.7)).

$$
E\left(l_{max}\right) = E\left(\infty\right) + A\left(l_{max}\right)^{-3} \quad \text{(Feller 4)} \tag{5.7}
$$

The parameters of the functions ($E\left(\infty\right)$,$E_{corr}\left(\infty\right)$, A, B, α and γ) were determined using the statistics toolbox of MATLAB [88]. The convergence was partly doubtful. The energies calculated with MOLPRO as well as the extrapolation using different functions can be seen in the figures 5.10 and 5.11.

The fitting procedure seems to give the better results for a fit with only three points (figure 5.10), although the results are not very reliable. Martin 1 and Lara-Castells 1 seem especially problematic. Both models have a power as a fit parameter. It is challenging to fit functions because of the sparse data set. There are only 3 or 4 points for the fitting procedure. The number of parameters in the functions is nearly as large as the number of points belonging to the function. Therefore making predictions for the functions is difficult and only possible with large uncertainties, especially if only three orders within the basis sets family are available. For different atoms, if there are up to five different basis sets available, this approach seems more promising.

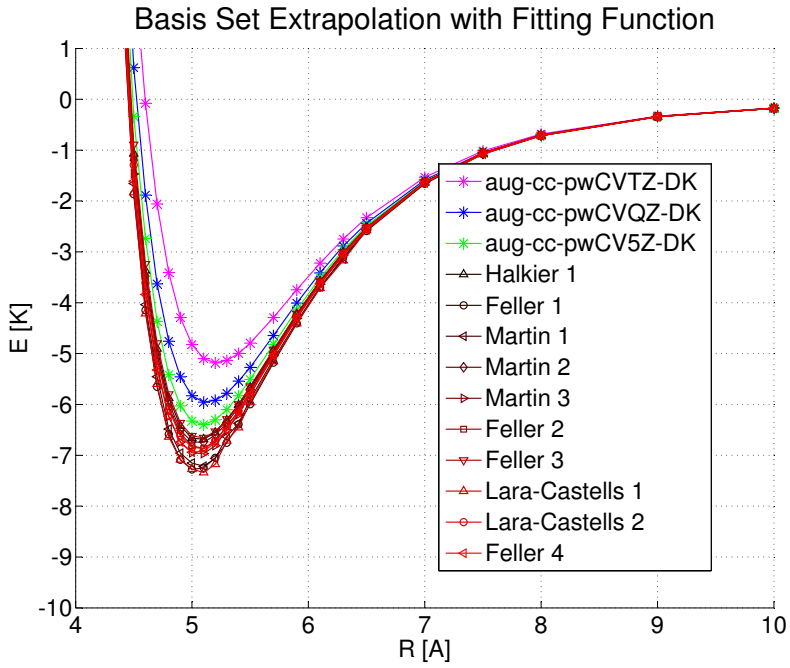

Figure 5.10: This figure shows the extrapolation to the basis set limit using different functions. The results for the aug-cc-pwCVNZ-DK basis set family are used.

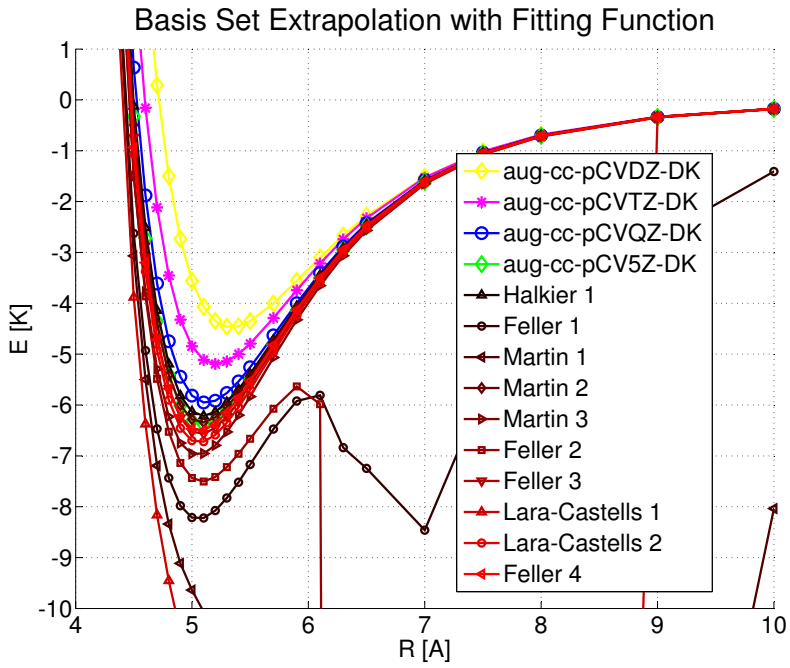

Figure 5.11: This figure shows the extrapolation to the basis set limit using different functions. The results for the aug-cc-pCVNZ-DK basis set family are applied. Although more points are available for the fitting procedure less meaningful results are obtained.

Formula

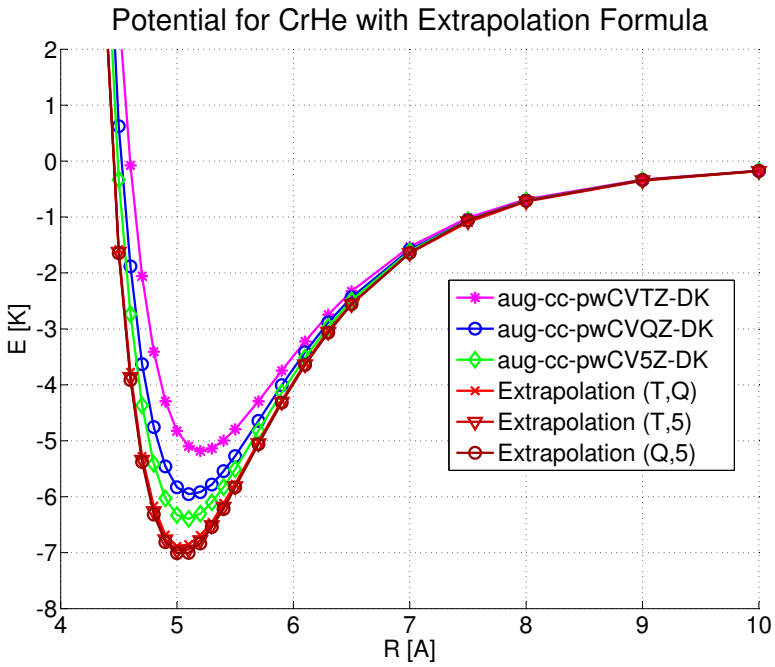

Figure 5.12: This figure shows the extrapolation to the basis set limit using the formula. The results for the aug-cc-pwCVNZ-DK basis set is displayed here.

The second method for performing the extrapolation is an extrapolation formula (equation (2.6), section 2.1.6). This approach seems more reliable than the fitting of functions, as discussed in the previous section.

The advantage of the formula is that you only need two points for the extrapolation, so you are able to compare the results for different extrapolations. Another advantage is that a search for good initial values is omitted. You do not need to fit a function to the data and so it is easier to handle.

The results are presented in the figures 5.12 and 5.13.

Since the fitted functions are quite problematic and partly depend on initial values, the extrapolation formula was selected to calculate the potential curve which will be used later on.

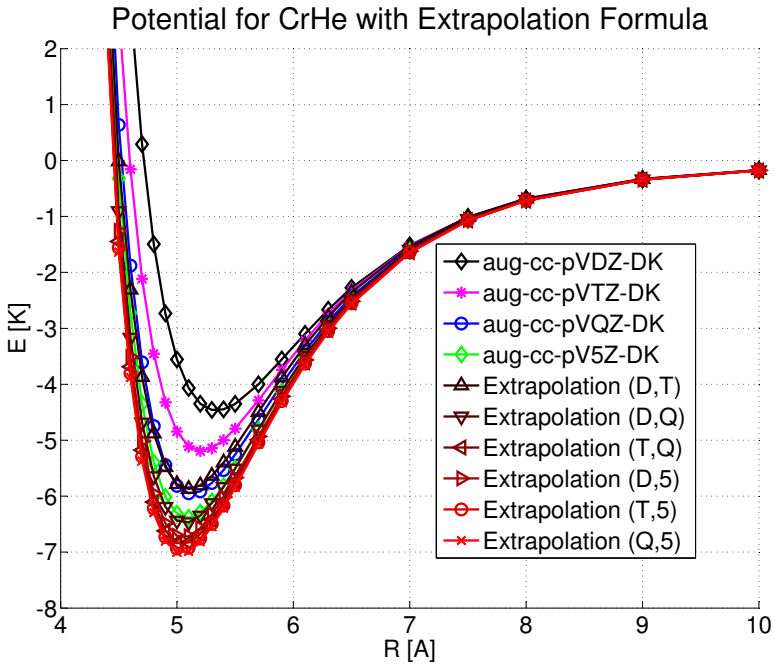

Figure 5.13: This figure shows the extrapolation to the basis set limit using the formula. This figure contains the results for the aug-cc-pCVNZ-DK basis set.

5.1.5 Counterpoise Correction

So far all shown curves (figures 3.1 to 3.3 and figures 5.1 to 5.13) where corrected with the counterpoise correction, see section 2.1.7. The necessity to use this correction can clearly be seen in the extrapolated diatomic potential, if the correction is neglected (figures 5.14 and 5.15).

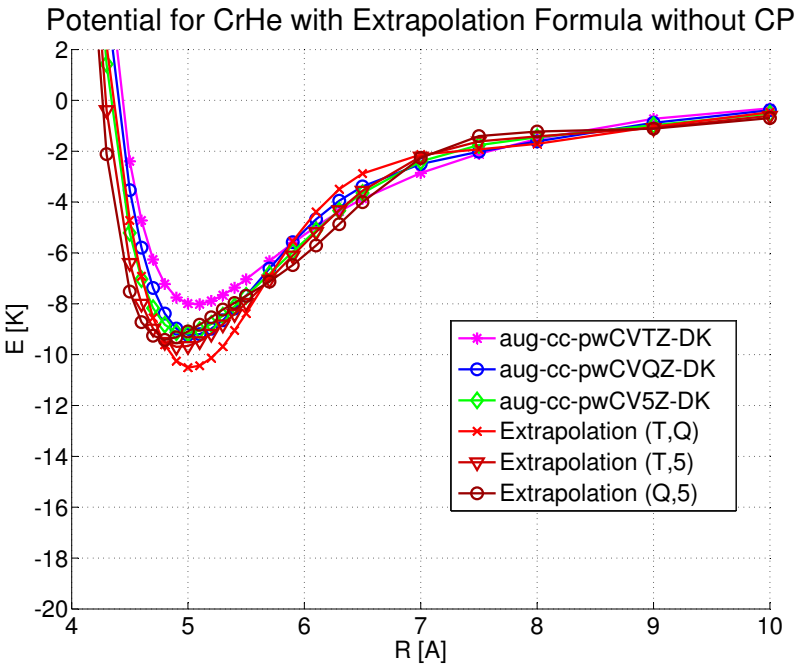

Figure 5.14: This figure shows the extrapolation to the basis set limit using the formula for uncorrected (no CP) curves, compare with figure 5.12. The results for the aug-cc-pwCVNZ-DK basis sets are displayed here. Neglecting the CP-correction deepens the potential and additonally the form of the potential curve becomes dependent on the size of the basis set.

The potential well deepens by neglecting the counterpoise correction. The form of the potential well changes additionally with the size of the basis set which leads to unphysical oscillations in the extrapolations. In comparing the figures 5.14 and 5.15 and the figures 5.12 and 5.13 it becomes clear that the counterpoise correction is meaningfull. The corrected potentials have no unphysical oscillation and additionally converge to the same potential independent of the basis set family, see section 5.1.4.

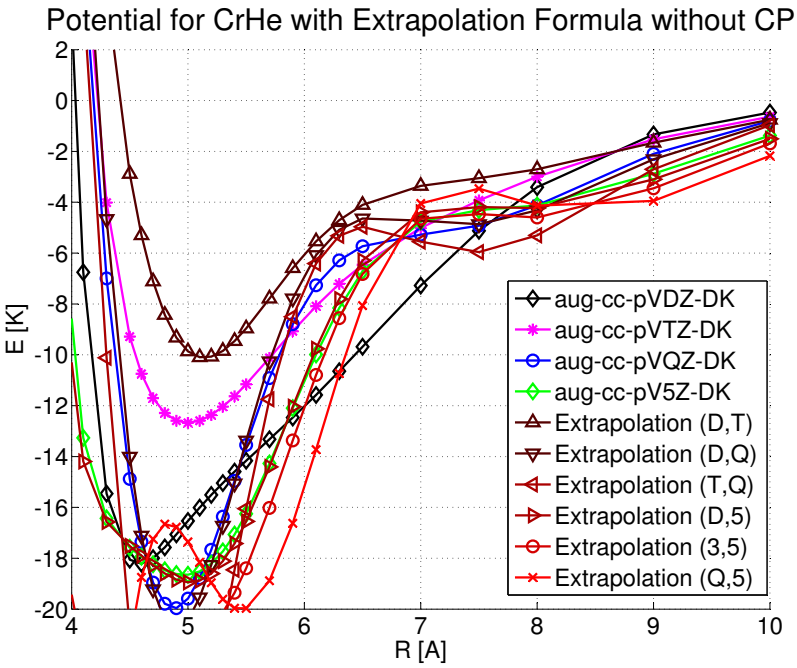

Figure 5.15: This figure shows the extrapolation to the basis set limit using the formula for uncorrected (no CP) curves, compare with figure 5.13. The results for the aug-cc-pCVNZ-DK basis set are shown. The depth and form of the potential well are strongly dependent on the basis set size and no trend can be determined.

5.1.6 Rovibrational Analysis

The same rovibrational analysis was performed for the CrHe diatomic molecule as for the CrHe cation, see section 3.4. For this analysis the potential curve of figure 5.12, that was derived by an extrapolation with formula (2.6), was used. The potential was calculated with the aug-cc-pwCVNZ-DK basis set and used the ROHF and CCSD(T) methods with a Dougals-Kroll correction.

The results for a fit with the Morse potential can be seen in table 5.1.

$D_e[cm^{-1}]$	$r_{min}[A^{circ}]$	a [d.u.]
4.8056	5.0521	1.1371

Table 5.1: Morse parameter for the CrHe ground state

The Lennard-Jones potential fit yields the parameters of table 5.2. These results were used for the LEVEL program.

m [d. u.]	n [d. u.]	$D_e[cm^{-1}]$	$r_{min}[A^{circ}]$
9	8	4.9188	5.0143

Table 5.2: Lennard-Jones parameter for the CrHe ground state

All three programs give similar results, showing a single vibrational level at about $-1\ cm^{-1}$, compare with table 5.3.

ν	J	MATLAB $[cm^{-1}]$	MORSE $[cm^{-1}]$	LEVEL 8 $[cm^{-1}]$
0	0	-1.0293	-0.8432	-0.9701

Table 5.3: Rovibrational levels for the CrHe ground state (ν ... vibrational quantum number, J ... rotational quantum number)

Using MATLAB this level can be illustrated like in figure 5.16. The single vibrational level is plotted and its probability density.

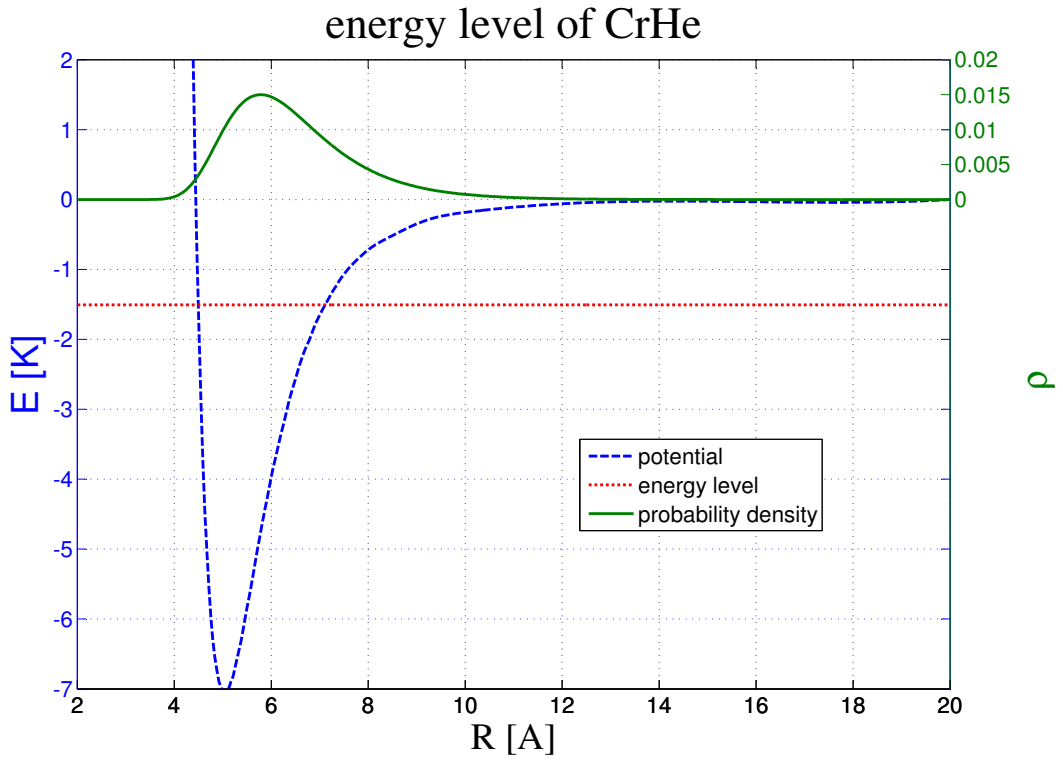

Figure 5.16: In the figure the vibrational level of CrHe and its probability density is depicted. The potential appearing in this figure is the counterpoise corrected and extrapolated of figure 5.12. The vibrational level has a energy of about $-1.4\ K \approx -1\ cm^{-1}$

5.1.7 Overview

For illustration the applied methods, basis sets and relativistic corrections are shown in figure 5.17.

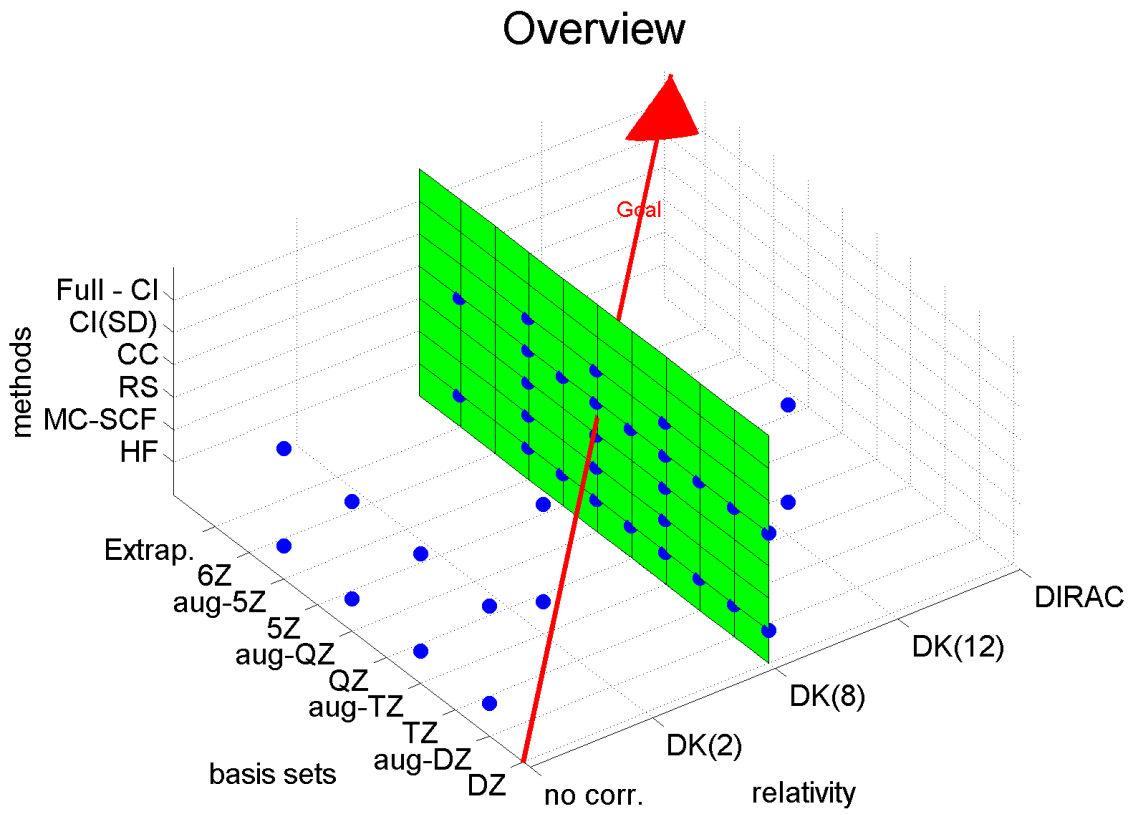

Figure 5.17: This figure gives an overview of applied basis sets and methods for the CrHe diatomic molecule.

Most of the calculations were performed with the Douglas-Kroll correction of 8^{th} order, plane in figure 5.17. The Hartree-Fock calculations were required as a starting point for the other calculations, so they appear for all used basis sets and relativistic corrections. The coupled cluster method was also applied extensively since it was very promising. The arrow points in the direction of improvement.

Primarily a basis set as large as possible is required for good accuracy.

Another improvement is the application of Post-Hartree-Fock methods and improving this by more and more accurate methods up to full CI.

Adding relativistic corrections can also improve the results. In this case the Douglas-Kroll correction was applied. Later on the Breit-Pauli operator will be used. The goal would be a complete relativistic calculation as it is possible with the DIRAC software package for small systems.

5.2 Excitations

For calculating the excited states of the diatomic molecule the same method was selected as for the excited states of the atom. The starting point is a ROHF calculation which is followed by a CASSCF calculation. A correction of the excited states by the Douglas-Kroll correction is neglected because the calculation for the atom has shown that this correction leads to greater inaccuracies in the description. The CASSCF calculation was challenging, which will be described in sections 5.2.1 and 5.2.2. The results of the following MRCI calculation are shown in section 5.2.3 which also contains a short discussion of accuracy. Section 5.2.4 contains the result of the subsequent spin-orbit coupling calculations.

The first excited level of He has an energy of 159856.0 cm^{-1} [1], whereas the first excited level of Cr lies at 7593.2 cm^{-1} [1]. The ionization energy of Cr is about 54575.6 cm^{-1} [1]. This means that the excited states of the diatomic molecule are dominated by the excitations of Cr. So a calculation of the excited states of the diatomic molecule at large distances should yield the excited states of the Cr atom.

5.2.1 Basis Sets

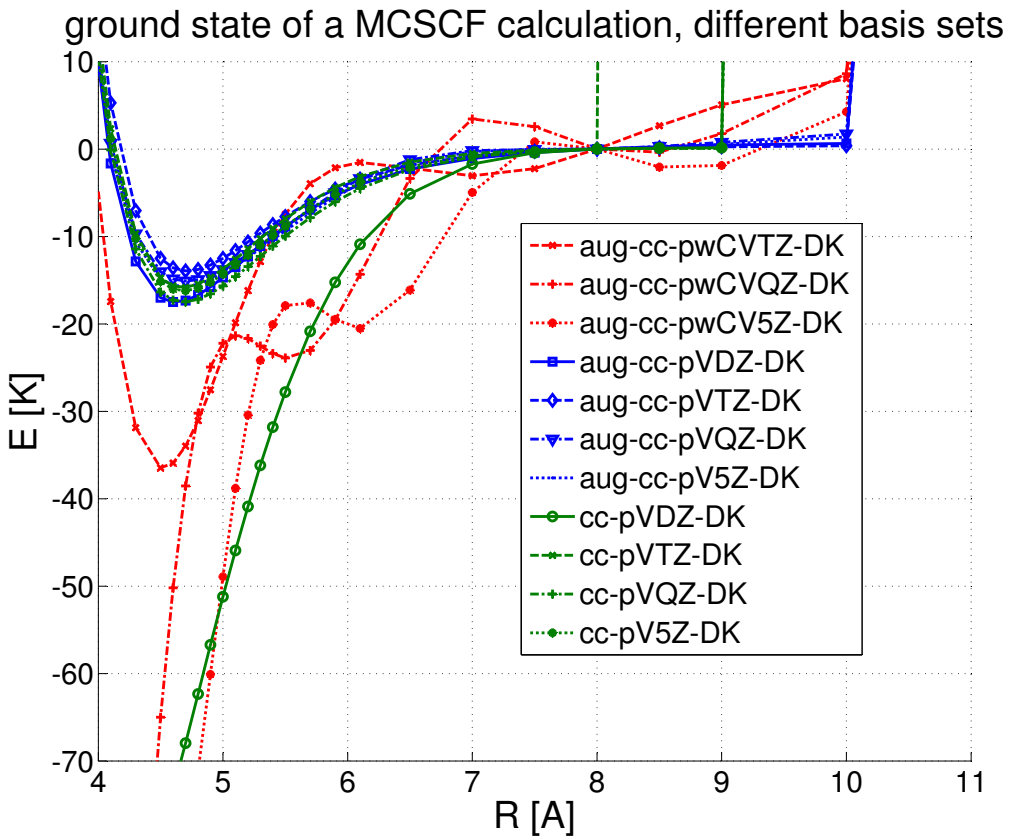

Figure 5.18: The ground state for a MCSCF calculation with an optimization of all states for different basis sets. All curves have been set to zero at 8 $\AA$. Several basis sets show unphysical oscillations.

The evaluation of the active space and the basis sets was done with a MCSCF calculation, since the MRCI-calculations for all relevant states are quite time consuming. The results for different basis sets for a MCSCF calculation are shown in figure 5.18.

The figure only contains the ground state which has already been extensively investigated and is known, see section 5.1. By comparing the results of different basis sets with the known solution an estimation of the accuracy of the approach can be determined. The difference between this approach and the results described in section 5.1.2 is the state-average. Instead of optimizing a single state numerous states are optimized in this CASSCF calculations. This results in orbitals which describe the whole system accurately, not only the ground state. Although the ground state is described less accurate, the result should still be meaningful.

Three basis set families were investigated, the aug-cc-pwCVNZ-DK, the aug-cc-pVNZ-DK, and the cc-pVNZ-DK basis set family. The aug-cc-pwCVNZ-DK basis set family has proven to be promising in section 5.1. However, in combination with state-averaged calculations it seems troublesome (figure 5.18). The ground state potential shows unphysical oscillations which also make any calculation based on this result doubtful. The aug-cc-pVNZ-DK and cc-pVNZ-DK basis set families give similar and meaningful results, except for the cc-pVDZ-DK basis set. This can be explained by the small size of the basis set.

The dependence on the active space is similar for the different basis set families. For the calculations in figure 5.18 the total number of orbitals was (10 / 4 / 4 / 1) with (5 / 2 / 2 / 0) closed orbitals. The number of states in each symmetry was (6 / 5 / 5 / 3).

In the end the aug-cc-pVTZ-DK basis set was selected which is a good trade-off between accuracy and computational effort.

5.2.2 Active Spaces

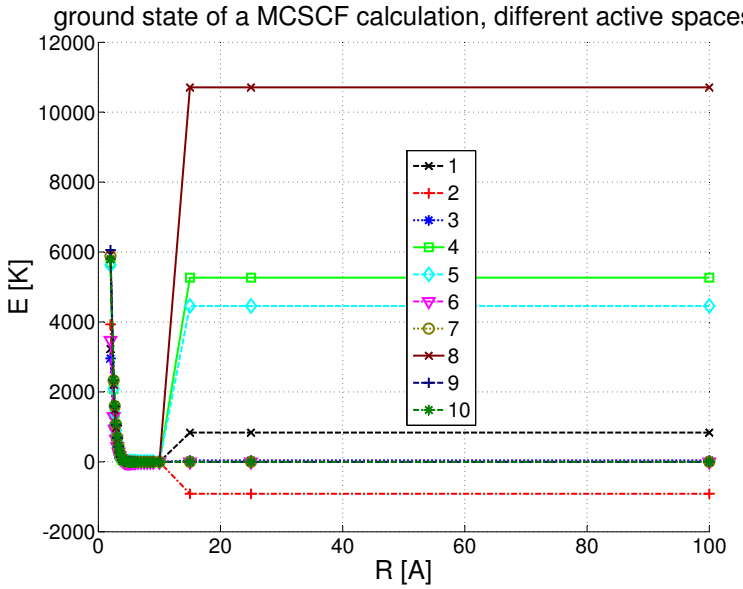

Figure 5.19: The ground state for a MCSCF calculation with an optimization of all states for different active spaces. The active spaces are shown in table 5.4. All curves have been set to zero at 10 $\mathring{A}$. A magnified section is displayed in figure 5.20. Some curves show unphysical steps.

Nr.	MCSCF (core)	MCSCF (total)	CSFs in MCSCF
1	5 / 2 / 2 / 0	10 / 4 / 4 / 1	303
2	5 / 2 / 2 / 0	11 / 4 / 4 / 1	917
3	4 / 2 / 2 / 0	10 / 4 / 4 / 1	2156
4	5 / 2 / 2 / 0	12 / 5 / 5 / 2	22635
5	5 / 2 / 2 / 0	12 / 5 / 5 / 1	11445
6	6 / 2 / 2 / 0	10 / 4 / 4 / 1	24
7	6 / 2 / 2 / 0	12 / 5 / 5 / 2	772
8	5 / 2 / 2 / 0	13 / 6 / 6 / 2	132674
9	6 / 2 / 2 / 0	13 / 6 / 6 / 2	3130
10	6 / 2 / 2 / 0	12 / 5 / 5 / 1	442

Table 5.4: active spaces for the results in figure 5.19 and figure 5.20

After selecting the basis set a study of different active spaces was performed to estimate its influence on the result. Such an analysis was already performed for the atom, see section 4.3.1. More details concerning the notation can be found there. The description of the active spaces as well as the number of configuration state functions can be extracted from table 5.4.

The abilities of describing the system can be judged looking at figure 5.19. The figure again contains the ground state of the diatomic molecule for different calculations, but this time the basis set is kept fixed, while the active space changes as described by table 5.4. All relevant states are calculated again, but only the ground state is displayed. Curves Nr. 1, 2, 4, 5 and 8 have large steps in their potential curves which is unphysical. So these active

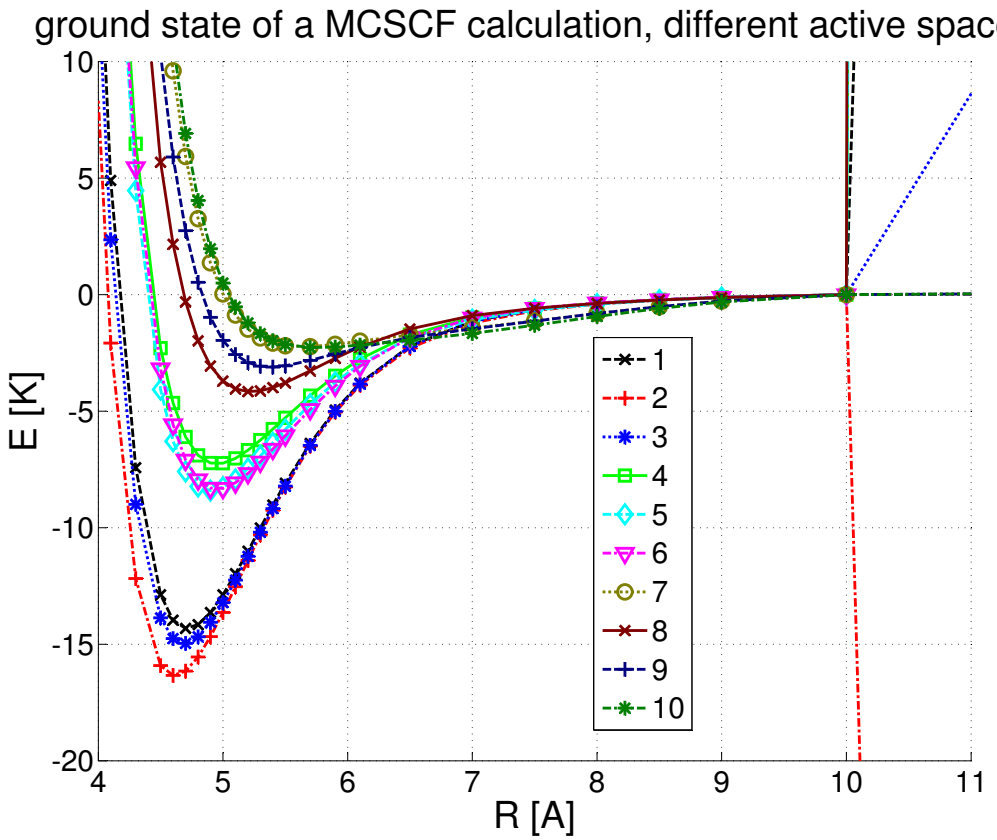

Figure 5.20: The ground state for a MCSCF calculation with an optimization of all states for different active spaces. The active spaces are shown in table 5.4. All curves have been set to zero at 10 $\AA$. This is a detail of figure 5.19. Some curves show unphysical steps.

spaces describe the system insufficiently. Curve number 3 also contains such a step, although it is much smaller.

In the end the active space of Nr. 7 was selected for further calculations. Its results are shown in the figures 5.21 and 5.22.

The following additional attempts were made to improve the results. Additional states were included and weights were used for the state averaging. However, no significant improvement in the description of the CrHe system was obtained. Therefore, these approaches were abandoned.

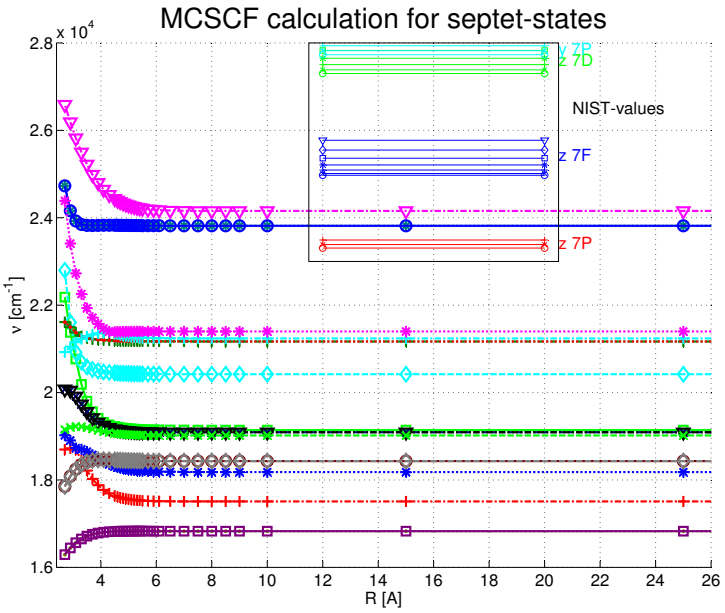

Figure 5.21: The MCSCF results for several septet-states are displayed. The active space of Nr. 7 was used and the aug-cc-pVTZ-DK basis set. The energy difference to the ground state can be seen, which should approach the NIST-values for large distances. The NIST-values are also shown in the figure. Neither level separation, nor absolute energy differences are reproduced well.

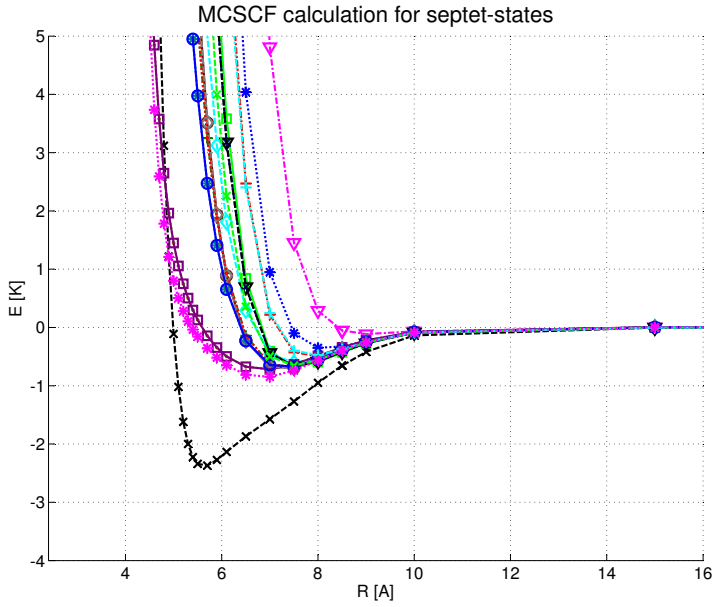

Figure 5.22: The MCSCF results for several septet-states are displayed. The active space of Nr. 7 was used and the aug-cc-pVTZ-DK basis set. All curves have been set to zero at 100 $\mathring{A}$. The potentials of the different states can be compared.

5.2.3 Potential Curves from MRCI

The figures 5.23, 5.24, 5.25, and 5.26 show the excited states of CrHe for two different calculations.

The first calculation was done with the aug-cc-pwCVTZ-DK basis set. In the MCSCF calculation a total number of (10 / 4 / 4 / 1) orbitals and (6 / 2 / 2 / 0) closed orbitals were used. The active space was increased in the MRCI calculation to (12 / 5 / 5 / 2) total orbitals but the closed orbitals were kept. The results for this calculation are shown in the figures 5.23 and 5.25.

The second calculation was done with the aug-cc-pVTZ-DK basis set, which showed more promising ground state potentials. The orbital numbers for the MCSCF calculation were (12 / 5 / 5 / 2) and (6 / 2 / 2 / 0). In the MRCI calculation a total of (12 / 5 / 5 / 2) orbitals was used with (5 / 2 / 2 / 0) closed ones. The results for this calculation can be found in the figures 5.24 and 5.26.

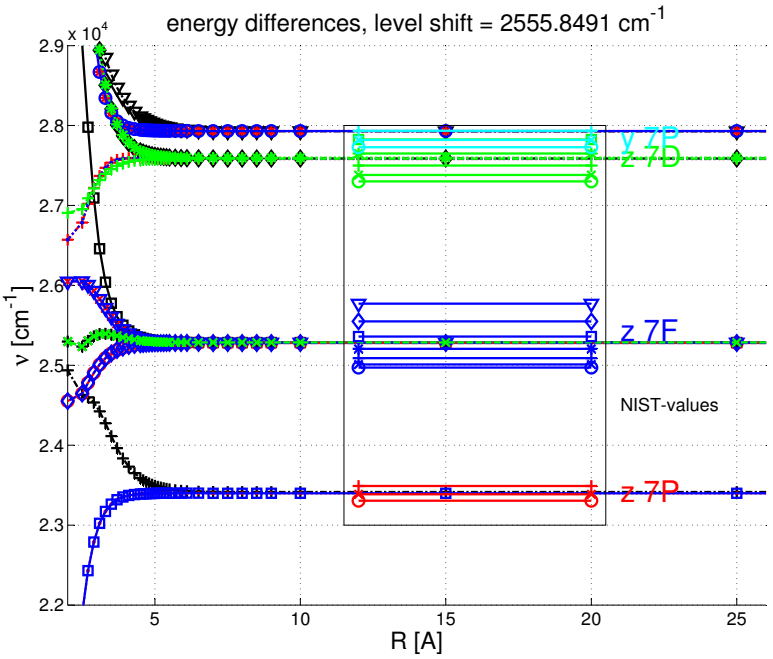

Figure 5.23: The MRCI results for several septet-states are displayed calculated with the first approach. The energy difference to the ground state can be seen, which should approach the NIST-values for large distances. The NIST-values are also shown in the figure. The energy separation is reproduced quite well. The curves have been shifted together to get a better agreement with the NIST-data. The level shift to larger differences is shown.

The basis sets were differently accurate in describing certain properties of the system. By comparing figure 5.23 with 5.24 it is obvious that the first calculation reproduces the experimental level separation of the excited states quite well. In contrast the total energy differences are further away from the NIST-values for the first calculation, which you can see if you compare the level shifts.

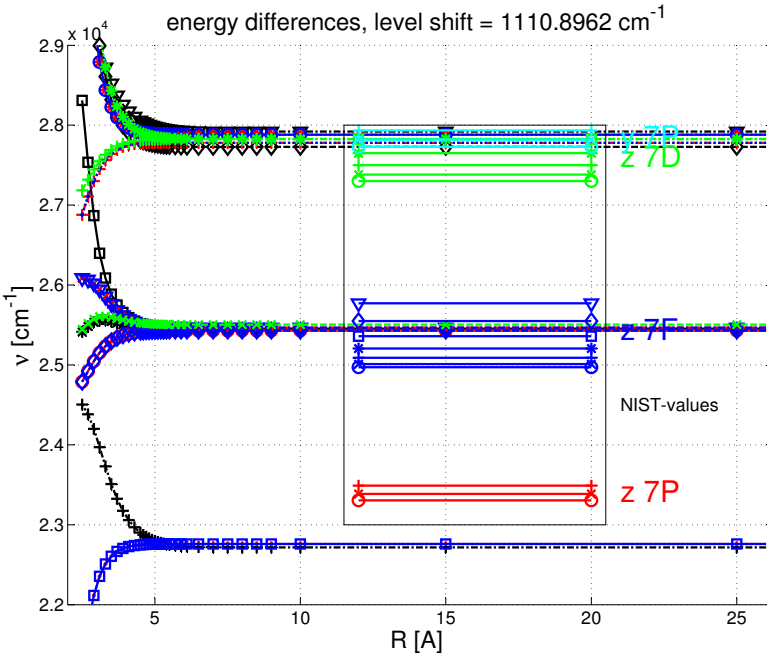

Figure 5.24: The MRCI results for several septet-states are displayed calculated with the second approach. The energy difference to the ground state can be seen, which should approach the NIST-values for large distances. The NIST-values are also shown in the figure. The energy separation is not reproduced accurately. Higher states are difficult to distinguish. The curves have been shifted together to get a better agreement with the NIST-data. The level shift to larger differences is shown.

By taking a look at figure 5.25 it can be observed that the first calculation completely fails in describing the interaction with the helium. All curves show the same oscillating behaviour, even the known groundstate. So the second calculation produces the more promising results.

These calculations were by far the most time consuming ones. They required a few weeks and the most costly part was the MRCI calculation. Additionally the spin-orbit operator was evaluated and these results can be found in the section 5.2.4.

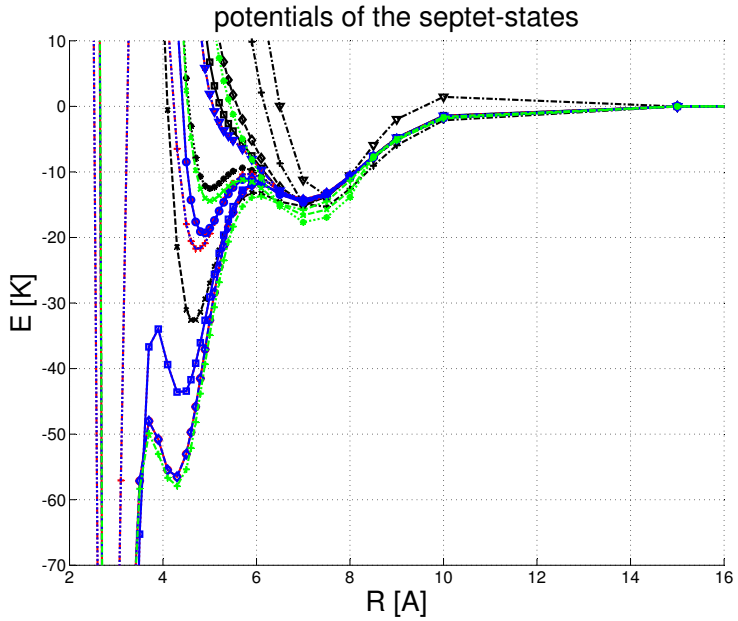

Figure 5.25: The MRCI results for several septet-states are displayed calculated with the first approach. All curves have been set to zero at 100 $\mathring{A}$ to be able to compare the potentials. Collective oscillations can be observed, an unphysical behaviour.

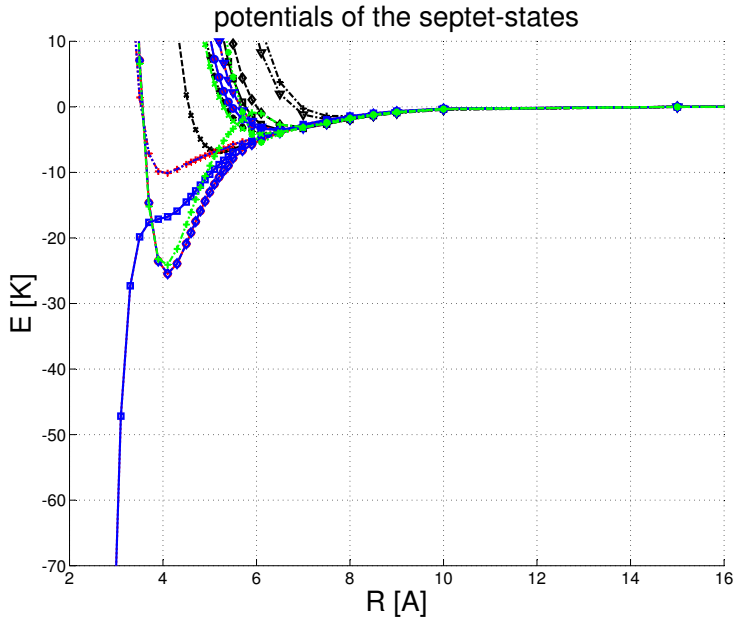

Figure 5.26: The MRCI results for several septet-states are displayed calculated with the second approach. All curves have been set to zero at 100 $\mathring{A}$ to be able to compare the potentials.

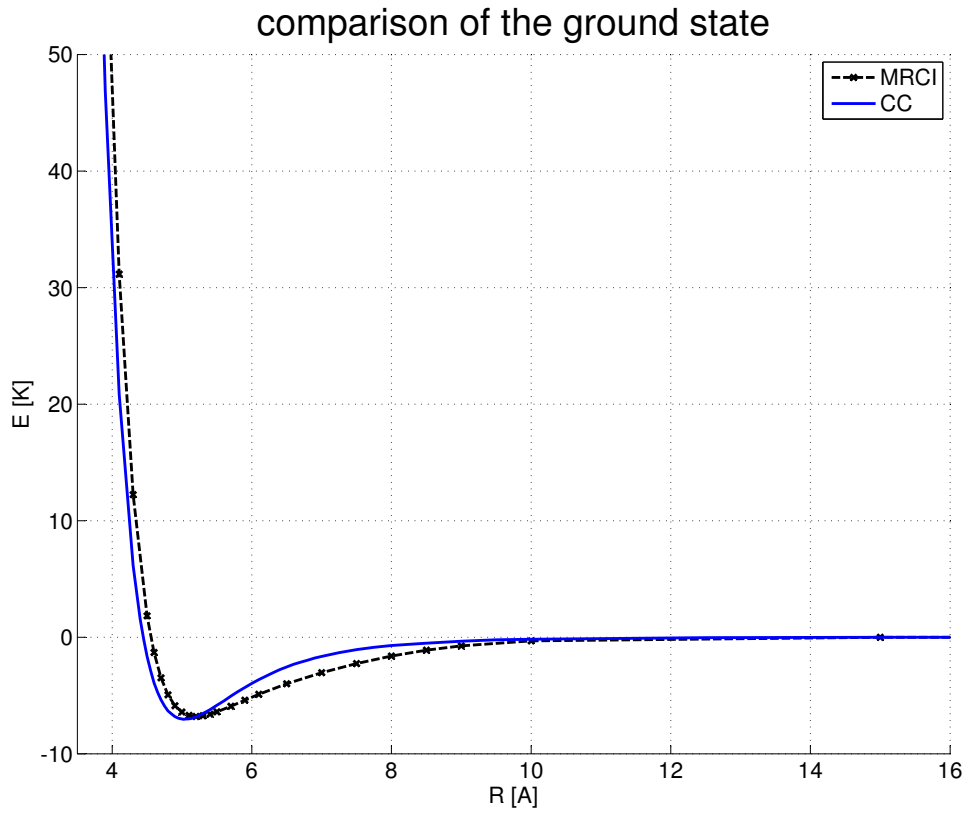

Figure 5.27: The ground state for the multistate MRCI calculation (the second calculation, figure 5.26) is compared with the extrapolated CC curve (figure 5.12).

A direct comparison of the ground state from the state-averaged MRCI calculation of this section and the final result for the CC calculation in section 5.1.4 is made in figure 5.27. There are differences between the curves, nevertheless they seem to be quite similar. The coupled cluster method is corrected with the counterpoise correction. Additionally the CC calculations include the Douglas-Kroll correction which might explain the shift of the potential minimum. The inclusion of the Douglas-Kroll correction shifts the potential slightly as can be seen in section 5.1.3. The form of the potential also seems to be changed in the state-averaged MRCI calculation.

5.2.4 Potential Curves with Spin-Orbit Coupling (SO)

Based on the calculations explained in the last section the Breit-Pauli operator for spin-orbit coupling was evaluated and the states are displayed in the figures 5.28, 5.29 5.30 and 5.31.

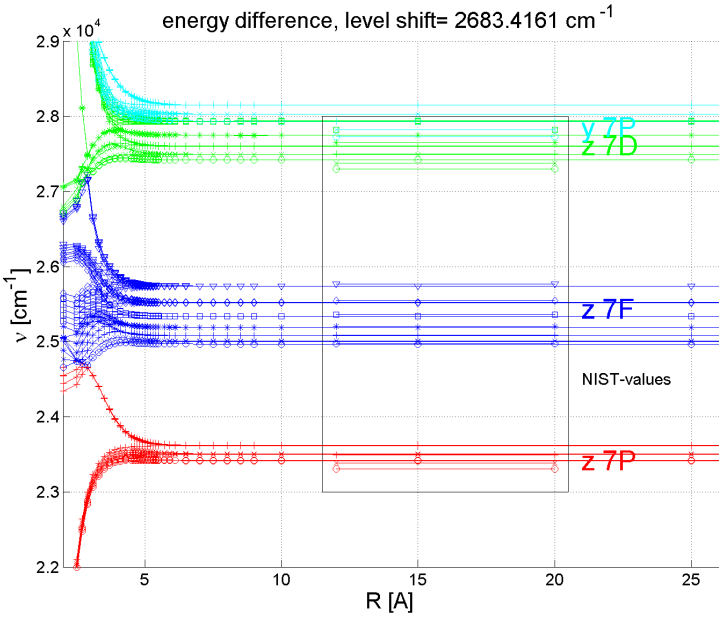

Figure 5.28: The results for several septet-states are displayed calculated with the first approach with the Breit-Pauli operator. The energy difference to the ground state can be seen, which should approach the NIST-values for large distances. The NIST-values are also shown in the figure. The energy splitting is reproduced quite well. The curves have been shifted together to get a better agreement with the NIST-data. The level shift to larger energy differences is shown.

Similar conclusions as in section 5.2.3 can be drawn. The first calculations describe the level splitting better, see figures 5.28 and 5.29. This is very obvious as the states y^7p and z^7D cannot be distinguished for the second calculation.

The first calculation obviously fails to describe the potentials. All states oscillate strongly and combined, see figure 5.30. The second calculation shows different potentials with different minima (figure 5.31). No collective behaviour can be seen, but some states show strange changes in their potential curves.

The different states show frequent level crossings, especially if the CrHe distance gets small. These crossings make associations of the states nearly impossible. It is next to impossible to distinguish the states for these calculations with He, especially if the atoms get close.

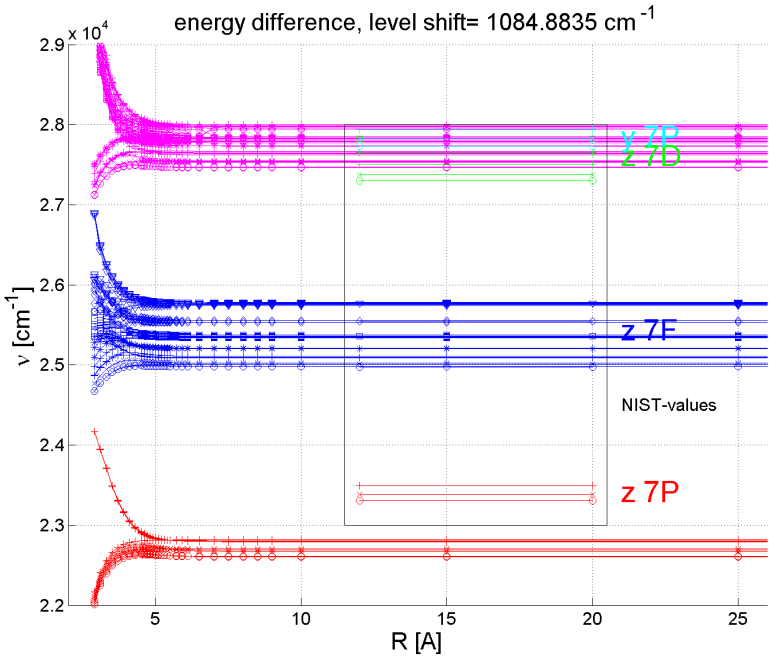

Figure 5.29: The results for several septet-states are displayed calculated with the second approach with the Breit-Pauli operator. The energy difference to the ground state can be seen, which should approach the NIST-values for large distances. The NIST-values are also shown in the figure. The energy splitting is not reproduced accurately. Higher states are difficult to distinguish. The curves have been shifted together to get a better agreement with the NIST-data. The level shift to larger energy differences is shown.

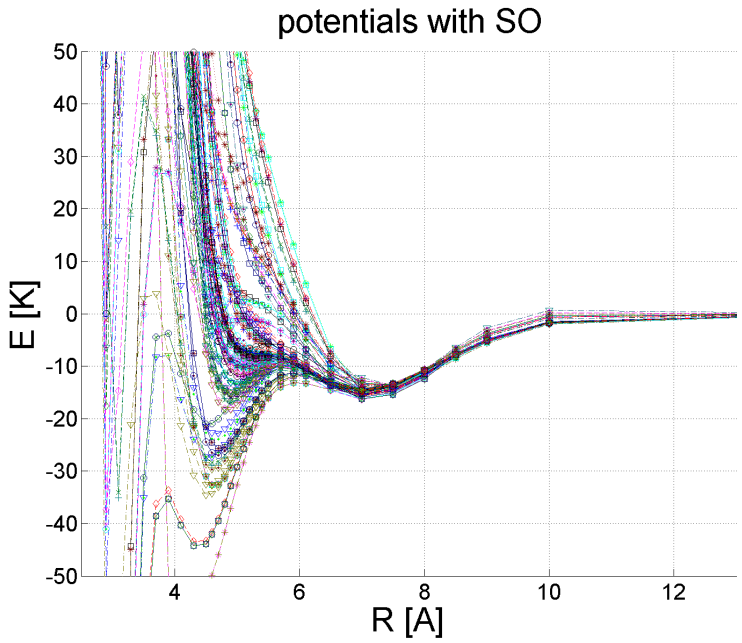

Figure 5.30: The SO results for several septet-states are displayed calculated with the first approach. All curves have been set to zero at 100 $\AA$ to be able to compare the potentials. Collective oscillations can be observed, a unphysical behaviour.

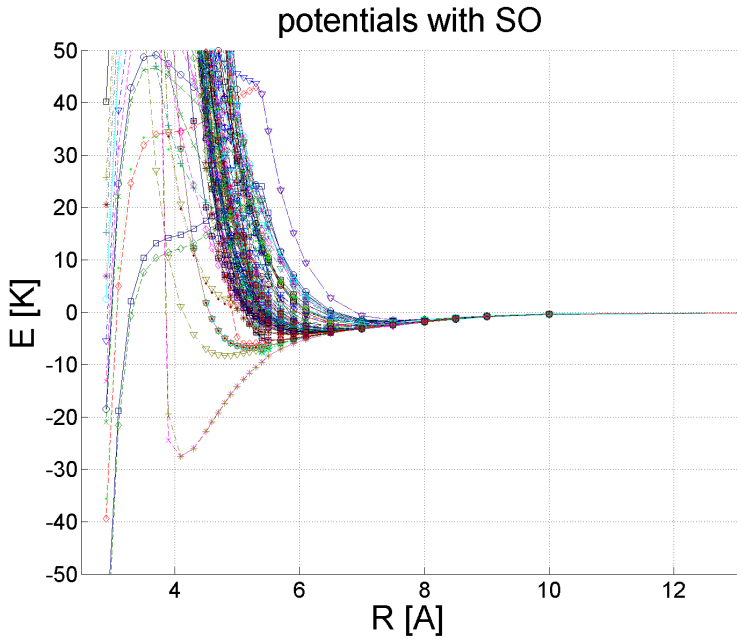

Figure 5.31: The SO results for several septet-states are displayed calculated with the second approach. All curves have been set to zero at 100 $\AA$ to be able to compare the potentials. Different potential minima can be determined. For certain states there is a sudden change from an ascending to descending potential.

5.2.5 Dipole Moment and Transition Probability

For the Cr atom itself a transition between states of different multiplicities is forbidden. This rule no longer needs to be fulfilled, if there is an additional interaction between Cr and He. Nevertheless, it still holds quite well and so the investigation of the excited state potentials of the diatomic molecule was also restricted to the septet-manifold.

Details on the symmetry numeration and other symmetry considerations can be found in section 4.4.

sym.	st.	$\hat{d}$	E_1 $[cm^{-1}]$	$\hat{d}_1$ $[a.u.]$	$\left\|\hat{d}_1\right\|^2$ $[a.u.]$	E_2 $[cm^{-1}]$	$\hat{d}_2$ $[a.u.]$	$\left\|\hat{d}_2\right\|^2$ $[a.u.]$
2	1	x	5741.37		0.00E+00	16827.83	4.24E-02	1.79E-03
2	2	x	5769.88	1.31E-02	1.71E-04	18442.19	3.33E-01	1.11E-01
2	3	x	6353.91	-3.25E-01	1.06E-01	19118.08	2.51E-02	6.28E-04
2	4	x	8005.26	-2.66E-03	7.06E-06	21178.88	1.50E-01	2.25E-02
2	5	x	19100.34	2.08E+00	4.34E+00	23822.27	2.18E+00	4.75E+00
3	1	y	5741.37		0.00E+00	16827.83	4.24E-02	1.79E-03
3	2	y	5769.88	-1.31E-02	1.71E-04	18442.19	-3.33E-01	1.11E-01
3	3	y	6353.91	3.25E-01	1.06E-01	19118.08	-2.51E-02	6.28E-04
3	4	y	8005.26	2.66E-03	7.06E-06	21178.88	-1.50E-01	2.25E-02
3	5	y	19100.34	-2.08E+00	4.34E+00	23822.27	-2.18E+00	4.75E+00
1	2	z	5758.24		0.00E+00	17558.91	0.00E+00	0.00E+00
1	3	z	5774.20	1.70E-02	2.88E-04	18237.88	4.02E-01	1.62E-01
1	4	z	6362.90	-3.29E-01	1.08E-01	19172.16	-1.01E-03	1.02E-06
1	6	z	19290.93	-2.08E+00	4.33E+00	24285.74	-2.20E+00	4.85E+00

Table 5.5: The excited states and transition properties for CrHe from a MCSCF calculation are shown. Symmetry (sym.) gives the irreducible representation of the state. The column states (st.) contains a numbering of the states in their respective symmetries. The third column shows the direction of the dipole operator which gives a non-zero contribution to the transition dipole moment. E_1 are the energy differences of the states in the first calculation, E_2 in the second calculation. $\hat{d}_1$ and $\hat{d}_2$ are the dipole moments in atomic units $(a_0 \cdot e)$ for the first and second calculation, respectively. Their squares can also be found in the table in atomic units $(a_0^2 \cdot e^2)$

Table 5.5 contains the dipole transition moments for the excited state of the diatomic molecule. As in the atomic case a distinct assignment of the calculated states is difficult for the MCSCF calculation.

Since the dipole moment depends on the interatomic distance a value for the distance needs to be selected. In tables 5.5 and 5.6 the results for 5 $\AA$ are displayed.

Again two calculations with different options were performed. The first calculation is based on the aug-cc-pwCVTZ-DK basis set. The MCSCF calculation contained (10 / 4 / 4 / 1) total and (6 / 2 / 2 / 0) closed orbitals, while the MRCI calculation was extended to (12 / 5 / 5 / 2) total and (6 / 2 / 2 / 0) closed orbitals. The second calculation with the aug-cc-pVTZ-DK basis set used an active space of (12 / 5 / 5 / 2) total and (6 / 2 / 2 / 0) closed orbitals for both calculations, MRCI and MCSCF.

Table 5.6 contains the dipole transition moments of the MRCI calculation of the diatomic molecule. The states are distinguishable and have been assigned. In comparing table 5.6 and table 4.3 an estimation of the influence of the He atom on the transition probability of the Cr

terms	sym.	st.	$\hat{d}$	$E_1\ [cm^{-1}]$	$\hat{d}_1\ [a.u.]$	$\left\|\hat{d}_1\right\|^2\ [a.u.]$	$E_2\ [cm^{-1}]$	$\hat{d}_2\ [a.u.]$	$\left\|\hat{d}_2\right\|^2\ [a.u.]$
z 7p	1	2	z	20937.26	-1.04E+00	1.07E+00	21687.90	-1.18E+00	1.39E+00
	2	1	x	20841.11	1.07E+00	1.14E+00	21646.66	1.20E+00	1.45E+00
	3	1	y	20841.11	-1.07E+00	1.14E+00	21646.66	-1.20E+00	1.45E+00
z 7f	1	3	z	22736.98	-7.14E-06	5.09E-11	24331.31	3.79E-06	1.44E-11
	1	4	z	22751.73	2.96E-02	8.77E-04	24366.45	-9.23E-03	8.52E-05
	2	2	x	22719.30	1.62E-02	2.64E-04	24314.61	1.71E-02	2.91E-04
	2	3	x	22748.64	2.89E-02	8.38E-04	24373.54	9.12E-03	8.31E-05
	3	2	y	22719.30	1.62E-02	2.64E-04	24314.61	1.71E-02	2.91E-04
	3	3	y	22748.64	-2.89E-02	8.38E-04	24373.54	-9.12E-03	8.31E-05
z 7d	1	5	z	25065.04	-3.06E-06	9.36E-12	26648.35	1.09E-05	1.20E-10
	2	4	x	25031.43	7.75E-02	6.01E-03	26668.01	-4.74E-01	2.25E-01
	3	4	y	25031.43	-7.75E-02	6.01E-03	26668.01	4.74E-01	2.25E-01
y 7p	1	6	z	25468.08	-1.98E+00	3.94E+00	26871.86	-1.89E+00	3.57E+00
	2	5	x	25380.69	1.98E+00	3.91E+00	26781.96	-1.80E+00	3.23E+00
	3	5	y	25380.69	-1.98E+00	3.91E+00	26781.96	1.80E+00	3.23E+00

Table 5.6: The excited states and transition properties for CrHe from a MRCI calculation are displayed. The headings are described in table 5.5. An additional column was added in the front for the term designations.

can be made. There is no distinctive feature, but all transition probabilities seem to decrease. This decrease seems more pronounced for the $z\ ^7P$ state than for the $y\ ^7P$ state.

This trend can also be observed in figure 5.32, where dipole transition moments for different distances are shown.

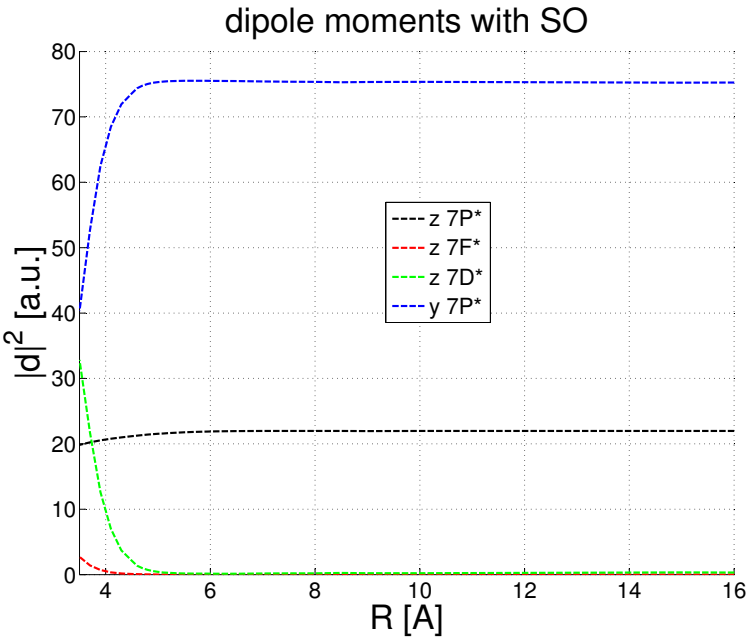

Figure 5.32: The results for several septet-states are displayed calculated with the first approach and the Breit-Pauli operator. This figure contains the dipole moments for the transitions in figure 5.30 and figure 5.28. All dipole moments belonging to one state were summed up to obtain these curves. The curve is shown for the region where clear designations are possible. The a. u. for the square of the dipole moment are $(a_0^2 \cdot e^2)$.

Chapter 6

Cr and a Superfliud He Nanodroplet

6.1 Ancilotto - Parameter

The position of Cr in or on He_N was an open question. Using the obtained parameters, predictions were made of the position of the dopant based on the Ancilotto-parameter λ_A (section 2.10). In table 6.1 the Ancilotto-parameter is displayed for several dopants. The parameters of the diatomic potential have been taken from various sources.

Quantum mechanical influences like the zero point energy also have an influence on the position of the dopant. The extent of these influences can be estimated by the de Boer quantum parameter (λ_{Boer}, section 2.10). A large value of this parameter means a strong effect. The dopant might be stabilised on the surface although its Ancilotto-parameter is above the threshold.

The He-value in table 6.1 refers to a ^{3}He atom on a ^{4}He droplet. H as well as He have strong quantum mechanical influences (large de Boer quantum parameter) and therefore they sit on the surface although the Ancilotto-parameter is above the threshold of 1.9.

Ions, especially cations, have large values of the Ancilotto-parameter, so they all are swallowed by the He_n. The ions unlike neutral atoms can polarize the He atoms and interact strongly with the cluster.

Most of the neutral alkali metal atoms and some neutral alkaline-earth metal atoms have been found to take a position on the surface of He_n. The position of Mg, which has a value closely to the threshold, is still not completely resolved [74, 89, 90]. Ca, also lying closely to the threshold, was determined to sit on the surface of He_n [91, 92].

dopant	ϵ_d $[K]$	r_{min} $\left[\mathring{A}\right]$	λ_A $[d.u.]$	m_d $[u]$	λ_{Boer} $[d.u.]$	source
H	6.80	3.70	1.93	1.0	20.59	[73]
H_2	14.21	3.44	3.75	2.0	5.70	[93]
^{3}He	11.00	2.97	2.51	4.0	4.94	[75]
Li	1.90	6.19	0.90	6.9	3.79	[73]
Na	1.70	6.41	0.84	23.0	1.19	[73]
Mg	3.31	5.60	1.42	24.3	0.76	[74]
Mg	7.19	5.10	2.81	24.3	0.42	[89]
K	1.40	7.18	0.77	39.1	0.68	[73]
Ca	4.17	7.40	2.37	40.1	0.21	[74]
Ca	4.93	5.90	2.23	40.1	0.28	[89]
Cu	8.13	4.62	2.88	63.5	0.17	[44]
Rb	1.40	7.33	0.79	85.5	0.30	[73]
Ag	17.11	4.54	5.96	107.8	0.05	[94]
Ag	9.80	4.64	3.49	107.8	0.08	[44]
Cs	1.20	7.73	0.71	132.9	0.20	[73]
Au	20.30	4.12	6.42	196.9	0.03	[44]
F-	249.46	2.89	55.38	19.0	0.05	[95]
Cl-	63.15	4.10	19.87	35.5	0.05	[95]
Cu-	6.29	6.61	3.19	63.5	0.11	[45]
Ag-	8.62	6.40	4.23	107.8	0.05	[45]
Au-	24.76	5.03	9.55	196.9	0.02	[45]
Li+	903.10	1.89	130.86	6.9	0.09	[95]
Li+	936.69	1.90	136.38	6.9	0.08	[96]
Na+	445.24	2.33	79.69	23.0	0.03	[95]
Na+	473.38	2.33	84.61	23.0	0.03	[96]
K+	211.57	2.91	47.23	39.1	0.03	[95]
K+	254.68	2.85	55.68	39.1	0.02	[96]
Cu+	1197.41	1.93	177.28	63.5	0.01	[45]
Rb+	204.32	3.10	48.59	85.5	0.01	[96]
Ag+	569.64	2.41	105.31	107.8	0.01	[45]
Cs+	168.35	3.38	43.65	132.9	0.01	[96]
Au+	565.32	2.44	105.81	196.9	0.00	[45]

Table 6.1: λ_{Boer} and λ_A are the parameters described in section 2.10. ϵ_d is depth of the potential and r_{min} the equilibrium distance. This two parameters were taken from various sources (source). Column m_d contains the mass of the dopant.

The previously obtained fit-parameters can now be used to make a prediction for Cr and Cr+ (table 6.2).

dopant	ϵ_d $[K]$	r_{min} $[\AA]$	λ_A $[d.u.]$	m_d $[u]$	λ_{Boer} $[d.u.]$	fit
Cr+	509.45	2.13	83.30	52.0	0.02	L.J.
Cr+	544.50	2.28	95.35	52.0	0.01	M.
Cr	6.87	5.05	2.66	52.0	0.21	L. J.
Cr	7.03	5.01	2.70	52.0	0.21	M.

Table 6.2: This table shows the Ancilotto-parameter for the calculated diatomic - potentials. The parameters have either been taken from a Lennard-Jones fit (L.J.) or a Morse fit (M), compare sections 3.4 and 5.1.6. The headings are explained in table 6.1.

The cation resides of course inside the superfluid droplet which is also confirmed by the Ancilotto-parameter and the de Boer-parameter. The neutral atom has values close to the threshold, similar to Mg. Simply using the Ancilotto-parameter is insufficient to make a reliable prediction for the Cr atom. Recent experimental and DFT results indicate a location of Cr inside the He_N.

6.1.1 Excited States

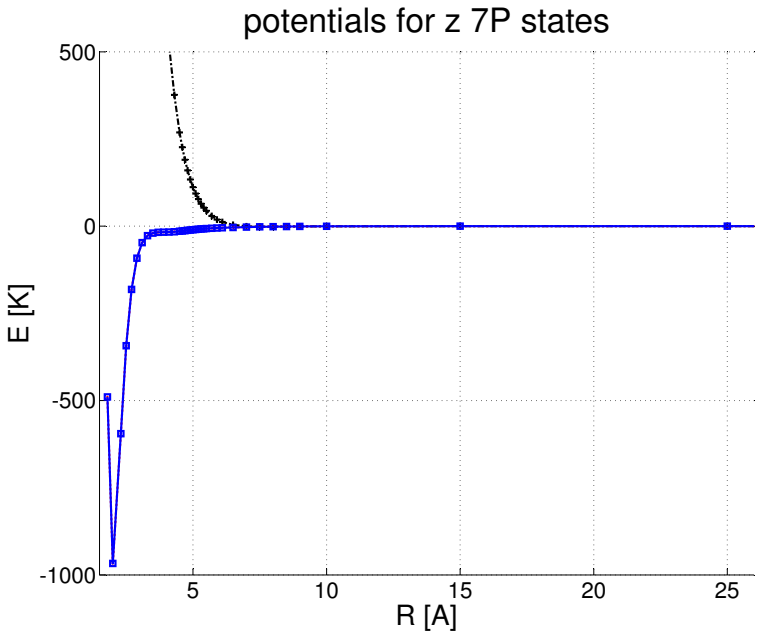

Figure 6.1: This is an extraction from figure 5.26. The potentials have been set to zero at 100 $\AA$. It shows the state $A\ ^7\Sigma$ (black) and $B\ ^7\Pi$ (red and blue).

Table 6.3 contains properties for the excited diatomic potentials and their Ancilotto-parameters. These properties were estimated from figure 6.1 and figure 6.2 which show both selected states from figure 5.26. The states $A\ ^7\Sigma$ and $B\ ^7\Pi$ arise from the atomic state z^7P and can be seen in figure 6.1. The states $C\ ^7\Sigma$ and $D\ ^7\Pi$ correspond to the atomic state

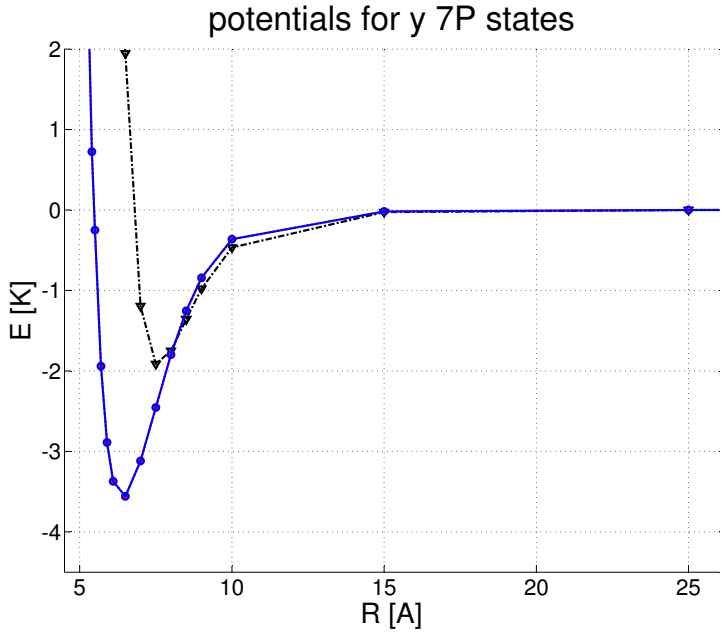

Figure 6.2: This is an extraction from figure 5.26. The potentials have been set to zero at 100 $\mathring{A}$. It shows the state $C\ ^7\Sigma$ (black) and $D\ ^7\Pi$ (red and blue).

state	ϵ_d $[K]$	r_{min} $[\mathring{A}]$	λ_A $[d.u.]$	m_d $[u]$	λ_{Boer} $[d.u.]$
$A\ ^7\Sigma$	1.43	8.0	0.88	52.0	0.40
$B\ ^7\Pi$	967.26	2.0	148.40	52.0	0.01
$C\ ^7\Sigma$	1.91	7.5	1.10	52.0	0.34
$D\ ^7\Pi$	3.56	6.5	1.77	52.0	0.25

Table 6.3: This table shows the Ancilotto-parameter for the calculated exited diatomic potentials. The parameter have been determined with figure 6.1 and 6.2. The headings are explained in table 6.1. Different states are compared here instead of different dopants.

y^7P and are displayed in figure 6.2. The letters A, B, C, and D were added in front of the terms for better identification. All states except $B\ ^7\Pi$ show less bonding and would clearly favour a position on the surface of the He_N. The state $B\ ^7\Pi$ is more strongly bound than the ground state, but it has a certain symmetry that could influence the behaviour. So far the calculations have not determined the potential minimum very accurately. The table shows the values of the deepest point calculated up to now.

Further analysis is therefore necessary to determine the location of the neutral Cr on the He_N and the behaviour of the states $A\ ^7\Sigma$ and $B\ ^7\Pi$. This can be done by a special DFT-code which captures the properties of a superfluid He_N. This is done by my colleague Martin Ratschek with a DFT-code that applies the Orsay-Trento functional [97].

Chapter 7

Conclusion

Within this thesis the interaction between chromium and helium was investigated. The ground state, the cation and excited states have been calculated with different ab initio methods. The results of these calculations were afterwards used to make predictions for the behaviour of the dopants on a superfluid helium nanodroplet. Besides these calculations the dipole transition moments were calculated for the excited states.

The first part of the investigation was a study of the CrHe cation. Experimental and theoretical results were already known [77, 78, 79]. So these calculations were a first attempt to compare the performance of different basis sets and methods. By comparing the results with the known data an estimation of the accuracy of different approaches can be achieved. The calculations yielded results similar to the known ones, but an exact agreement was not found. An additional rovibrational analysis was performed and the results are in good agreement with the theoretical results of Wilson [78, 79].

The second part of the investigation was focused on the Cr atom as a test system for the CrHe diatomic molecule at large distances. Especially optical properties were investigated extensively because they are significant for the experiment. The excited states were calculated with the ROHF, MCSCF and MRCI methods. The calculated level splittings are in quite good agreement with the experimental level splittings from the NIST-database [1]. Especially, the aug-cc-pwCV5Z-DK basis set reproduces the spectral features very well. The absolute level differences to the ground state, however, were not reproduced as accurately as the level splitting. But after including spin-orbit coupling with the Breit-Pauli operator good agreement was found. The transition dipole moment was also calculated since it corresponds to the experimental intensities of the spectrum. The order of the different states was reproduced, but the absolute values differed.

The third part of the investigation was focused on the CrHe diatomic molecule. First, its ground state was determined as accurately as possible in an extensive study. Different basis sets were compared and in the end the aug-cc-pwCVNZ-DK basis set family was selected. Also the self-made basis set and bond functions were attempted, but discarded. The ROHF, MCSCF, CI, RS, and CC methods were used for calculating the ground state. The CC

method seemed to yield the most promising results. Also relativistic corrections proved to be necessary and were included by the Douglas-Kroll formalism. The rovibrational state of the resulting potential was determined to have a bonding energy of about $-1\ cm^{-1}$.

Second, the excited states of the CrHe diatomic molecule have been studied. Most of the calculations were done with two basis sets. It was observed that different basis sets describe different properties of the system better. The aug-cc-pwCVTZ-DK basis set was very good at reproducing optical properties, like the level splitting. Especially the inclusion of spin-orbit coupling made this obvious. In contrast the aug-cc-pVTZ-DK basis set seemed to capture the CrHe interaction better, probably because the He atom was described in all calculations with a basis set of the same type. These differences can be observed in section 5.2.3. The dipole transition moments were calculated for the excited states of the CrHe diatomic molecule. No significant changes in comparison to the atomic dipole transition moments could be determined for a distance of 5 $\mathring{A}$.

In the end the results from the previous chapters were applied to deducing the Ancilotto-parameter. The CrHe cation clearly sits inside the He_N. For the neutral diatomic molecule a prediction is rather difficult. The parameters of the CrHe potential give a value of the Ancilotto-parameter close to the threshold between surface residing and in the droplet sitting dopants. The excited states show varying behaviour. The most important state, the y^7P state, is clearly very weakly bound and the Cr would sit on the surface of He_N. For the z^7P state different symmetries show diverse behaviour. One state is extremely weakly bound. The other two states show bonding in the same order of magnitude as the cation. The prediction of its behaviour will require more sophisticated approaches. The transition dipole moments of these two states are barely influenced by the He environment, but their potentials show large differences. An interesting question is, if these differences influence the experimental findings.

Outlook

An investigation of other multiplicities seems important. So far only the septet-multiplicity was investigated. The interaction between the different multiplicities might also be interesting.

As already mentioned a more sophisticated analysis using a He-DFT code will be done with the obtained potential curves. This should give a conclusive prediction of the location of Cr on or inside He_N. Also the behaviour of the excited state with the symmetry dependent potentials (z^7P) might be investigated.

Bibliography

[1] Y. Ralchenko, A.E. Kramida, J. Reader, and NIST ASD Team (2011). Nist atomic spectra database (ver. 4.1.0), [online]. *National Institute of Standards and Technology, Gaithersburg, MD*, 2011. xix, xx, 34, 37, 42, 51, 52, 73, 93, 104, 105, 109

[2] J. Sugar and C. Corliss. Atomic-energy levels of the iron-period elements - potassium through nickel. *Journal of Physical and Chemical Reference Data*, 14:1–&, 1985. xix, 51, 105

[3] D. Feller. The role of databases in support of computational chemistry calculations. *Journal of Computational Chemistry*, 17(13):1571–1586, October 1996. xx, 43

[4] K. L. Schuchardt, B. T. Didier, T. Elsethagen, L. S. Sun, V. Gurumoorthi, J. Chase, J. Li, and T. L. Windus. Basis set exchange: A community database for computational sciences. *Journal of Chemical Information and Modeling*, 47(3):1045–1052, May 2007. xx, 9, 43

[5] M. Theisen, F. Lackner, and W. E. Ernst. Forming Rb(+) snowballs in the center of he nanodroplets. *Physical Chemistry Chemical Physics*, 12(45):14861–14863, 2010. 2

[6] M. Theisen, F. Lackner, G. Krois, and W. E. Ernst. Ionization thresholds of alkali metal atoms on helium droplets. *Journal of Physical Chemistry Letters*, 2(21):2778–2782, November 2011. 2

[7] M. Theisen, F. Lackner, and W. E. Ernst. Cs atoms on helium nanodroplets and the immersion of Cs(+) into the nanodroplet. *Journal of Chemical Physics*, 135(7):074306, August 2011. 2

[8] G. Auböck, J. Nagl, C. Callegari, and W. E. Ernst. Electron spin pumping of Rb atoms on He nanodroplets via nondestructive optical excitation. *Phys. Rev. Lett.*, 101(3):035301–&, July 2008. 2

[9] A. W. Hauser. The electronic structure of alkali trimers in their doublet and quartet manifolds: shell models and quantum chemistry calculations. Dissertation, Graz University of Technology, 2009. 2

[10] M. Koch. Magnetic resonance spectroscopy of single alkali-metal atoms isolated in superfluid helium nanodroplets. Dissertation, Graz University of Technology, 2009. 2

[11] Thomas Gruber. Ab-initio Spindichten alkalimetaldotierter Heliumcluster. Masterarbeit, Graz University of Technology, 2011. 2

[12] M. Ratschek, M. Koch, and W. E. Ernst. Doping helium nanodroplets with high temperature metals: Formation of chromium clusters. *Journal of Chemical Physics*, 136(10):104201, March 2012. 2

[13] M. Ratschek. Doping helium droplets: Development of a high-temperature pickup source. Master thesis, Graz University of Technology, 2010. 2

[14] M. Hasewend. Photoionization spectroscopy on single Cr atoms in superfluid helium nanodroplets. Master thesis, Graz University of Technology, 2012. 2

[15] F. W. Payne, W. Jiang, and L. A. Bloomfield. Magnetism and magnetic isomers in free chromium clusters. *Physical Review Letters*, 97(19):193401–&, November 2006. 2, 42

[16] P. I. Premovic, J. Ciesielczuk, G. Bzowska, and M. G. Dordevic. Geochemistry and electron spin resonance of hydrothermal dickite (nowa ruda, lower silesia, poland): vanadium and chromium. *Geologica Carpathica*, 63(3):241–252, June 2012. 2

[17] V. Singh, R. P. S. Chakradhar, J. L. Rao, K. Al-Shamery, M. Haase, and Y. D. Jho. Electron paramagnetic resonance and photoluminescence properties of alpha-Al2O3:Cr3+ phosphors. *Applied Physics B-Lasers and Optics*, 107(2):489–495, May 2012. 2

[18] S. Khamlich, V. V. Srinivasu, O. Nemraoui, R. McCrindle, N. Cingo, and M. Maaza. Electron spin resonance study of alpha-Cr2O3 and Cr2O3 . nH(2)O quasi-spherical nanoparticles. *Nanoscience and Nanotechnology Letters*, 3(4):550–555, August 2011. 2

[19] T. Ishiyama, T. Tsurukawa, Y. Mori, Y. Kamiura, and Y. Yamashita. Electron spin resonance of chromium-platinum pair in silicon. *Japanese Journal of Applied Physics*, 50(8):081302, August 2011. 2

[20] E. Baibekov, I. Kurkin, M. Gafurov, B. Endeward, R. Rakhmatullin, and G. Mamin. Coherence times and rabi oscillations in CaWO4:Cr5+ crystal. *Journal of Magnetic Resonance*, 209(1):61–68, March 2011. 2

[21] S. B. M. Krishna, P. M. V. Teja, and D. K. Rao. Role of chromium ion valence states in ZnO-As2O3-Sb2O3 glass system by means of spectroscopic and dielectric studies. *Materials Research Bulletin*, 45(12):1783–1791, December 2010. 2

[22] D. Soundararajan, D. Mangalaraj, D. Nataraj, L. Dorosinskii, J. Santoyo-Salazar, and M. J. Riley. Magnetic and magneto-optical studies on Zn 1-xCr xTe (x = 0.05) films grown on glass substrate. *Journal of Magnetism and Magnetic Materials*, 321(24):4108–14, 2009. 2

[23] R. M. El-Shazly. Synthesis and characterization of 3-methyl-5-oxo-N,1-diphenyl-4, 5-dihydro-1-H-pyrazole-4-carbothioamide and its metal complexes. *Spectrochimica Acta Part A-molecular and Biomolecular Spectroscopy*, 74(1):259–264, September 2009. 2

[24] I. V. Hertel and C.-P. Schulz. *Atome, Moleküle und optische Physik 1.* Springer-Verlag Berlin Heidelberg, 2008. 2, 33

[25] I. V. Hertel and C.-P. Schulz. *Atome, Moleküle und optische Physik 2.* Springer-Verlag Berlin Heidelberg, 2008. 2, 28

[26] H. Haken and H. C. Wolf. *Atom- und Quantenphysik*. Springer-Verlag Berlin Heidelberg, 1996. 2

[27] H. Haken and H. C. Wolf. *Molekülphysik und Quantenchemie*. Springer-Verlag Berlin Heidelberg, 2006. 2

[28] H.-J. Werner, P. J. Knowles, G. Knizia, F. R. Manby, M. Schütz, P. Celani, T. Korona, R. Lindh, A. Mitrushenkov, G. Rauhut, K. R. Shamasundar, T. B. Adler, R. D. Amos, A. Bernhardsson, A. Berning, D. L. Cooper, M. J. O. Deegan, A. J. Dobbyn, F. Eckert, E. Goll, C. Hampel, A. Hesselmann, G. Hetzer, T. Hrenar, G. Jansen, C. Köppl, Y. Liu, A. W. Lloyd, R. A. Mata, A. J. May, S. J. McNicholas, W. Meyer, M. E. Mura, A. Nicklass, D. P. O'Neill, P. Palmieri, K. Pflüger, R. Pitzer, M. Reiher, T. Shiozaki, H. Stoll, A. J. Stone, R. Tarroni, T. Thorsteinsson, M. Wang, and A. Wolf. Molpro, version 2010.1, a package of ab initio programs, 2010. see http://www.molpro.net/. 7

[29] Frank Jensen. *Introduction to Computational Chemistry*. John Wiley & Sons, Ltd, 2007. 7, 11, 12

[30] T. Helgaker, W. Klopper, H. Koch, and J. Noga. Basis-set convergence of correlated calculations on water. *Journal of Chemical Physics*, 106(23):9639–9646, June 1997. 11

[31] K. L. Bak, P. Jorgensen, J. Olsen, T. Helgaker, and W. Klopper. Accuracy of atomization energies and reaction enthalpies in standard and extrapolated electronic wave function/basis set calculations. *Journal of Chemical Physics*, 112(21):9229–9242, June 2000. 11, 12

[32] A. Halkier, T. Helgaker, P. Jorgensen, W. Klopper, H. Koch, J. Olsen, and A. K. Wilson. Basis-set convergence in correlated calculations on Ne, N-2, and H2O. *Chemical Physics Letters*, 286(3-4):243–252, April 1998. 12, 63

[33] A. Halkier, T. Helgaker, P. Jorgensen, W. Klopper, and J. Olsen. Basis-set convergence of the energy in molecular hartree-fock calculations. *Chemical Physics Letters*, 302(5-6):437–446, March 1999. 12, 63

[34] J. M. L. Martin. Ab initio total atomization energies of small molecules - towards the basis set limit. *Chemical Physics Letters*, 259(5-6):669–678, September 1996. 12, 63

[35] D. Feller and J. A. Sordo. A CCSDT study of the effects of higher order correlation on spectroscopic constants. I. first row diatomic hydrides. *Journal of Chemical Physics*, 112(13):5604–5610, April 2000. 12, 64

[36] M. P. de Lara-Castells, R. V. Krems, A. A. Buchachenko, G. Delgado-Barrio, and P. Villarreal. Complete basis set extrapolation limit for electronic structure calculations: Energetic and nonenergetic properties of HeBr and HeBr2 van der waals dimers. *Journal of Chemical Physics*, 115(22):10438–10449, December 2001. 12, 64

[37] A. J. C. Varandas. Extrapolating to the one-electron basis-set limit in electronic structure calculations. *Journal of Chemical Physics*, 126(24):244105, June 2007. 12

[38] T. G. Williams, N. J. DeYonker, and A. K. Wilson. Hartree-fock complete basis set limit properties for transition metal diatomics. *Journal of Chemical Physics*, 128(4):044101, January 2008. 12

[39] D. Feller, K. A. Peterson, and J. G. Hill. On the effectiveness of ccsd(t) complete basis set extrapolations for atomization energies. *Journal of Chemical Physics*, 135(4):044102, July 2011. 12, 63, 64

[40] S. F. Boys and F. Bernardi. Calculation of small molecular interactions by differences of separate total energies - some procedures with reduced errors. *Molecular Physics*, 19(4):553–&, 1970. 12

[41] M. Mladenovic, M. Lewerenz, G. Cilpa, P. Rosmus, and G. Chambaud. Exploration of the NH3-H-2 van der Waals interaction by high level ab initio calculations. *Chemical Physics*, 346(1-3):237–246, May 2008. 13

[42] F. M. Tao. An accurate ab-initio potential-energy surface of the He-H2 interaction. *Journal of Chemical Physics*, 100(7):4947–4954, April 1994. 13

[43] F. M. Tao, Z. R. Li, and Y. K. Pan. An accurate ab initio potential energy surface of He-H2O. *Chemical Physics Letters*, 255(1-3):179–186, June 1996. 13, 37

[44] X. F. Tong, C. L. Yang, Y. P. An, M. S. Wang, X. G. Ma, and D. H. Wang. Theoretical characteristics of the bound states of M-X complexes (M=Cu, Ag, and Au, and X=He, Ne, and Ar). *Journal of Chemical Physics*, 131(24):244304, December 2009. 13, 37, 90

[45] X. F. Tong, C. L. Yang, M. S. Wang, X. G. Ma, and D. H. Wang. Interactions of M(z)-X complexes (M = Cu, Ag, and Au; X = He, Ne, and Ar; and z = +/- 1). *Journal of Chemical Physics*, 134(2):024306, January 2011. 13, 90

[46] R. Polly, H. J. Werner, F. R. Manby, and P. J. Knowles. Fast Hartree-Fock theory using local density fitting approximations. *Molecular Physics*, 102(21-22):2311–2321, November 2004. 18

[47] P. J. Knowles and H.-J. Werner. An efficient second order MCSCF method for long configuration expansions. *Chem. Phys. Letters*, 115:259–267, 1985. 19

[48] H.-J. Werner and P. J. Knowles. A second order MCSCF method with optimum convergence. *J. Chem. Phys.*, 82:5053, 1985. 19

[49] H. J. Werner and W. Meyer. A quadratically convergent multiconfiguration-self-consistent field method with simultaneous-optimization of orbitals and Cl coefficients. *Journal of Chemical Physics*, 73(5):2342–2356, 1980. 19

[50] H. J. Werner, M. Kallay, and J. Gauss. The barrier height of the F+H(2) reaction revisited: Coupled-cluster and multireference configuration-interaction benchmark calculations. *Journal of Chemical Physics*, 128(3):034305, January 2008. 20

[51] H. J. Werner and E. A. Reinsch. The self-consistent electron pairs method for multiconfiguration reference state functions. *Journal of Chemical Physics*, 76(6):3144–3156, 1982. 20

[52] H.-J. Werner and P. J. Knowles. An efficient internally contracted multiconfiguration reference CI method. *J. Chem. Phys.*, 89:5803–5814, 1988. 20

[53] P. J. Knowles and H.-J. Werner. An efficient method for the evaluation of coupling coefficients in configuration interaction calculations. *Chem. Phys. Letters*, 145:514–522, 1988. 20

[54] T. J. Lee and P. R. Taylor. A diagnostic for determining the quality of single-reference electron correlation methods. *International Journal of Quantum Chemistry*, 36:199–207, 1989. 21, 59

[55] A. I. Krylov. Equation-of-motion coupled-cluster methods for open-shell and electronically excited species: The Hitchhiker's guide to Fock space, 2008. 21

[56] M. Kallay and J. Gauss. Approximate treatment of higher excitations in coupled-cluster theory. *Journal of Chemical Physics*, 123(21):214105, December 2005. 21

[57] P. J. Knowles, C. Hampel, and H.-J. Werner. Coupled cluster theory for high spin open shell reference wavefunctions. *J. Chem. Phys.*, 99:5219–5227, 1993. 21

[58] C. Hampel, K. A. Peterson, and H. J. Werner. A comparison of the efficiency and accuracy of the quadratic configuration-interaction (QCSID), coupled cluster (CCSD), and brueckner coupled cluster (BCCD) methods. *Chemical Physics Letters*, 190(1-2):1–12, February 1992. 21

[59] H. J. Werner. Third-order multireference perturbation theory - the CASPT3 method. *Molecular Physics*, 89(2):645–661, October 1996. 21

[60] P. Celani and H. J. Werner. Multireference perturbation theory for large restricted and selected active space reference wave functions. *Journal of Chemical Physics*, 112(13):5546–5557, April 2000. 21

[61] P. Hohenberg and W. Kohn. Inhomogeneous electron gas. *Physical Review B*, 136(3B):B864–&, 1964. 22

[62] W. Kohn and L. J. Sham. Self-consistent equations including exchange and correlation effects. *Physical Review*, 140(4A):1133–&, 1965. 22

[63] A. Wolf, M. Reiher, and B. A. Hess. The generalized Douglas-Kroll transformation. *Journal of Chemical Physics*, 117(20):9215–9226, November 2002. 24

[64] M. Reiher and A. Wolf. Exact decoupling of the Dirac Hamiltonian. I. General theory. *Journal of Chemical Physics*, 121(5):2037–2047, August 2004. 24

[65] M. Reiher and A. Wolf. Exact decoupling of the Dirac Hamiltonian. II. The generalized Douglas-Kroll-Hess transformation up to arbitrary order. *Journal of Chemical Physics*, 121(22):10945–10956, December 2004. 24

[66] B. A. Hess, R. J. Buenker, and P. Chandra. Toward the variational treatment of spin-orbit and other relativistic effects for heavy-atoms and molecules. *International Journal of Quantum Chemistry*, 29(4):737–753, April 1986. 24

[67] A. Berning, M. Schweizer, H. J. Werner, P. J. Knowles, and P. Palmieri. Spin-orbit matrix elements for internally contracted multireference configuration interaction wavefunctions. *Molecular Physics*, 98(21):1823–1833, November 2000. 24

[68] Robert J. Le Roy. *LEVEL 8.0 A Computer Program for Solving the Radial Schrödinger Equation for Bound and Quasibound Levels.* University of Waterloo, 2007. Chemical Physics Research Report. 25, 112

[69] P. M. Morse. Diatomic Molecules According to the Wave Mechanics. II. Vibrational Levels. *Phys. Rev.*, 34:57–64, 1929. 25

[70] R. J. Le Roy. Level 8.0: A computer program for solving the radial schrödinger equation for bound and quasibound levels. University of Waterloo Chemical Physics Research Report CP-663, 2007. see: http://leroy.uwaterloo.ca/programs/. 26

[71] H. Sponer and E. Teller. Electronic spectra of polyatomic molecules. *Reviews of Modern Physics*, 13(2):0075–0170, April 1941. 30

[72] I. V. Hertel and C.-P. Schulz. *Atome, Moleküle und optische Physik 1.* Springer-Verlag Berlin Heidelberg, 2008. 34

[73] F. Ancilotto, E. Cheng, M. W. Cole, and F. Toigo. The binding of alkali atoms to the surfaces of liquid-helium and hydrogen. *Zeitschrift für Physik B-Condensed Matter*, 98(3):323–329, September 1995. 35, 90

[74] J. Reho, U. Merker, M. R. Radcliff, K. K. Lehmann, and G. Scoles. Spectroscopy of Mg atoms solvated in helium nanodroplets. *Journal of Chemical Physics*, 112(19):8409–8416, May 2000. 35, 89, 90

[75] J. P. Toennies and A. F. Vilesov. Superfluid helium droplets: A uniquely cold nanomatrix for molecules and molecular complexes. *Angewandte Chemie-international Edition*, 43(20):2622–2648, 2004. 35, 90

[76] E. Cheng, M. W. Cole, W. F. Saam, and J. Treiner. Wetting transitions of classical liquid films: A nearly universal trend. *Phys. Rev. B*, 48(24):18214–18221, December 1993. 35

[77] P. R. Kemper, M. T. Hsu, and M. T. Bowers. Transition-metal ion rare-gas clusters - bond strengths and molecular-parameters for Co+(He/Ne)n, Ni+(He/Ne)n, and Cr+(He/Ne/Ar). *Journal of Physical Chemistry*, 95(26):10600–10609, December 1991. 37, 93

[78] D. J. D. Wilson, C. J. Marsden, and E. I. von Nagy-Felsobuki. Ab initio calculations on first row transition metal hydrides TMHn+ and helides TMHe(n+1)+ (TM = Sc-Cu, n=0-2). *Physical Chemistry Chemical Physics*, 5(2):252–258, 2003. 37, 41, 93

[79] D. J. D. Wilson, C. J. Marsden, and E. I. von Nagy-Felsobuki. Ab initio structures and stabilities of doubly charged diatomic metal helides for the first row transition metals. *Journal of Physical Chemistry A*, 106(32):7348–7354, August 2002. 37, 93

[80] A. J. Wachters. Gaussian basis set for molecular wavefunctions containing third-row atoms. *Journal of Chemical Physics*, 52(3):1033–&, 1970. 37

[81] C. W. Bauschlicher, S. R. Langhoff, H. Partridge, and L. A. Barnes. Theoretical-studies of the 1st-row and 2nd-row transition-metal methyls and their positive-ions. *Journal of Chemical Physics*, 91(4):2399–2411, August 1989. 37

[82] A. K. Rappe, T. A. Smedley, and W. A. Goddard. Flexible d basis-sets for Sc through Cu. *Journal of Physical Chemistry*, 85(18):2607–2611, 1981. 37

[83] N. B. Balabanov and K. A. Peterson. Systematically convergent basis sets for transition metals. I. All-electron correlation consistent basis sets for the 3d elements Sc-Zn. *Journal of Chemical Physics*, 123(6):064107, August 2005. 38, 54, 63

[84] D. E. Woon and T. H. Dunning. Gaussian-basis sets for use in correlated molecular calculations .4. calculation of static electrical response properties. *Journal of Chemical Physics*, 100(4):2975–2988, February 1994. 38, 54, 63

[85] K. Andersson. Different forms of the 0th-order hamiltonian in 2nd-order perturbation-theory with a complete active space self-consistent-field reference function. *Theoretica Chimica Acta*, 91(1-2):31–46, April 1995. 56

[86] B. O. Roos and K. Andersson. Multiconfigurational perturbation-theory with level shift - the Cr-2 potential revisited. *Chemical Physics Letters*, 245(2-3):215–223, October 1995. 56

[87] T. H. Dunning. A road map for the calculation of molecular binding energies. *Journal of Physical Chemistry A*, 104(40):9062–9080, October 2000. 63

[88] MATLAB. *version 7.11.0.584 (R2010b)*. The MathWorks Inc., Natick, UNITED STATES, 1994 - 2012. 64

[89] R. J. Hinde. Mg-He and Ca-He van der Waals interactions: approaching the Born-Oppenheimer limit. *Journal of Physics B-atomic Molecular and Optical Physics*, 36(14):3119–3128, July 2003. 89, 90

[90] M. Mella, G. Calderoni, and F. Cargnoni. Predicting atomic dopant solvation in helium clusters: The $MgHe_n$ case. *Journal of Chemical Physics*, 123(5):054328, August 2005. 89

[91] F. Stienkemeier, F. Meier, and H. O. Lutz. Alkaline earth metals (Ca, Sr) attached to liquid helium droplets: Inside or out? *Journal of Chemical Physics*, 107(24):10816–10818, December 1997. 89

[92] Y. Ren and V. V. Kresin. Surface location of alkaline-earth-metal-atom impurities on helium nanodroplets. *Physical Review A*, 76(4):043204, October 2007. 89

[93] A. I. Boothroyd, P. G. Martin, and M. R. Peterson. Accurate analytic he-h(2) potential energy surface from a greatly expanded set of ab initio energies. *Journal of Chemical Physics*, 119(6):3187–3207, August 2003. 90

[94] F. Cargnoni, T. Kus, M. Mella, and R. J. Bartlett. Ground state potential energy surfaces and bound states of M-He dimers (M=Cu,Ag,Au): A theoretical investigation. *Journal of Chemical Physics*, 129(20):204307, November 2008. 90

[95] R. Ahlrichs, H. J. Bohm, S. Brode, K. T. Tang, and J. P. Toennies. Interaction potentials for alkali ion-rare gas and halogen ion-rare gas systems. *Journal of Chemical Physics*, 88(10):6290–6302, May 1988. 90

[96] D. Bellert and W. H. Breckenridge. Bonding in ground-state and excited-state A(+) . Rg van der Waals ions (A = atom, Rg = rare-gas atom): A model-potential analysis. *Chemical Reviews*, 102(5):1595–1622, May 2002. 90

[97] F. Dalfovo, A. Lastri, L. Pricaupenko, S. Stringari, and J. Treiner. Structural and dynamical properties of superfluid-helium - a density-functional approach. *Physical Review B*, 52(2):1193–1209, July 1995. 92

[98] H. J. Werner and P. J. Knowles. *MOLPRO Users Manual Version 2010.1.* University College Cardiff Consultants Limited, 2008. 106

Part III

Appendix

Chapter 8

Nist-Table for the Septet-Multiplicity

Table 8.1 contains the levels of the Cr atom. These results were obtained from the NIST-database [1]. In the column "configuration" the electronic configurations are given (sections 2.9 and 4). All orbitals up to the [Ar] configuration are doubly occupied. Therefore, only the outer shells are stated. The term designations of the different states are displayed in the second column ("Term", section 2.9). The third column contains the total angular momentum of the electron (J). The next two columns contain the level separations and level splittings. The last two columns contain the Lande g-factor and the percentage of the contributions of this state to a transition, because a transition of a certain energy might be realised with different states.

Configuration	Term	J	Level (cm-1)	Level Splittings (cm-1)	Lande-g	Leading percentages
$3d^5(6S)4s$	a 7S	3	0.00		2.00183	100
$3d^5(6S)4s$	a 5S	2	7 593.16	7 593.16	2.006	100
$3d^44s^2$	a 5D	0	7 750.78	157.62		
		1	7 810.82	60.04	1.50060	
		2	7 927.47	116.65	1.50060	
		3	8 095.21	167.74	1.50060	
		4	8 307.57	212.36	1.50060	
$3d^5(4G)4s$	a 5G	2	20 517.40	12 209.83	0.37	100
		6	20 519.60	2.20	1.33	100
		3	20 520.92	1.32	0.93	100
		4	20 523.69	2.77	1.13	100
		5	20 523.94	0.25	1.25	100
$3d^5(4P)4s$	a 5P	3	21 840.84	1 316.90	1.6	98
		2	21 847.88	7.04	1.847	98
		1	21 856.94	9.06	2.500	100
$3d^44s^2$	a 3P	0	23 163.27	1 306.33		
		1	23 512.00	348.73		
		2	24 093.16	581.16		
$3d^5(6S)4p$	z 7P	2	23 305.01	-788.15	2.334	67
		3	23 386.35	81.34	1.9176	67
		4	23 498.84	112.49	1.7510	67
$3d^44s^2$	a 3H	4	23 933.90	435.06		
		5	24 056.11	122.21		
		6	24 200.23	144.12		
$3d^5(4D)4s$	b 5D	0	24 277.06	76.83		100
		4	24 282.34	5.28	1.51	100
		1	24 286.54	4.20	1.48	100
		2	24 299.89	13.35	1.51	98
		3	24 303.94	4.05	1.55	98
$3d^5(4G)4s$	a 3G	3	24 833.86	529.92		100
		4	24 897.55	63.69		100
		5	25 038.61	141.06		100
$3d^44s^2$	a 3F	2	24 940.61	-98.00		
		3	25 106.34	165.73		
		4	25 177.39	71.05		
$3d^4(5D)4s4p(3P)$	z 7F	0	24 971.21	-206.18		100
		1	25 010.64	39.43	1.52	100
		2	25 089.20	78.56	1.50	100
		3	25 206.02	116.82	1.49	100
		4	25 359.62	153.60	1.51	100
		5	25 548.64	189.02	1.51	100
		6	25 771.40	222.76	1.53	100
$3d^5(6S)4p$	z 5P	3	26 787.50	1 016.10	1.670	92
		2	26 796.28	8.78	1.830	91
		1	26 801.93	5.65	2.512	92
$3d^5(4P)4s$	b 3P	0	27 163.20	361.27		100
		1	27 176.22	13.02		100
		2	27 223.05	46.83		98
$3d^4(5D)4s4p(3P)$	z 7D	1	27 300.19	77.14	3.01	99
		2	27 382.18	81.99	1.99	99
		3	27 500.37	118.19	1.76	99
		4	27 649.71	149.34	1.66	99
		5	27 825.45	175.74	1.61	100
$3d^44s^2$	b 3G	3	27 597.22	-228.23		
		4	27 703.84	106.62		
		5	27 816.88	113.04		
$3d^4(5D)4s4p(3P)$	y 7P	2	27 728.87	-88.01	2.341	66
		3	27 820.23	91.36	1.929	66
		4	27 935.26	115.03	1.761	67

Table 8.1: energy levels for chromium from the NIST - database[1, 2]

Chapter 9

MOLPRO

This section contains the input-file for a MOLPRO calculation and its discussion. The MOLPRO Manual [98] was helpful in writing the programs. The calculation of the dipole moment of CrHe for a distance of 5 A has been taken as an example. The results of this calculation can be found in section 4.4.

```
***CrHe dipole moment calculation
gthresh,energy=1.d-09,oneint=1.d-14,twoint=1.d-14;
gthresh,prefac=1.d-14,zero=1.d-14;
memory, 900, m
```

The parameters for the execution of the program are set. The command "gthresh" determines the thresholds for the convergence in the different methods. Additionally the memory the program can use, is given.

```
gprint,orbitals, civector
gexpec, dm
ANGSTROM
```

The command "gprint" is used to determine which information should be printed in the output - file. "gexpec" is used to determine globally which operators should be evaluated. In this case the dipole moment (dm) is requested. The command "ANGSTROM" forces the software to interpret the distances in the input-file in Ångström instead of atomic units.

```
basis
!  aug-cc-pVTZ-DK  EMSL  Basis Set Exchange Library   9/7/12 8:01 AM
! Original basis sets:
! Elements                             References
! --------                             ----------
! H     : T.H. Dunning, Jr. J. Chem. Phys. 90, 1007 (1989).
! He    : D.E. Woon and T.H. Dunning, Jr. J. Chem. Phys. 100, 2975
(1994).
! B - Ne: T.H. Dunning, Jr. J. Chem. Phys. 90, 1007 (1989).
! Al - Ar: D.E. Woon and T.H. Dunning, Jr.  J. Chem. Phys. 98, 1358
(1993).
! Ga - Kr: A.K. Wilson, D.E. Woon, K.A. Peterson, T.H. Dunning, Jr.,
```

```
! J. Chem. Phys., 110, 7667 (1999).
! Original exponents recontracted: W.A. de Jong, R.J. Harrison and
D.A. Dixon,
! J. Chem. Phys. 114, 48 (2001).
! Sc - Zn: (20s,16p,8d,2f,1g) -> [7s,6p,4d,2f,1g] N.B. Balabanov and
K.A.
! Peterson, J. Chem. Phys.,
! 123, 064107 (2005)
! Y Zr Nb Mo Tc Ru Rh Pd      : K.A. Peterson, D. Figgen, M. Dolg,
H. Stoll, Energy-consistent relativistic pseudopotentials and
correlation consistent basis sets for the 4d elements Y-Pd, Journal
of Chemical Physics 126, 124101 (2007).
!

! HELIUM       (7s,3p,2d) -> [4s,3p,2d]
! HELIUM       (6s,2p,1d) -> [3s,2p,1d]
! HELIUM       (1s,1p,1d)
s, HE , 234.0000000, 35.1600000, 7.9890000, 2.2120000, 0.6669000,
0.2089000, 0.0513800
c, 1.4, 0.0026127, 0.0195588, 0.0910316, 0.2720643
c, 5.5, 1
c, 6.6, 1
c, 7.7, 1
p, HE , 3.0440000, 0.7580000, 0.1993000
c, 1.1, 1
c, 2.2, 1
c, 3.3, 1
d, HE , 1.9650000, 0.4592000
c, 1.1, 1
c, 2.2, 1
! CHROMIUM       (21s,17p,9d,3f,2g) -> [8s,7p,5d,3f,2g]
! CHROMIUM       (20s,16p,8d,2f,1g) -> [7s,6p,4d,2f,1g]
! CHROMIUM       (1s,1p,1d,1f,1g)
s, CR , 6177194.0000000, 924929.5000000, 210486.5000000, 59620.0500000,
19450.7600000, 7022.0560000, 2738.7630000,1135.8140000, 495.0923000,
224.7487000, 105.3836000, 50.1935900, 22.2495700, 10.9826500,
5.3836650, 2.3436850, 1.1052020, 0.4878480, 0.0895990, 0.0334230, 0.0124700
c, 1.19, 0.0000840, 0.0002410, 0.0006580, 0.0016730, 0.0042480,
0.0108890, 0.0278590, 0.0678880, 0.1468020, 0.2556230,0.2984080,
0.1745600, 0.0696900, 0.1141840, 0.0840700, 0.0099260, -0.0003160,
0.0000590, 0.0000160
c, 1.19, -0.0000460, -0.0001340, -0.0003640, -0.0009270, -0.0023610,
-0.0060760, -0.0157230, -0.0390780, -0.0887110, -0.1701120, -0.2472980,
-0.1863810, 0.1584390, 0.5481250, 0.3885790, 0.0492810, -0.0043050,
0.0001110, -0.0000270
c, 1.19, 0.0000100, 0.0000290, 0.0000780, 0.0002000, 0.0005110,
```

```
0.0013170, 0.0034470, 0.0086680, 0.0204950, 0.0417010, 0.0693000,
0.0581890, -0.0761810, -0.3561380, -0.3726510, 0.2838030, 0.7149340,
0.2908760, 0.0069090
c, 1.19, -0.0000020, -0.0000070, -0.0000180, -0.0000450, -0.0001170,
-0.0002980, -0.0007900, -0.0019570, -0.0047250, -0.0093680,
-0.0162500, -0.0125490, 0.0155500, 0.0916910, 0.0854260, -0.0662500,
-0.2868520,-0.1703030, 0.6967260
c, 1.19, 0.0000040, 0.0000130, 0.0000360, 0.0000880, 0.0002390,
0.0005570, 0.0016820, 0.0034900, 0.0105120, 0.0153920, 0.0402770,
0.0073940, 0.0140570, -0.2936730, 0.0030100, -0.1758500, 1.5006460,
-1.1269400, -1.2270880
c, 1.19, -0.0000070, -0.0000210, -0.0000580, -0.0001450, -0.0003840,
-0.0009370, -0.0026480, -0.0060270, -0.0162070, -0.0279550,
-0.0593480, -0.0278590, 0.0170670, 0.4205010, 0.2026980, -0.4517940,
-1.9067910, 2.8955150, -2.2377970
c, 20.20, 1
c, 21.21, 1
p, CR , 14454.2000000, 3421.6760000, 1111.3870000, 425.1918000,
180.2623000, 82.0611700, 39.2972600, 19.4195900, 9.8288990, 5.0168100,
2.4870910, 1.1987800, 0.5586950, 0.2093660, 0.0847220, 0.0332780,
0.0130700
c, 1.15, 0.0001150, 0.0005600, 0.0026530, 0.0106120, 0.0358670, 0.0993240,
0.2135250, 0.3339970, 0.3282920, 0.1505820, 0.0200020,
-0.0015630, -0.0012910, -0.0002120, 0.0000240
c, 1.15, -0.0000400, -0.0001940, -0.0009220, -0.0037110, -0.0127060,
-0.0361210, -0.0805400, -0.1323120, -0.1340350, 0.0347070, 0.3356300,
0.4612780, 0.2785730, 0.0412210, -0.0038000
c, 1.15, 0.0000090, 0.0000460, 0.0002190, 0.0008780, 0.0030300,
0.0085680, 0.0193430, 0.0315600, 0.0330560, -0.0135900, -0.0940090,
-0.1498470, -0.0657160, 0.2711740, 0.5750590
c, 1.15, 0.0000120, 0.0000590, 0.0002770, 0.0011210, 0.0038200,
0.0109400, 0.0243010, 0.0405940, 0.0407730, -0.0134400, -0.1211060,
-0.1827370, -0.1200720, 0.4449520, 0.6413430
c, 1.15, 0.0000250, 0.0001160, 0.0006020, 0.0021980, 0.0083680,
0.0212190, 0.0545450, 0.0746730, 0.1147010, -0.0783210, -0.2465150,
-0.6773230, 0.7479410, 0.9845060, -1.0295180
c, 16.16, 1
c, 17.17, 1
d, CR , 89.4745000, 26.3368000, 9.5342900, 3.8211800, 1.5716900,
0.6264220, 0.2330550, 0.0763030, 0.0249800
c, 1.7, 0.0036170, 0.0255390, 0.0968340, 0.2351220, 0.3574460,
0.3691600, 0.2380780
c, 1.7, -0.0041240, -0.0290980, -0.1143160, -0.2719580, -0.3162730,
0.0374570, 0.5894820
c, 1.7, 0.0059530, 0.0422270, 0.1730970, 0.3927110, 0.1544870,
-0.8070190, 0.0009440
```

```
c, 8.8, 1
c, 9.9, 1
f, CR , 2.2211000, 0.5231000, 0.1724900
c, 1.1, 1
c, 2.2, 1
c, 3.3, 1
g, CR , 1.4199000, 0.4989600
c, 1.1, 1
c, 2.2, 1
end
```

The information for the basis set are given in between the commands "basis" and "end". The basis set was taken from the NIST-database [1]. First, there are the citations, commented with "!". Next, the different orbitals, functions for Cr and He are defined. The command "s,Cr, ..." is used to give the exponentials for the s-type Gauss orbitals. Similar commands are used for the rest of the orbitals. The command "c, ..." determines how many functions are contracted to describe a single orbital. These parameters determine the $\psi_i(\mathbf{r}_j)$ in equation 2.4.

```
radi=5.0;
symmetry, x,y
geometry={
Cr;
He,Cr, radi;}
```

These commands determine the geometry of the system. "symmetry, x,y" is used to set the point group for the calculation to C_{2v} The command "geometry" is used to describe the system, in this case it is a Cr and a He atom with the distance "radi".

```
{hf-scf;wf,26,1,6;maxit,120}
```

This requests a ROHF calculation. The command "wf,26,1,6" gives the properties of the solution. The wave function for system containing 26 electrons should be calculated. The wave function should belong to the first symmetry, the A_1. The number "6" determines the multiplicity, in this case a septet-multiplicity.

```
{multi;
occ,12,5,5,2
closed,6,2,2,0
wf,26,1,6;state,6;
wf,26,2,6;state,5;
wf,26,3,6;state,5;
wf,26,4,6;state,3;
canonical}
cas_e=energy;
ccas_e=(cas_e-cas_e(1))*TOCM;
{table, cas_e, ccas_e, radi;
digits, 9, 9, 9, 9
save, Cr_ANR_acpwCVTZ_MCSCF.txt}
```

The command “multi” demands a MCSCF calculation. “occ, ...” and “closed, ...” are used to define the orbitals of the active space, see sections 4.3.1 and 5.2.2. Next the commands “wf, ...” determine the symmetries in the calculation. “state, ...” gives the number of states calculated in the respective symmetry. The orbitals need to be transformed to be used by the MRCI-program which is done with the command “canonical”. The results then are saved to variables and printed to a file with “table, ... save, ...”.

```
{ci, maxit=500, maxiti=100
wf,26,1,6;
save,3000.1
state,1;}
```

The ground states is calculated in a MRCI calculation with the above commands. The result is saved to the internal file 3000.1.

```
{ci, maxit=500, maxiti=100
wf,26,1,6;
save,3100.1
state,6;}
e_ground=energy(1);
ci_e1=(energy-e_ground)*TOCM;
{table, ci_e1, energy, radi;
digits, 9, 9, 9
save, Cr_ANR_acpwCVTZ_MCSCF_CI.txt}
```

Six states of the first symmetry are calculated in a MRCI calculation and saved. The results are saved in variables and printed to a file.

```
{ci; trans,3000.1,3100.1,dm,qm,lop}
{ci; trans,3000.1,3000.1,dm,qm,lop}
{ci; trans,3100.1,3100.1,dm,qm,lop}
```

The command “ci; trans, ...” can be used to calculate the transition properties between two saved states. In this case the dipole and the quadrupole moment are requested as well as the orbital angular momentum.

```
{ci, maxit=500, maxiti=100
wf,26,2,6;
save,3200.1
state,5;}

ci_e2=(energy-e_ground)*TOCM;
{table, ci_e2, energy, radi;
digits, 9, 9, 9
save, Cr_ANR_acpwCVTZ_MCSCF_CI.txt}

{ci; trans,3000.1,3200.1,dm,qm,lop}
{ci; trans,3200.1,3200.1,dm,qm,lop}
```

```
{ci, maxit=500, maxiti=100
wf,26,3,6;
save,3300.1
state,5;}

ci_e3=(energy-e_ground)*TOCM;
{table, ci_e3, energy, radi;
digits, 9, 9, 9
save, Cr_ANR_acpwCVTZ_MCSCF_CI.txt}

{ci; trans,3000.1,3300.1,dm,qm,lop}
{ci; trans,3300.1,3300.1,dm,qm,lop}

{ci, maxit=500, maxiti=100
wf,26,4,6;
save,3400.1
state,3;}

ci_e4=(energy-e_ground)*TOCM;
{table, ci_e4, energy, radi;
digits, 9, 9, 9
save, Cr_ANR_acpwCVTZ_MCSCF_CI.txt}

{ci; trans,3000.1,3400.1,dm,qm,lop}
{ci; trans,3400.1,3400.1,dm,qm,lop}
```

The MRCI-calculations are performed for the other symmetries one by one with the text above. Their results are saved and printed to a file. After each MRCI calculation the transition properties are calculated.

Chapter 10

LEVEL 8

This section shows an input-file for a calculation of rovibrational levels with the LEVEL program. For writing this program the manual was used [68]. The results of this calculation are displayed in section 5.1.6.

```
1: 0 30  0 30   0  1                  % IAN1 IMN1 IAN2 IMN2 CHARGE NUMPOT
2: 'He' 4.00                          % NAME1 MASS1
3: 'Cr' 52.00                         % NAME2 MASS2
4: 'rovibrational levels for a Lennard-Jones potential'
5: 0.0020  2.0  99.  1.d-6            % RH RMIN RMAX EPS
6: 0  -1  0  0.D0                     % NTP LPPOT IOMEG VLIM
7: 1  8 9 0  0  0  4.9188d0  5.0143D0 % IPOTL MPAR NSR NVARB NCMM IBOB DSCM REQ
8: -998  1  2  -1  0 1  2 -1          % NLEV1 AUTO1 LCDC LXPCT NJM JDJR IWR LPRWF
9: 0 0                                % IV(1) IJ(1)
```

The text after "%" are only comments. The first four numbers determine the atomic numbers and the mass of the two atoms. The zeros for the atomic numbers cause the program to read the second and third row for these details. The atomic number is given by the abbreviations of the atoms which are followed by the mass. The fifth number in the first row gives the charge of the system. The last number determines the number of potentials used, two would be necessary for calculating transition properties. The fourth row contains a title. The fifth row gives details for the numerical treatment. These numbers are the step length, the minimum at maximum radius and the accuracy. The next two rows (6,7) contain details describing the potential. In the seventh row the Lennard-Jones parameters are given. The second and third number in the seventh row determine the powers of the potential and the last two numbers in this row the potential depth in $cm^{-}1$ and the position of the potential well in Å, compare with table 5.2. The last two rows (8,9) determine how many rovibrational states should be calculated. For details refer to the manual [68].